



# UNIVERSIDAD NACIONAL AUTÓNOMA DE MÉXICO

---

---

## FACULTAD DE MEDICINA

**El Canal Inespecífico Mitocondrial de *Saccharomyces cerevisiae* (ScMUC).**

**Tesis**

**Que para obtener el título de:**

**Licenciado en Investigación Biomédica Básica**

**Presenta:**

**JUAN ESPINASA JARAMILLO**

**Director:**

**Dr. Salvador Uribe Carvajal**

**Ciudad Universitaria 2014**



**UNAM – Dirección General de Bibliotecas**

**Tesis Digitales**  
**Restricciones de uso**

**DERECHOS RESERVADOS ©**  
**PROHIBIDA SU REPRODUCCIÓN TOTAL O PARCIAL**

Todo el material contenido en esta tesis está protegido por la Ley Federal del Derecho de Autor (LFDA) de los Estados Unidos Mexicanos (México).

El uso de imágenes, fragmentos de videos, y demás material que sea objeto de protección de los derechos de autor, será exclusivamente para fines educativos e informativos y deberá citar la fuente donde la obtuvo mencionando el autor o autores. Cualquier uso distinto como el lucro, reproducción, edición o modificación, será perseguido y sancionado por el respectivo titular de los Derechos de Autor.



## 1. ÍNDICE

1. Índice	3
2. Resumen	7
3. Introducción	11
3.1. Las células, el metabolismo y la bioquímica	11
3.2. La bioenergética, la teoría quimiosmótica y la mitocondria	13
3.3. La fosforilación oxidativa, la cadena transportadora de electrones y la ATP sintasa	20
3.3.1. Composición en mamíferos	20
3.3.2. Composición en <i>Saccharomyces cerevisiae</i>	22
3.3.3. Regulación	24
3.4. La transición de la permeabilidad y el Canal Inespecífico Mitocondrial	26
3.4.1. Descubrimiento y función	27
3.4.2. Efectores y composición	28
3.4.2.1. CsA y CyP-D	29
3.4.2.2. ADP, ATP y el transportador de Adenin Nucleótidos	30
3.4.2.3. VDAC	31
3.4.2.4. PiC y H <sub>2</sub> PO <sub>4</sub> <sup>-</sup>	33
3.4.2.5. ATP sintasa	34
3.4.2.6. Efecto de Cationes	34
4. Hipótesis y Objetivos	37
4.1. Hipótesis	37
4.2. Objetivos	37

5. Material y Métodos	39
5.1. Material	39
5.2. Cultivo de Levaduras	39
5.3. Aislamiento de mitocondrias	40
5.4. Determinación de proteína	41
5.5. Función mitocondrial	41
5.6. Consumo de oxígeno	41
5.7. Potencial transmembranal	43
5.8. Hinchamiento y contracción mitocondrial	44
5.9. Producción de especies reactivas de oxígeno	44
6. Resultados	47
6.1. Consumo de oxígeno	47
6.2. Potencial transmembranal	50
6.3. Hinchamiento y contracción mitocondrial	54
6.4. Producción de especies reactivas de oxígeno	58
7. Discusión	61
8. Conclusiones	65
8.1. Efecto sinérgico de $\text{Ca}^{2+}$ , $\text{Mg}^{2+}$ y $\text{H}_2\text{PO}_4^-$	65
8.2. Regulación dinámica del <i>ScMUC</i> por iones	65
8.3. En busca de aperturas parciales del <i>ScMUC</i>	65
8.4. MUC y ROS	65
9. Referencias	67
10. Agradecimientos	79

11. Lista de Abreviaturas	81
---------------------------	----

12. Anexos	83
------------	----

12.1. Cabrera-Orefice, A., Chiquete-Félix, N., Espinasa-Jaramillo, J., Rosas-	84
---	----

Lemus, M., Guerrero-Castillo, S., Peña, A., & Uribe-Carvajal, S. (2014).

The branched respiratory chain from *Debaryomyces hansenii*: Components

and supremolecular organization. *Biochimica et Biophysica acta*, 1837, 73-

84.

12.2 Guerrero-Castillo, S., Araiza-Olivera, D., Cabrera-Orefice, A., Espinasa-	96
--	----

Jaramillo, J., Gutiérrez-Aguilar, M., Luévano-Martínez, L. A., Zepeda-Bastida,

A., & Uribe-Carvajal, S. (2011). Physiological uncoupling of mitochondrial

oxidative phosphorylation. Studies in different yeast species. *Journal of*

*Bioenergetics and Biomembranes*, 43, 323-331.



## 2. RESUMEN

### “Dinámica del Canal Inespecífico Mitocondrial de *Saccharomyces cerevisiae* (ScMUC)”

Una característica de todos los seres vivos, incluyendo los virus, es la necesidad de transformar energía. Para esto existen diferentes mecanismos que permiten llevar a cabo este proceso. La bioenergética es la disciplina encargada de estudiar los procesos de obtención de energía a partir de la oxidación de sustratos o la luz.

En el caso de las células eucarióticas una parte importante de la energía que se obtiene para el funcionamiento celular proviene de la mitocondria, en donde se lleva a cabo la oxidación de sustratos como el NADH, succinato, piruvato, entre otros. La mitocondria es un organelo de suma importancia por su rol energético y como señalizador en diversos procesos celulares. Ésta cuenta con dos membranas, una externa (MOM) y una interna (MIM), que le permiten regular de forma muy precisa qué entra y sale de la matriz mitocondrial. La oxidación de estos sustratos, por la cadena respiratoria, ocasiona el bombeo de protones al espacio intermembranal generando una diferencia de carga entre la matriz y éste. La diferencia de cargas es usada por la ATP sintasa para llevar a cabo la reacción de síntesis del ATP.

Se han propuesto diversos mecanismos para regular la producción de ATP, los cuales se han dividido en dos grandes categorías: 1) enzimas redox que no bombean protones, como es el caso de componentes alternos como las deshidrogenasas de *S. cerevisiae* que sustituyen al complejo I o la Oxidasa Alterna de *Y. Lypolitica*, y 2) los sumideros de protones, como las enzimas desacoplantes y el canal inespecífico mitocondrial que abaten

el potencial transmembranal.

La transición de la permeabilidad (PT) se definen como un aumento en la permeabilidad de MIM a moléculas de hasta 1.5 KDa. Ésta es ocasionada por la apertura del canal inespecífico mitocondrial (MUC); y si se mantiene por mucho tiempo produce pérdida del potencial transmembranal, hinchamiento mitocondrial y posteriormente ruptura de la membrana externa.

El papel fisiológico del MUC y la relevancia de la PT en vivo sigue siendo un tema de debate hoy en día, por lo que nos interesó estudiar si el MUC podía, *in vitro*, ser regulador por iones como el  $\text{Ca}^{2+}$ ,  $\text{Mg}^{2+}$  y  $\text{H}_2\text{PO}_4^-$ , ya que creemos que la PT es un mecanismo de detoxificación mitocondrial y regulación de la producción de ATP y de especies reactivas.

Vimos un acoplamiento en la respiración y un aumento en los valores del potencial transmembranal proporcionales a las concentraciones de  $\text{Ca}^{2+}$ ,  $\text{Mg}^{2+}$  y  $\text{H}_2\text{PO}_4^-$  usadas en los ensayos. También evaluamos la posibilidad del MUC de abrirse y cerrarse, en una misma preparación, por el efecto de cationes divalentes como el  $\text{Ca}^{2+}$  y  $\text{Mg}^{2+}$  dentro de valores fisiológicos.

En ensayos adicionales estudiamos la posibilidad de que el MUC tuviera diferentes aperturas, con diferentes diámetros, a varias concentraciones de iones y por último medimos la producción de Especies Reactivas de Oxígeno.

El papel de los iones para regular la apertura y cierre del MUC es muy claro. Además de ser una estructura con apertura dinámica. En cuanto a la apertura con diferentes diámetros y el papel del MUC en la formación de ROS no podemos concluir mucho debido a que no detectamos aperturas parciales con la prueba de polietilén glicol y los datos de la

formación de ROS no tienen diferencias con valor estadístico significativas.



### 3. INTRODUCCIÓN

*Una de las propiedades que convierte a los seres vivos  
en algo maravilloso y diferente;  
es que crean y mantienen orden en un universo tendiente al caos.*  
BRUCE ALBERTS

#### 3.1 Las células, el metabolismo y la bioquímica

Con la excepción posible de los virus, todas las formas de vida en este planeta —a pesar de la diversidad y complejidad que tienen— están formadas por al menos una célula que en su interior cuenta con la maquinaria necesaria para sobrevivir y reproducirse (Alberts y cols., 2009). La variedad de reacciones químicas que esta maquinaria puede mediar es casi tan amplia como la podamos imaginar. Puede ir desde un microorganismo que debe modificar su metabolismo por cambios en el charco en el que vive o que está siendo utilizado para fermentar azúcares para la producción de cerveza, hasta una planta que enfrenta una sequía extrema o cambios de temperatura. Los seres vivos dependen durante toda su existencia de estas reacciones para poder sobrevivir.

La ciencia que se encarga de estudiar los fenómenos químicos que ocurren dentro de las células es la bioquímica. Para su estudio, estas reacciones químicas se han dividido en dos categorías: la primera, el catabolismo, incluye las reacciones que permiten descomponer macromoléculas de las cuales se obtiene energía y moléculas más pequeñas que sirven para construir la célula. La segunda es el anabolismo y está constituido por las reacciones biosintéticas que utilizan la energía y moléculas simples obtenidas de las reacciones

catabólicas para la construcción de las membranas, el DNA, las proteínas y todos los organelos presentes en una célula. Al conjunto de reacciones, tanto catabólicas como anabólicas, que ocurren dentro de una célula se le llama metabolismo (Horton y cols., 2008).

El estudio bioquímico del metabolismo comienza a inicios del siglo XIX al demostrarse que a partir de moléculas sencillas, y por medio de una transformación química, era posible sintetizar compuestos químicos presentes sólo en los seres vivos (Horton y cols., 2008). Es hasta inicios del siglo XX que comienza a desarrollarse esta disciplina de forma generalizada en las universidades y centros de investigación, y se realizan grandes descubrimientos. Hay dos hallazgos que vale la pena mencionar, pues sentaron las bases para la imagen que hoy en día se tiene de la biología:

1. El descubrimiento de las enzimas como catalizadores de las reacciones que ocurren dentro de los organismos (eficientes dispositivos moleculares que determinan los patrones de las reacciones químicas dentro de las células), ya que gran parte de éstas sólo podrían darse a temperaturas muy elevadas. Si no contáramos con catalizadores que faciliten estas reacciones químicas la vida no existiría (Horton y cols., 2008).
2. El descubrimiento del papel de los ácidos nucleicos como almacenadores y transportadores de información (Horton y cols., 2008) explicando en términos moleculares la herencia de caracteres entre padres e hijos y dando lugar a la rama de la biología molecular.

### 3.2 La bioenergética, la teoría quimiosmótica y la mitocondria

Una característica que comparten los seres vivos, incluyendo los virus, es la necesidad de transformar energía para poder realizar las funciones que se llevan a cabo dentro de una célula. Cabe mencionar que, aunque en las reacciones que ocurren dentro de la célula hay una transformación energética, la rama de la bioenergética se especializa en estudiar los mecanismos por los cuales se obtiene energía a partir de la oxidación de sustratos o de la absorción de la luz (Nicholls y Ferguson, 2002).

Cuando la disciplina de la bioquímica comenzó formalmente a mediados del siglo XX, gran parte de las rutas metabólicas ya habían sido elucidadas pero aún no se entendía de qué forma las células transformaban la energía de la luz o de las fuentes de carbono en energía, almacenada en moléculas como el ATP (intermediario altamente energético que participa en una gran diversidad de procesos biológicos) de manera tan eficiente (Slater, 1953).

En 1966, Peter Mitchell postuló la teoría quimiosmótica, que sentó las bases para el estudio moderno de la bioenergética (Mitchell, 1966). La teoría quimiosmótica propone que las reacciones de oxidoreducción, que se llevan a cabo en los complejos respiratorios y fotosintéticos, ocasionan el bombeo de protones de un lado a otro de la membrana, lo que genera un potencial transmembranal (una diferencia electroquímica entre un lado y otro) que después es usado para la síntesis de ATP y diferentes procesos que requieren de energía (Fig. 1).

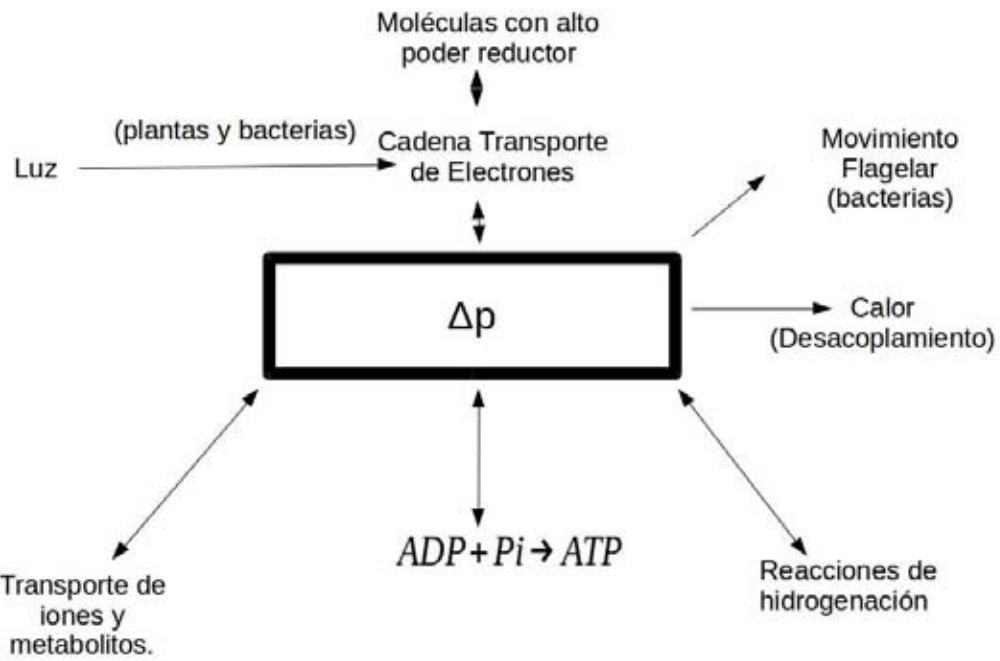


**Figura 1. Esquema de formación y uso de la fuerza protónica.** En el esquema podemos ver cómo la luz, metabolitos o reductores se transforman en una fuerza protón motriz que es utilizada para distintas funciones como son la síntesis de ATP, el movimiento de flagelos, generar calor y reacciones de hidrogenación. (Imagen modificada de *Bioenergetics 3* de Nicholls y Ferguson, 2002).

La diferencia en la concentración de protones junto con la diferencia de cargas eléctricas generada de cada lado de la membrana, es descrita en la siguiente ecuación y es llamada fuerza protónmotriz:

$$\Delta P(mV) = -(\Delta \mu H^+)/F$$

$$\Delta P(mV) = \Delta \Psi + 59 \Delta pH$$

La ecuación describe la fuerza protón motriz ( $\Delta P$ ) que consta de dos componentes.

El  $\Delta\Psi$ , la diferencia de cargas ocasionada por diferentes concentraciones de iones en ambos lados de la membrana interna, y la diferencia de pH ( $\Delta\text{pH}$ ) entre el espacio intermembranal y la matriz. Este proceso de transformación de energía puede verse como un análogo a un circuito eléctrico, excepto que en lugar de electrones fluyen protones, tal como se ve en la Fig. 2.

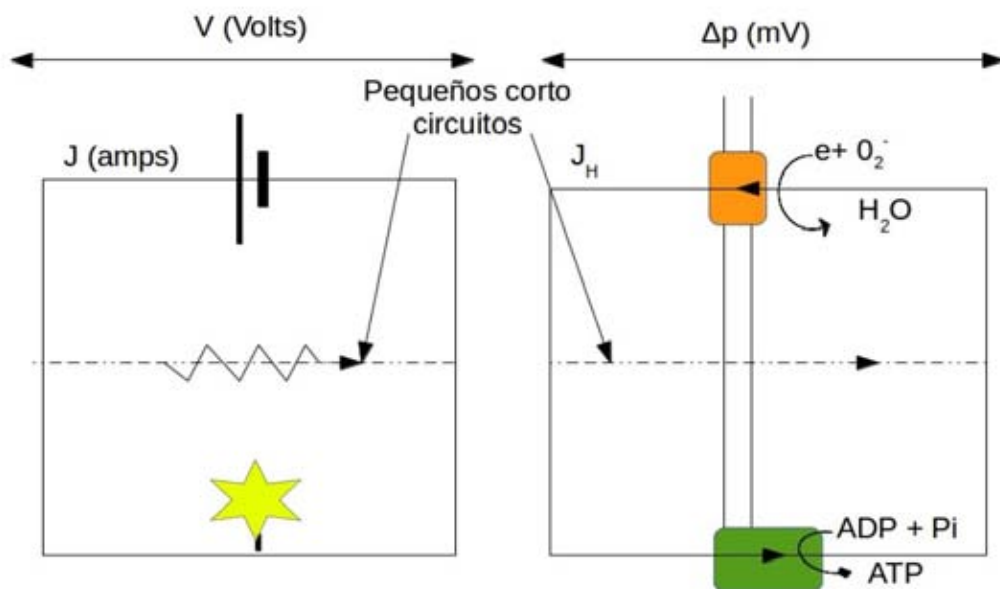


**Figura 2. La cadena de transporte de electrones es similar a un circuito eléctrico.** A la izquierda tenemos una representación gráfica de un circuito en el que una diferencia de voltaje genera el transporte de carga a través del circuito y transforma la energía a luz en el foco. Del lado derecho tenemos una representación gráfica de la membrana interna mitocondrial, en donde la cadena transportadora de electrones genera una diferencia de potencial entre la matriz y el espacio intermembranal que es usado por la ATP sintasa para llevar a cabo la catálisis de un ADP y un fosfato a ATP. (Imagen modificada de *Bionergetics 3* de Nicholls y Ferguson, 2002).

La mitocondria y el cloroplasto son considerados los organelos energéticos por excelencia. Se cree que la mitocondria tuvo su origen en un proceso endosimbiótico que sucedió hace más de mil millones de años (Sagan, 1967). Ésta presenta dos membranas: una interna mitocondrial (MIM; por sus siglas en inglés) con alta selectividad y una externa (MOM; por sus siglas en inglés) con mayor permeabilidad al paso de especies químicas (Fig. 3).

La MIM le permite a la mitocondria compartamentalizar iones, metabolitos y generar diferencias de concentraciones entre un lado de la membrana y otro.

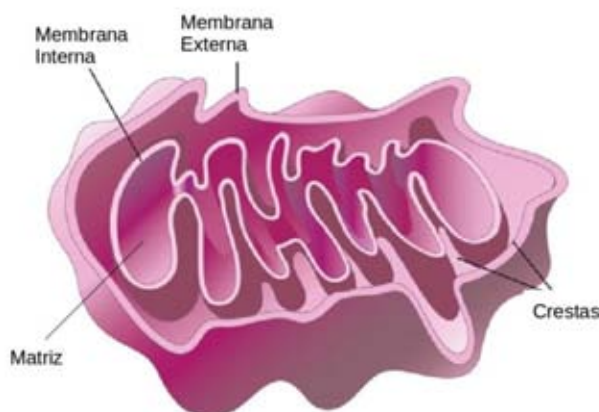


**Figura 3. Esquema de una mitocondria.** En ésta se puede ver la membrana externa mitocondrial, la membrana interna, las crestas y la matriz. (Imagen modificada de Nature Scitable).

Para que los sustratos y los iones puedan llegar a la matriz mitocondrial o al espacio intermembranal deben cruzar primero la membrana externa. Este fenómeno es mediado por el canal aniónico dependiente de voltaje (VDAC; por sus siglas en inglés) (Colombini, 2004).

La mitocondria presenta en su membrana interna una diversidad de proteínas entre

las que se encuentran: la cadena respiratoria y los transportadores de moléculas como iones ( $\text{Ca}^{2+}$ ,  $\text{Mg}^{2+}$ ,  $\text{HPO}_4^{2-}$ ), sustratos del ciclo de Krebs, ATP, ADP (Bernardi, 1999). Todos estos transportadores le permiten a la mitocondria abastecerse de los co-factores, sustratos y grupos prostéticos necesarios para llevar a cabo reacciones como la síntesis de ATP y otras reacciones metabólicas (Fig. 4).

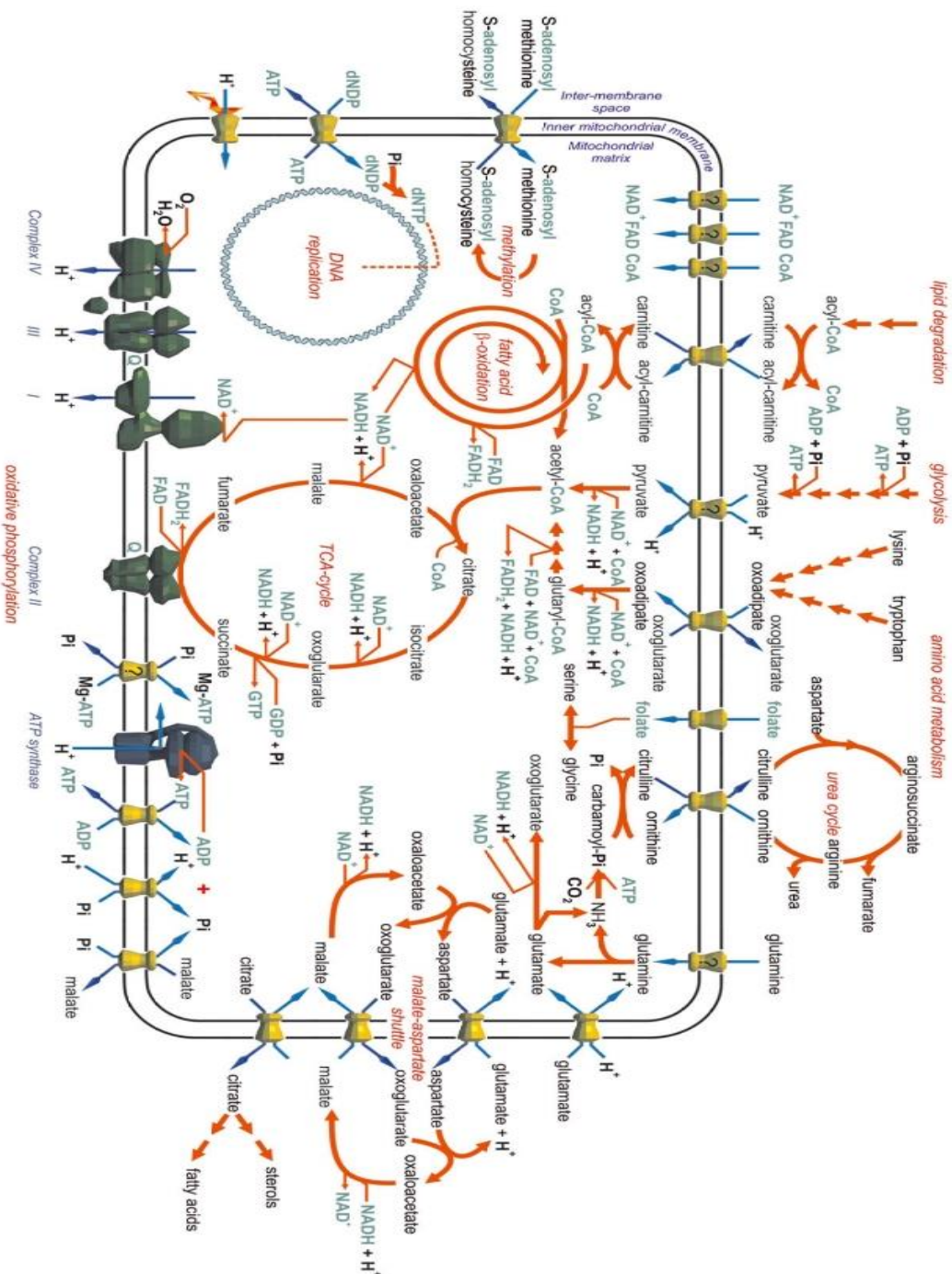


**Figura 4. Transportadores y rutas metabólicas mitocondriales.** En amarillo: podemos ver a los transportadores de diferentes especies químicas.

En gris: la cadena transportadora de electrones. Y en rojo las rutas metabólicas. (Imagen modificada de Kunji, 2004).

La relación simbiótica entre la  $\alpha$ -proteobacteria que dio origen a la mitocondria y el huésped llevó a que gran parte del genoma de la  $\alpha$ -proteobacteria migrara hacia el núcleo y que las vías metabólicas de ambos organelos fueran complementándose (Adams y Palmer, 2003). Las mitocondrias conservan todavía un genoma y ribosomas en su interior y llevan a cabo síntesis de algunas subunidades de proteínas de membrana (Constanzo y Fox, 1990).

Al migrar parte de los genes mitocondriales al núcleo, también tuvo que ocurrir, la aparición de un mecanismo que permitió importar proteínas del citosol al interior de la mitocondria. La mayoría de las proteínas que tienen como destino la mitocondria poseen una secuencia de importación y cuentan con translocadores en cada membrana (Dolezal y cols., 2006). La presecuencia puede ser muy variable en extensión y composición, y se cree que lo que principalmente lleva a que estas proteínas se trasloquen hacia el interior es una carga positiva en la presecuencia (Saint-Georges y cols., 2001) y, en otros casos, su importación es catalizada por chaperonas (Dolezal y cols., 2006).

Otra característica de este organelo es que se divide de forma independiente del ciclo celular. La división mitocondrial y los cambios en su morfología son estimulados por altas demandas energéticas (Scott y Youle, 2010).

Es importante mencionar que aunque la principal función de la mitocondria es energética, ésta lleva a cabo otras funciones que son vitales para la célula (Kroemer y Reed, 2000). En su interior ocurre el ciclo de Krebs, participa en vías de señalización, como es el caso de la necrosis y la apoptosis, la oxidación de ácidos grasos, etcétera.

### 3.3 La fosforilación oxidativa, la cadena transportadora de electrones y la ATP sintasa

Una parte de la oxidación de los sustratos acoplada a la síntesis de ATP ocurre en el citosol y en algunos otros organelos, pero la parte más significativa y que es considerada la respiración celular ocurre en la mitocondria. El proceso que acopla la oxidación de un sustrato con alto potencial reductor (esto quiere decir que puede donar sus electrones con facilidad), obtenido del metabolismo como el NADH o el succinato, al bombeo de protones, se le denomina fosforilación oxidativa (OXPHOS; por sus siglas en inglés) (Nicholls y Ferguson, 2002). Éste comprende dos grandes pasos:

Primero, la oxidación de sustratos por medio de una cadena respiratoria (grupo de enzimas redox presentes en la membrana interna mitocondrial) que está acoplada al bombeo de protones desde la matriz mitocondrial hacia el espacio intermembranal. La composición de la cadena respiratoria es de cuatro complejos canónicos que se encuentran presentes en una gran variedad de organismos (Mitchell, 1966).

Segundo, el uso de ese gradiente de protones por la ATP sintasa o complejo V para llevar a cabo la síntesis de ATP (Adenosin Trifosfato) (Mitchell, 1966).

#### 3.3.1 Composición en mamíferos

La cadena respiratoria de mamíferos llamada canónica, presenta cuatro complejos respiratorios, de los cuales sólo tres son bombas de protones (Wittig y Schägger, 2009) (Fig. 5):

El Complejo I o NADH:ubiquinona oxidoreductasa cataliza la reacción de

transferencia de electrones del NADH a la quinona. La estructura cristalográfica y una propuesta para el mecanismo por el cual este complejo bombea los protones acoplados a la transferencia de los electrones por las subunidades fue publicado recientemente (Baradaran y cols., 2013). Éste tiene una estequiometría de bombeo de cuatro protones por molécula de NADH oxidada (Brown y Brand, 1988).

El complejo II o succinato deshidrogenasa no está acoplado al bombeo de protones y sólo presenta un segundo punto de entrada para el complejo III y IV desde el ciclo de Krebs (Singer y cols., 1973).

El complejo III o ubiqüinol:citocromo c oxidorreductasa que cataliza la transferencia de electrones del ubiqüinol al citocromo. El estudio de este complejo llevó a la propuesta del ciclo Q que describe el mecanismo de acción por el cual una molécula de ubiqüinol es reducida totalmente para generar dos moléculas de citocromo c reducido y bombear cuatro protones (Trumpower, 1990).

El complejo IV o citocromo c oxidasa transfiere los electrones desde el citocromo c al oxígeno para formar agua y es el paso final para el bombeo de protones (Wikström, 1977). La regulación de esta bomba es interesante; al aumentar el potencial transmembranal y tener un flujo acelerado por la cadena sufre un fenómeno llamado *slipping* en el que cambia la estequiometría de bombeo de los protones (Murphy, 1989).

El complejo V o ATP sintasa está conformada por dos dominios. Uno soluble llamado F<sub>1</sub> y otro que está embebido en la membrana interna y es denominado F<sub>0</sub>. Por el dominio insoluble regresan los protones que fueron bombeados previamente por los otros complejos; esto ocasiona un cambio conformacional que se transmite a la parte soluble de la enzima, lo que conlleva a la formación de ATP a partir de ADP y H<sub>2</sub>PO<sub>4</sub><sup>-</sup> (Boyer, 1997).

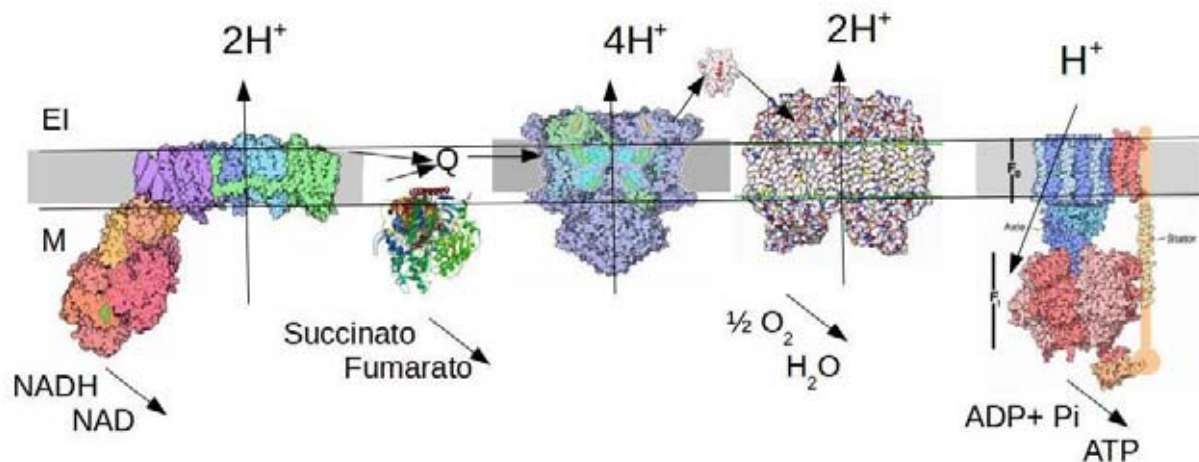


**Figura 5. Cadena respiratoria de mamíferos.** Se observan los cuatro complejos respiratorios llamados canónicos, a la ATP sintasa así como su disposición en la membrana interna, su sustrato y la estequiométría en el bombeo de protones. (CI) Baradaran y cols., 2013; CII) Sun y cols., 2005; CIII) Xia y cols., 1997; CIV) Michel y cols., 1998; y CV) Stock y cols., 1999).

### 3.3.2 Composición en *Saccharomyces cerevisiae*

*Saccharomyces cerevisiae* es conocida como la levadura del pan (Baker's yeast). Su taxonomía se presenta en la tabla 1 (Uniprot):

**Tabla 1.** Clasificación taxonómica de *Saccharomyces cerevisiae*

Dominio	Fungi
Filum	Ascomycota
Clase	Saccharomycetes
Orden	Saccharomycetales
Familia	Saccharomycetaceae
Género	<i>Saccharomyces</i>
Especie	<i>Cerevisiae</i>

Este es un organismo facultativo, ya que puede crecer con diferentes fuentes de energía (en algunos casos crecen en condiciones donde la mitocondria es poco o nada funcional) (Sherman, 2002) y es importante en diversos sectores, tales como: la industria cervecera y la alimenticia (para la producción de pan). También *S. cerevisiae* es importante como modelo de estudio, porque presenta ventajas prácticas: crece de forma rápida y a bajos costos; conserva rutas bioquímicas con otros organismos; su genoma está completamente secuenciado, y es fácil de manipular genéticamente, entre otras cosas (Sherman, 2002).

La fosforilación oxidativa de *Saccharomyces* difiere de la de mamíferos, pues sólo cuenta con los complejos II, III, IV y V. Además, esta levadura tiene tres NADH deshidrogenasas (que no bombean protones): una interna Ndip y dos externas, Ndep1 y Ndep2, que permiten la entrada de electrones desde el NADH, ya sea en el espacio intermembranal o en la matriz mitocondrial (Overkamp y cols., 2000) (Fig. 6).

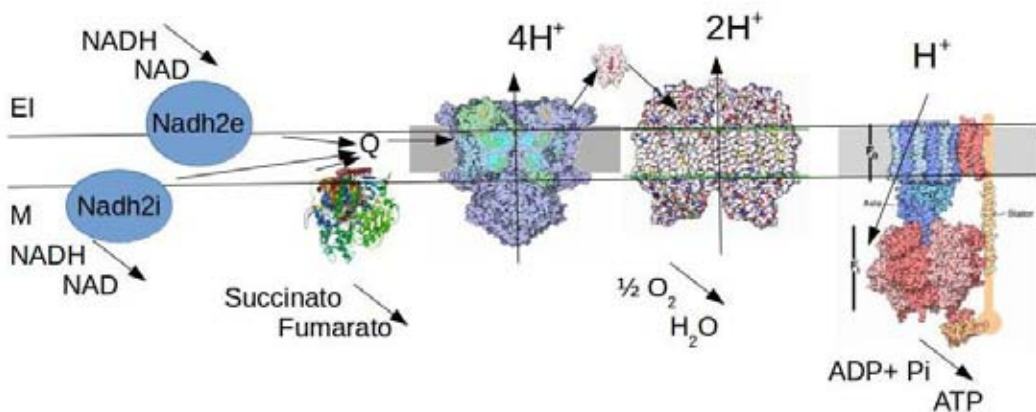


**Figura 6. Cadena Respiratoria de *S. cerevisiae*.** Se presenta la cadena respiratoria de *S. cerevisiae*, a diferencia de la de mamíferos, ésta no cuenta con complejo I y contiene múltiples deshidrogenasas alternas. (CII) Sun y cols., 2005; CIII) Xia y cols., 1997; CIV) Michel y cols., 1998; y CV) Stock y cols., 1999).

### 3.3.3 Regulación

La eficiencia de la fosforilación oxidativa varía mucho entre especies, línea celular, etc. Esta eficiencia se debe en gran medida al acoplamiento entre el potencial transmembranal formado por los complejos I, III y IV y su uso por la ATP sintasa para fosforilar ADP (Guerrero-Castillo y cols., 2011).

En trabajos previos en el laboratorio se han propuesto dos grandes mecanismos de desacoplamiento fisiológico (Guerrero-Castillo y cols., 2011) (Fig. 7):

El primero corresponde a enzimas redox que no bombean protones y que permiten la entrada —como es el caso de las NADH deshidrogenasas tipo II de *S. cerevisiae*— y la salida de electrones —como es el caso de la oxidasa alterna (AOX) de *Y. lypolitica*

(Guerrero-Castillo y cols., 2009) y *D. hansenii* (Cabrera-Orefice y cols., 2014) (Anexo 9.1).

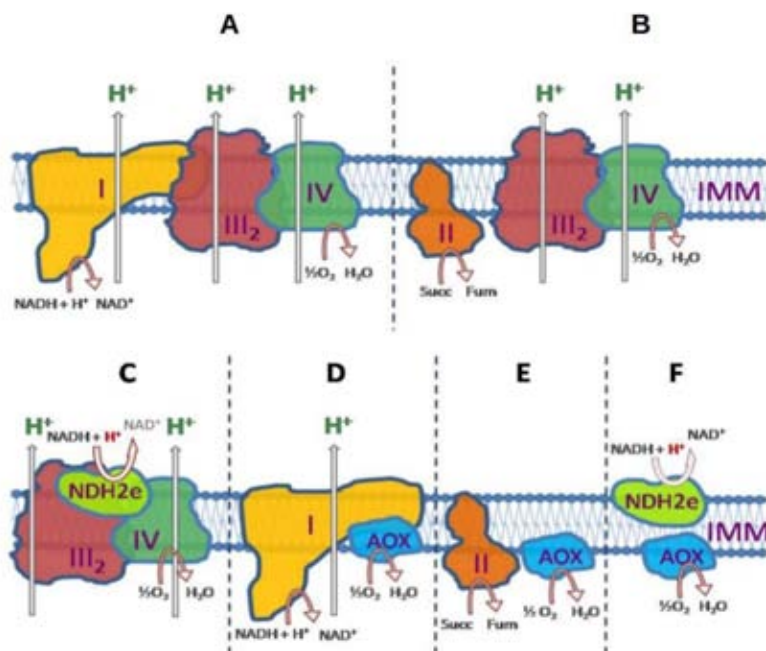


**Figura 7. Diferentes estequiométrias propuestas para el bombeo de protones en *Y. lypolitica*.**

A) El CI, CIII y CIV brindan un camino para el paso de electrones por la cadena con una estequiometría máxima de bombeo; B) el CII, CIII y CIV brindan un desacoplamiento parcial para la entrada de electrones desde la matriz, ya que el CII no bombea protones; C) la NDH2e, el CIII y CIV brindan un desacoplamiento parcial para la entrada de electrones a la cadena desde el espacio intermembranal; D) el CI y la AOX brindan un transporte de electrones desde la matriz con muy poco bombeo de protones; E y F) son ciclos fútiles en el transporte de electrones, ya que no tienen ningún bombeo de protones acoplado (Guerrero-Castillo y cols., 2011).

El segundo se refiere a los sumideros de protones (Fig. 8) como las enzimas desacoplantes (UCP; por sus siglas en inglés) y el canal inespecífico mitocondrial (MUC; por siglas en inglés) (Guerrero- Castillo y cols., 2011). En mamíferos existen varias isoformas de UCPs que tienen una expresión en tejidos específicos. La UCP3 ha sido

descrita en mitocondrias del tejido adiposo y se propone como una proteína que induce la termogénesis en mamíferos que hibernan (Palou y cols., 1998).

*S. cerevisiae* presenta un canal inespecífico (ScMUC) que se ha propuesto como el responsable de un mecanismo para detoxificar de iones a la mitocondria y regular la producción de ATP durante el ciclo celular (Bernardi y Petronilli, 1996).

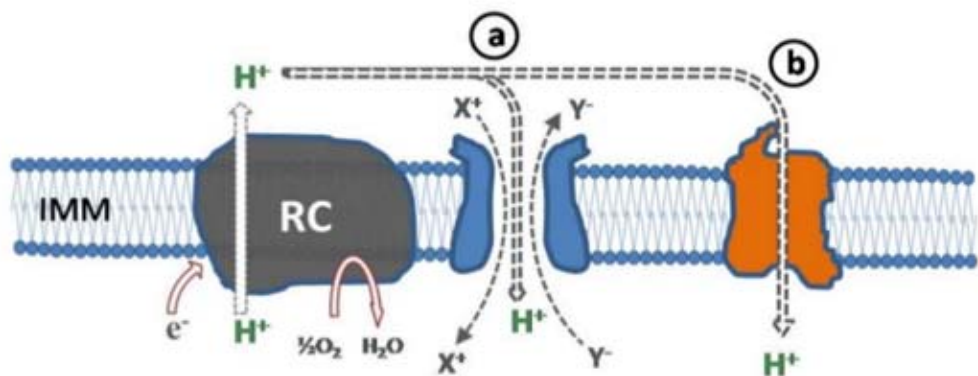


**Figura 8. Imagen de mecanismos de desacoplamiento inducidos por UCP's y MUC.** a) Esquema del MUC en donde se ejemplifica el regreso de protones a la matriz y la fuga de iones y metabolitos al espacio intermembranal; b) muestra una UCP y cómo facilita el regreso de protones a la matriz (Guerrero y cols., 2011).

### 3.4 La transición de la permeabilidad y el Canal Inespecífico Mitocondrial

La transición de la permeabilidad (PT) se define como un aumento en la permeabilidad de MIM a moléculas de hasta 1.5 KDa. Ésta es ocasionada por la apertura del canal inespecífico mitocondrial (MUC; por sus siglas en inglés) (Halestrap, 2009) que tiene como consecuencia: la pérdida del potencial transmembranal y la depleción de purín nucleótidos de la matriz. En condiciones *in vitro* es acompañada por hinchamiento, ruptura de la MOM,

liberación del citocromo c y de otras proteínas del espacio intermembranal (Crompton, 1999).

La función fisiológica del MUC no se ha logrado dilucidar. Sin embargo, se le han propuesto diferentes papeles como la señalización en muerte celular o la detoxificación de iones, y/o la regulación de la producción de ATP, aunque aún no se ha llegado a un consenso (Bernardi y cols., 2006).

### 3.4.1 Descubrimiento y función del MUC

Debido a que el estudio de las mitocondrias se ha desarrollado, en su gran mayoría, en condiciones *in vitro* y debido a que los procedimientos de aislamiento y almacenamiento buscan disminuir lo más posible la pérdida del acoplamiento entre el bombeo de protones y el uso por la ATP sintasa, la PT se consideró durante muchos años un artificio (Bernardi y cols., 2006).

El primero en describir el fenómeno fue Chateaubodeau (Chateaubodeau y cols., 1976), pero fue hasta que Haworth y su grupo mostró que una inducción con  $\text{Ca}^{2+}$  en mitocondrias de la corteza adrenal llevaba a que nucleótidos del citoplasma pudieran tener acceso a la matriz mitocondrial, que la PT se aceptó (Hunter y Haworth, 1979).

Otro descubrimiento trascendental para afianzar esta idea fue la desensibilización de la PT en mamíferos, por cantidades submicromolares de ciclosporina A (CsA) (Crompton y Costi, 1988). La CsA se une a la ciclofilina D (CyP-D) (peptidil-prolil isomerasa), presente en la matriz mitocondrial, en las mismas concentraciones en las que se bloquea la PT (Nicoll y cols., 1993). (Ver apartado CsA y CyP-D).

Hallazgos que reafirmaron la presencia de un canal inespecífico fueron los estudios electrofisiológicos que se desarrollaron con la mitocondria y en los cuales se mostró que en la membrana interna había un canal con una conductancia de 1 nS, el MMC (Mitochondrial Mega Channel; por sus siglas en inglés) que posee las mismas características del MUC (Szabó y Zoratti, 1992).

En los organismos en los que se ha estudiado el fenómeno de la transición de la permeabilidad, los moduladores del MUC pueden no ser los mismos y no tener el mismo efecto, lo que en un principio llevó a pensar que eran fenómenos que no tenían relación (Azzolin y cols., 2010). La visión que se tiene hoy en día es que la modulación del MUC parece haber evolucionado en respuesta a las condiciones de vida de cada especie (Bernardi y cols., 2006).

### 3.4.2 Efectores y composición

Entre los efectores del MUC se encuentran una amplia gama de factores y de compuestos químicos, tales como: el potencial transmembranal, el ATP y ADP (Haworth y Hunter, 2000), los cationes divalentes (Pérez-Vázquez y cols., 2003), el  $\text{H}_2\text{PO}_4^-$  (Cortés y cols., 2000), las especies reactivas de oxígeno (Kowaltowski y cols., 2000) y la ciclosporina A (Crompton y Costi, 1988). En la tabla 2 se presentan los efectores más importantes y su blanco.

<b>Tabla 2.</b> Efectores del MUC y blanco.		
K <sup>+</sup>	Abre: <i>ScMUC</i>	Cortés y cols., 2000.
H <sub>2</sub> PO <sub>4</sub> <sup>-</sup>	Cierra mMUC y <i>ScMUC</i>	Jung y cols., 1997. Gutiérrez-Aguilar y cols., 2010.
Ca <sup>2+</sup> , Mg <sup>2+</sup>	Cierra: <i>ScMUC</i> Abre: mMUC	Pérez-Vázquez y cols., 2003.
ADP	Cierra: <i>ScMUC</i> y mMUC	Haworth y Hunter, 2000.
ATP	Abre: <i>ScMUC</i> y mMUC	Haworth y Hunter, 2000.
CsA	Sólo tiene efecto sobre mMUC	Halestrap, 1989.
ROS	Abre mMUC	García y cols., 2005.
ΔΨ	↓ΔΨ Abre <i>ScMUC</i> ↑ΔΨ Abre mMUC	Szabó y cols., 1992.

En la tabla 2 sólo se exponen los reguladores del MUC más comunes y de interés para el trabajo. Para obtener mayor información de reguladores del MUC se refiere al lector a la siguiente revisión (Uribe-Carvajal y cols., 2011).

### 3.4.2.1 CsA y CyP-D

La ciclosporina A (CsA), un fármaco inmunosupresor utilizado ampliamente en trasplantes ya que inhibe la calcineurina, se une también a la CyP-D, una peptidil-prolil isomerasa presente en la matriz mitocondrial. Esto ocasiona una desensibilización (o inhibición) de la PT (Handschumacher y cols., 1984).

Las primeras indicaciones sobre el papel de CyP-D en la PT fueron propuestas por

el grupo de Halestrap, en donde se vio que el calcio desplaza a CsA de los sitios de unión de alta afinidad en mitocondrias de hígado de rata y que esto lleva a que las concentraciones de CsA necesarias para inhibir la PT sean mayores (Halestrap, 1989; Davidson y Halestrap, 1990).

Estudios en los que se desactivó el gen de CyP-D (Ppif) en ratón (Baines y cols., 2005; Basso y cols., 2005) mostraron la presencia de una PT con diferentes propiedades como: el aumento en la capacidad de retención de calcio (elevando el umbral para activar el mMUC) y la pérdida del efecto por CsA. Estos datos apuntan hacia un papel regulatorio de CyP-D, más que estructural.

Por otro lado, el grupo de Pfeiffer trabajando en *S. cerevisiae*, demostró que ésta presenta una PT que se regula de manera distinta a la de mamíferos, en algunos casos, los efectores tienen consecuencias opuestas pero se conserva la permeabilidad de la MIM a solutos de hasta 1.5 KDa (Jung y cols., 1997).

#### 3.4.2.2 ADP, ATP y el Transportador de Adenin Nucleótidos

La mitocondria requiere, para llevar a cabo la fosforilación oxidativa, del intercambio de ATP recién sintetizado en la matriz por ADP, que viene del metabolismo del citoplasma para ser fosforilado. El encargado de llevar a cabo esta función es el Transportador de Adenín Nucleótidos (ANT; por sus siglas en inglés) (Chappell, 1968). Éste pertenece a la familia de acarreadores mitocondriales (MCF; por sus siglas en inglés) (Bernardi y cols., 2006).

Hoy en día se cuenta con una estructura cristalográfica de 2.2 Å de resolución

(Pebay-Peyroula y cols., 2003) del ANT y se ha caracterizado su inhibición por atractilato y bongrekato (Schultheiss y Klingenberg, 1984).

Por estudios de microscopía se describió que el ANT forma, junto con el acarreador de fosfato y la ATP sintasa, un complejo llamado sintasoma que se ha propuesto para canalizar los sustratos necesarios para la síntesis de ATP (Cheng y cols., 2003).

La apertura del MUC es estimulada por el ATP, mientras que es inhibida por el ADP (Haworth y Hunter, 2000). Además, ligandos del transportador como el atractilato y el bongrekato tienen efectos sobre el MUC de mamíferos (mMUC) que en levaduras son opuestos (Uribe-Carvajal y cols., 2011).

Fue hasta que se demostró en mitocondrias, en las que no se contaba con ninguna de las isoformas del ANT que la PT seguía ocurriendo aunque se perdía la regulación por bongrekato y atractilato, y que se descartó la idea del ANT como componente estructural (Kokoszka y cols., 2004).

Se ha propuesto que gran parte de los efectores del MUC coinciden en que generan alteraciones en el potencial transmembranal y que esto ocasiona la apertura del MUC. En el caso del atractilato y bongrekato se ha planteado que variaciones en las cargas de los fosfolípidos derivadas del cambio de conformación del ANT es lo que provoca la apertura o cierre del MUC (Bernardi y cols., 2006).

### 3.4.2.3 El VDAC

El canal aniónico dependiente de voltaje (VDAC) es la proteína más abundante en la MOM y regula el paso de gran parte de iones y sustratos que se necesitan en el espacio

intermembranal (Colombini, 2004).

Dentro de las mitocondrias existen sitios de contacto entre la MIM y la MOM, en éstos la concentración de proteínas como el ANT, VDAC y hexocinasa es mayor. Se ha propuesto que en estos “sitios de contacto” puede darse una interacción entre la ANT, el VDAC y otras enzimas del citoplasma (Brenner y Grimm, 2006).

Se ha propuesto la participación del VDAC en la PT debido a la posibilidad de formar un mega canal con propiedades similares a las de MUC (regulado por NADH, Ca<sup>2+</sup>, glutamato) cuando es reconstituido en bicapas de fosfolípidos (Szabó y cols., 1993).

El VDAC presenta tres isoformas en modelos murinos de laboratorio (Szabó y cols., 1993). El estudio de esta proteína por medio de mutantes en ratones ha sido complicada, ya que se piensa que cualquiera de las tres isoformas puede sustituir la función de la otra y al mutar las tres se ha visto que ocasiona letalidad (Cheng y cols., 2003).

Todos los datos que apuntan a la participación del VDAC en la formación del MUC no brindan pruebas que permitan concluir qué papel juega el VDAC, ya que hablan sobre la posibilidad de formar canales con propiedades similares, pero ninguno ha visto la participación fisiológica del VDAC en la PT. Además, cada componente que se proponga debe ser cuestionado qué tan necesario es para que ocurra la PT (Bernardi y cols., 2006).

En reportes recientes se ha descrito la posibilidad de regulación del VDAC por su estado de fosforilación y el potencial transmembranal (Sheldon y cols., 2011). Esto es de relevancia, ya que si el VDAC se encuentra en una conformación cerrada, el paso de ATP, ADP y cationes hacia la membrana interna es casi nulo lo que promueve una PT, mientras que si está abierto estos pueden cruzar libremente hasta el espacio intermembranal. La posibilidad de que exista un canal que atraviese ambas membranas sigue abierta.

### 3.4.2.4 PiC y H<sub>2</sub>PO<sub>4</sub><sup>-</sup>

Para realizar la síntesis de ATP es necesario de fosfato inorgánico (H<sub>2</sub>PO<sub>4</sub><sup>-</sup>). El encargado de transportarlo a la mitocondria es el acarreador de fosfato (PiC; por sus siglas en inglés); que al igual que el ANT pertenece a la MCF (Bernardi y cols., 2006). Este acarreador presenta un mecanismo de antiporte H<sub>2</sub>PO<sub>4</sub><sup>-</sup>/OH<sup>-</sup> que permite la entrada de fosfato a la matriz en donde participa en la síntesis del ATP (Stappen y Krämer, 1994).

El papel del PiC en la PT comenzó a evaluarse cuando se vio que el efecto de la ciclosporina A era dependiente de la concentración de H<sub>2</sub>PO<sub>4</sub><sup>-</sup>. En columnas de afinidad, con mitocondrias de mamíferos, se vio que la ciclofilina D se une al acarreador de fosfato (Leung y cols., 2008).

Aunado a esto se ha propuesto una posible interacción entre el ANT, el PiC y el complejo V, el sintasoma (Chen y cols., 2004).

En estudios de mitocondrias donde se eliminó el gen del acarreador de fosfato hubo diversas consecuencias, entre éstas: la pérdida de regulación por mersalil (inhibidor específico del acarreador del PiC), además de una disminución en el tamaño del MUC (Gutiérrez-Aguilar y cols., 2010).

#### 3.4.2.5 ATP sintasa

La regulación por ATP y ADP de la PT fue descrita por Haworth y Hunter (2000). Para abril de 2013, el grupo de Bernardi mostró que una de las subunidades del dominio F<sub>0</sub> de la ATP sintasa participa en la formación del MUC (Giorgio y cols., 2013). En este trabajo propusieron que la estructura del MUC consiste en dímeros de la ATP sintasa. Aunado a esto, la idea del sintasoma y la disminución del tamaño del MUC en levaduras sin PiC (Gutiérrez-Aguilar y cols., 2010) muestran que el MUC está formado por este grupo de proteínas.

Otro dato interesante es la participación de la ATP sintasa en la formación de las crestas mitocondriales, en donde se ha visto que mutaciones en ciertas subunidades que son necesarias para la oligomerización, ocasionan una pérdida de las crestas y cambios en la morfología de la membrana interna mitocondrial. Todo parece apuntar que la ATP sintasa forma parte de la estructura de esta mega canal (Paumard y cols., 2002).

#### 3.4.2.6 Efecto de cationes

En un artículo publicado hace algunos años se vio que el efecto de cationes como el Mg<sup>2+</sup> o el Ca<sup>2+</sup> sobre el MUC de *S. cerevisiae* era dependiente de la concentración de H<sub>2</sub>PO<sub>4</sub><sup>-</sup> (Pérez-Vázquez y cols., 2003). La modulación por iones se propuso como un mecanismo regulatorio de la producción de energía, funcionando como una válvula que permanece cerrada en momentos de alta demanda energética y que se abre en períodos de baja demanda energética, para disipar el gradiente y evitar la formación de ROS (especies

reactivas de oxígeno; por sus siglas en inglés) en levaduras (Guerrero-Castillo y cols., 2011). En mamíferos ocurre el fenómeno contrario, en donde el aumento de las concentraciones citosólicas lleva a una apertura del MUC y si esta apertura es prolongada ocasiona muerte celular (Honda y cols., 2005). Una de las diferencias es que en mamíferos las mitocondrias cuentan con un transportador de calcio (Gunter y Pfeiffer, 1990), mientras que en *S. cerevisiae* éste no se encuentra.

En *S. cerevisiae* el  $\text{H}_2\text{PO}_4^-$  se acumula en condiciones donde hay un gasto de energía utilizado para la producción de biomasa. A su vez, el  $\text{Ca}^{2+}$  controla el ciclo celular, aumentando la concentración citosólica en momentos de alta demanda energética, lo que corresponde al cierre del MUC (Pringle y Hartwell, 1981).

Tomando en cuenta los datos descritos se propone que la transición de la permeabilidad podría ser un mecanismo de desacoplamiento fisiológico y por lo tanto, reversible. Los resultados obtenidos en esta tesis indican que se puede abrir y cerrar alternativamente el MUC mediante la adición de  $\text{Ca}^{2+}$  y EGTA o bien  $\text{Mg}^{2+}$  y EDTA. También se evaluaron las condiciones de apertura a distintas concentraciones de estos iones en busca de aperturas parciales.



## 4. HIPÓTESIS Y OBJETIVOS

### 4.1 Hipótesis:

La apertura del MUC y la transición de la permeabilidad forman parte de un evento reversible, de regulación de la cadena respiratoria, que evita la producción de ROS.

### 4.2 Objetivos:

- Evaluar la reversibilidad de la apertura y cierre del MUC ocasionada por  $\text{Ca}^{2+}$  o  $\text{Mg}^{2+}$ .
- Evaluar si existen estados de apertura parcial del MUC a diferentes concentraciones de Pi inorgánico y/o  $\text{Ca}^{2+}$ .
- Evaluar la producción de ROS en condiciones del MUC abierto o cerrado.



## 5. MATERIALES Y MÉTODOS

### 5.1 Material

Todos los compuestos utilizados fueron de grado reactivo analítico. El CaCl<sub>2</sub>, MES, manitol, MgCl<sub>2</sub>, albúmina sérica y safranina-o fueron de Sigma-Aldrich, Co.

La cepa auxotrófica de *S. cerevisiae* utilizada fue donada por el Dr. Fred Sherman de la Universidad de Rochester, EUA.

Las características genéticas de las cepas de *S. cerevisiae* utilizadas son:

- Cepa Industrial: La Azteca (adquirida periódicamente en una panadería ubicada en 19°19'22.00"N 99°09'31.34"W).
- Cepas Auxotróficas: B-7553: MATa CYC1+ cyc7-738:CYH2 ura3-52 his3-Δ1 leu2-3, 112trp1 289cyh2

### 5.2 Cultivo de levaduras

La cepa usada fue resembrada periódicamente en medio sólido YPD (extracto de levadura 1%, peptona de gelatina 2%, dextrosa 2% y agar 2%). De aquí se inoculó una asada en un matraz con 50 mL de precultivo YPD líquido (extracto de levadura 1%, peptona de gelatina 2% y dextrosa 2%) y se incubó a 30°C durante 24 hrs. Los 50 mL se inocularon en matraces con 1 L de medio YPD (extracto de levadura 1%, peptona de gelatina 1%, glucosa al 2%) a 30°C durante 24 hrs. con agitación constante para las cepas del marco B-7553. |

Para los estudios que utilizaron levaduras de la cepa industrial fue necesario cultivar

a las células durante 8 hrs. en medio rico (De Klöet y cols., 1961), lavarlas dos veces con agua destilada y ayunar a las células durante 16 hrs. previas a la obtención de mitocondrias (Pérez-Vázquez y cols., 2003).

### 5.3 Aislamiento de mitocondrias

Se llevó a cabo por el método mecánico (Peña y cols., 1977). Una vez obtenido alrededor de 2 L de cultivo, se cosecharon las células, lavándolas tres veces por centrifugación en un rotor Beckman a 3500 rpm por 5 min. Después de la última centrifugación se determinó el peso seco de las células para mantener igualdad de condiciones durante el aislamiento de las mitocondrias (Guérin y cols., 1990). Las células fueron resuspendidas al 50% W/V en el amortiguador de MES 5mM, manitol 0.6 M y albumina al 1%, y se incubaron durante 15 min a 4°C en agitación. Al terminar la incubación se rompieron con perlas de vidrio de 1 mm en un fraccionador Rib. Una vez lavadas las células homogenizadas, se realizó una centrifugación diferencial:

- 3000 rpm por 5 min, se toma el sobrenadante.
- 9500 rpm por 10 min tomar el precipitado y se homogeniza con un pincel con medio MES 5mM, manitol 0.6 M, albumina 1%.
- 5000 rpm por 5 min, se toma el sobrenadante.
- 12000 rpm 10 min, el precipitado se homogeneiza con un pincel con medio de MES 5mM, manitol 0.6 M.
- Se coloca la muestra en hielo.

#### 5.4 Determinación de proteína

La concentración de proteínas mitocondriales fue determinada por medio del método de Gornal o biuret utilizando albúmina sérica bovina como estándar (Gornall y cols., 1949).

#### 5.5 Función mitocondrial

Las mitocondrias utilizadas en este estudio mostraron alto cociente respiratorio y/o U/4, capacidad para sintetizar ATP y un  $\Delta\Psi$  estable (ver los experimentos control en cada inciso de los resultados).

Una característica común del ScMUC tanto en las cepas industriales como en las cepas de laboratorio, es la posibilidad del Pi de regular su apertura (Gutiérrez-Aguilar y cols., 2010). En todas las cepas en que se ha medido el efecto del Pi hasta la fecha, se ha observado que: a bajas concentraciones de Pi el ScMUC permanece abierto, mientras que a 2 mM y arriba de esta concentración, el ScMUC se cierra. En las cepas de *S. cerevisiae* usadas en este estudio, se observó que las mitocondrias resuspendidas en un soporte isoosmótico y en presencia de 4 mM Pi, no presentan hinchamiento mitocondrial. En otras palabras, el ScMUC está cerrado en esas condiciones, mientras que a 0.4 mM Pi el ScMUC está abierto.

#### 5.6 Consumo de oxígeno

En mitocondrias recién aisladas se midió la velocidad de consumo de oxígeno en dos

estados: Estado 4 y Estado desacoplado (Estado U) (Fig. 9, ver más adelante). Se usó un oxímetro YSI 5300 equipado con un electrodo de Clark, acoplado a un registrador analógico que contaba con una cámara de 3 mL con camisa de agua recirculante en baño a 30°C, utilizando una concentración final de mitocondrias de 0.5 mg/mL (Estabrook, 1967). El medio de reacción fue manitol 0.6 M, MES 5 mM, pH 6.8 ajustado con TEA y 10 µL/mL de etanol como sustrato respiratorio.

El consumo de oxígeno por la cadena respiratoria está regulado principalmente por el potencial transmembranal. Cuando el potencial transmembranal es elevado, el consumo de oxígeno es lento. A esta condición se le conoce como estado de reposo de la cadena respiratoria y se le llama Estado 4. Cuando se abate el potencial transmembranal, la cadena respiratoria aumenta su actividad y se acelera el consumo de oxígeno. Un mecanismo de abatimiento del potencial transmembranal es la fuga controlada de H<sup>+</sup> hacia el interior de la matriz a través de la F<sub>1</sub>F<sub>0</sub> ATP sintasa, hecho que ocurre durante la síntesis de ATP. Éste es el Estado fosforilante o Estado 3. En el Estado desacoplado (*uncoupled*) la caída de ΔΨ se da por la fuga de H<sup>+</sup> mediada por un protonóforo. La diferencia entre el Estado 4 y los estados acelerados indica que la mitocondria es capaz de sostener un potencial transmembranal adecuado y de reaccionar a la pérdida de ese potencial. Por ello una medida de integridad mitocondrial es el cociente U/4 o Edo. 3 /Edo. 4. Esta medida es adimensional y sólo constituye un indicador de la eficiencia de la fosforilación oxidativa en las mitocondrias aisladas (Nicholls y Ferguson, 2002).

En este protocolo se decidió utilizar el agente desacoplante FCCP en vez de ADP, que interfiere con la regulación del MUC. Así, se midió un cociente U/4 que se calculó dividiendo la actividad respiratoria del Estado U sobre la del Estado 4. Estrictamente

hablando, éste no es un control respiratorio, ya que no se evalúa la fosforilación oxidativa (respiración acoplada a la síntesis de ATP) sino la capacidad respiratoria en ausencia o presencia de un desacoplante.

### 5.7 Potencial transmembranal

El potencial transmembranal fue determinado en un espectrofotómetro de doble haz en modo dual (511-533 nm), utilizando anaranjado de safranina como cromóforo y su incorporación a las membranas energizadas. El espectrofotómetro de doble haz en modo dual se usa para medir los cambios de absorbancia específicos que sufren ciertas sustancias. Por lo general, se usan dos longitudes de onda: una donde se observa un cambio máximo y otra en la que no se distinguen cambios y que corresponde al punto isosbéstico. La safranina-o es un catión hidrofílico que tiene un punto de cambio máximo de absorbancia en respuesta a la polaridad del medio a 511 nm y un isosbéstico a 533 nm. Por ello, la safranina-o es atraída hacia la membrana proporcionalmente al potencial transmembranal, cambiando su absorbancia a 511 nm. Cualquier cambio inespecífico dado por difracción de la luz que incida en las mitocondrias, turbidez u otros factores es detectado a 533 nm y restado del valor registrado a 511 nm. Para promover el colapso del potencial se añadió FCCP 1 mM (Åkerman y Wikström, 1976).

## 5.8 Hinchamiento y contracción mitocondrial

Las mitocondrias se comportan como osmómetros, es decir, cuando aumenta la concentración de solutos en su interior captan agua para compensar el aumento en la presión osmótica y viceversa: Si pierden osmolitos, exportan agua y se contraen. Ópticamente, el hinchamiento-deshinchamiento mitocondrial puede seguirse porque la mitocondria hinchada se vuelve transparente y la turbidez de la suspensión decrece (Kaasik y cols., 2007).

Se ha reportado que con compuestos de polietilen glicol (PEG) de 1.5 KDa se obstruye el MUC y ocasiona una recontracción. Existen PEG's de diferentes tamaños que van desde 0.4 KDa a 1.5 KDa, lo que permite evaluar la posibilidad de una apertura parcial (Jung y cols., 1997).

El hinchamiento mitocondrial fue evaluado monitoreando el cambio en la absorbancia a 540 nm en un espectrofotómetro Aminco DW2000 en modo “split”. Se utilizó una celda de cuarzo de 2 mL y se adicionó amortiguador de manitol 0.6 M, MES 5 mM, pH 6.8 (TEA). El sustrato respiratorio fue etanol 5 $\mu$ L/mL.

## 5.9 Producción de especies reactivas de oxígeno

Para medir la producción de especies reactivas se utilizó un sistema comercial proporcionado por Life Technology, de Amplex Red. Este compuesto sufre un cambio de color al ser oxidado por peróxido de hidrógeno, lo que permite observar la producción de especies reactivas (Reszka y cols., 2005).

La producción de especies reactivas fue evaluada monitoreando el cambio en la absorbancia a 600 nm en un lector de placas POLARstar Omega multifuncional (fluorómetro, espectrofotómetro, etc.). Se utilizaron placas oscuras de 8X12 y se adicionó amortiguador de manitol 0.6 M, MES 5 mM, pH 6.8 (TEA). Las condiciones para los ensayos fueron; como sustrato respiratorio etanol 5 $\mu$ L/mL o NADH y lo indicado en las figuras.



## 6. RESULTADOS

En un estudio previo en el laboratorio se demostró que la fosforilación oxidativa es regulada por  $K^+$  y  $H_2PO_4^-$  a través del MUC (Castrejón y cols., 2002). Al titular con diferentes concentraciones de  $K^+$ , y evaluar la repercusiones en la síntesis de ATP y el volumen mitocondrial, notaron que los efectos disminuían al aumentar la concentración de Pi (Cortés y cols., 2000). En otro trabajo reportaron el efecto de cationes divalentes sobre la mitocondria, demostrando que estos actúan de forma sinérgica para desencadenar reacciones a concentraciones fisiológicas en experimentos *in vitro* (Pérez-Vazquéz y cols., 2003).

La propuesta de este estudio fue evaluar la posibilidad de que el  $H_2PO_4^-$ ,  $Ca^{2+}$  y  $Mg^{2+}$  ocasionasen la apertura o cierre del MUC en relación a los requerimientos energéticos y del ciclo celular. Este mecanismo funciona como una válvula que libera la fuerza protón-motriz, evitando así la formación de ROS por saturación de la cadena y regulando la síntesis de ATP de acuerdo a las demandas energéticas celulares.

A continuación se presentan los datos obtenidos de pruebas funcionales mitocondriales como oximetrías, pruebas de potencial transmembranal, hinchamiento mitocondrial y formación de ROS por parte de la cadena transportadora de electrones y el papel que juega el  $H_2PO_4^-$ ,  $Ca^{2+}$  y  $Mg^{2+}$  en la apertura o cierre del MUC.

### 6.1 Consumo de oxígeno

El consumo de oxígeno, como se explicó en el apartado 3 “Materiales y Métodos”, se

utiliza para obtener una medida adimensional denominada cociente respiratorio (CR). El CR o estado U/3 llega a variar dependiendo de múltiples factores como: protonóforos como el CCCP o FCCP, ADP, pH, etcétera.

Cuando el CR tiene valores cercanos a dos en levaduras como *S. cerevisiae*, se habla de que existe acoplamiento entre el consumo de oxígeno y la formación de un potencial transmembranal (Gutiérrez-Aguilar y cols., 2010). Un CR cercano a 1 indica que no se está estableciendo un potencial; esto se puede deber a daños en la membrana interna durante el aislamiento de las mitocondrias o que existen proteínas desacoplantes o que el MUC se encuentren abierto.

En la Fig. 9A, en el eje de las abscisas, se muestran diferentes concentraciones de  $\text{H}_2\text{PO}_4^-$  (éstas son 0 M a 1 mM) y de  $\text{Ca}^{2+}$  (desde 0 M hasta 1 M). En el eje de las ordenadas se observa un aumento progresivo en el consumo de oxígeno mientras aumenta la concentración de  $\text{H}_2\text{PO}_4^-$  y  $\text{Ca}^{2+}$ . Es claro el efecto del Pi sobre la respiración, ya que al ir incrementando las concentraciones se eleva el CR (columnas azules). Al adicionar simultáneamente calcio y Pi se vio un mayor efecto (líneas verdes) alcanzando valores superiores a 2 desde concentraciones de 1 mM de Pi y 0.6 mM de calcio (líneas amarillas y rojas). En la Fig. 9B se muestra un trazo donde se agregó, además de lo anterior, 0.5 mM de  $\text{Mg}^{2+}$ . A diferencia de la Fig. 9A, el CR llegó a un máximo a 0.5 mM de  $\text{Ca}^{2+}$ , 0.6 mM de  $\text{H}_2\text{PO}_4^-$  y 0.5 mM de  $\text{Mg}^{2+}$  (columnas amarillas).

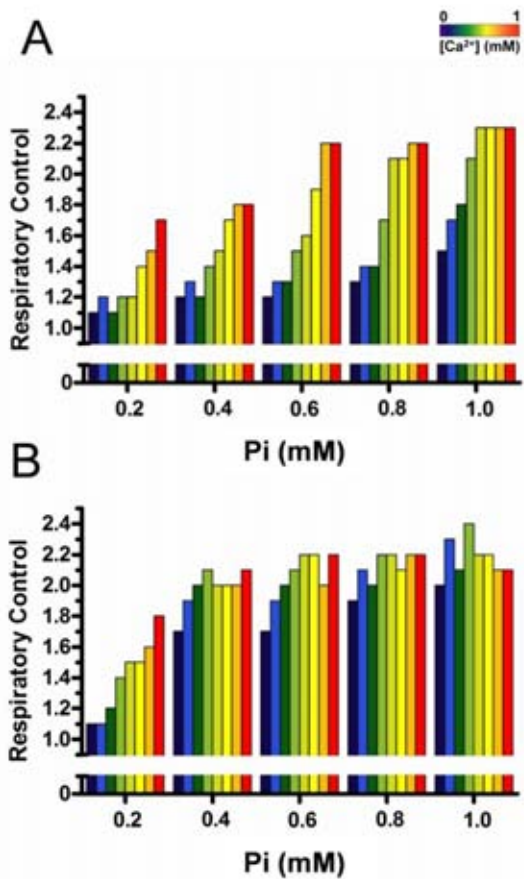


**Figura 9. Efecto Sinérgico de iones sobre el Cociente Respiratorio.** Los experimentos fueron realizados en amortiguador de respiración (5mM MES, 0.6 M manitol) sin  $Mg^{2+}$ , además de las concentraciones de iones indicadas. La gráfica A corresponde a una titulación calcio: 0 M (morado), 50 mM (azul), 0.3 mM (verde oscuro), 0.45 mM (verde claro), 0.6 mM (amarillo-verde), 0.75 mM (amarillo brillante), 0.9 mM (naranja), 1 mM (rojo). A diferentes concentraciones de Pi (0.2 mM, 0.4 mM, 0.6 mM, 0.8 mM y 1 M). La gráfica B contiene además 0.5 mM de  $Mg^{2+}$ .

El  $Ca^{2+}$ ,  $Mg^{2+}$  y  $H_2PO_4^-$  muestran un efecto sinérgico en el acoplamiento mitocondrial.

## 6.2 Potencial transmembranal

Otra medida que es importante para establecer el papel sobre la fosforilación oxidativa y el efecto de alguna sustancia sobre el MUC es su papel sobre el potencial transmembranal. El potencial transmembranal es un indicador de la capacidad de la mitocondria para generar y mantener una diferencia de iones entre un lado y otro de la membrana interna, así como ser un marcador de funcionalidad de la cadena respiratoria (Szabó y cols., 1992).

En la Fig. 10 se evaluó el efecto del  $\text{Ca}^{2+}$ ,  $\text{Mg}^{2+}$  y  $\text{H}_2\text{PO}_4^-$  sobre el potencial transmembranal en las mismas condiciones que en la Fig. 9. Ésta muestra el efecto de diferentes concentraciones de Pi (de 0 M a 1 mM) y  $\text{Ca}^{2+}$  (de 0 a 1 mM) y los valores del potencial transmembranal ( $\Delta\Psi$ ) que se alcanzaron en miliVolts (mV). A concentraciones mayores de 0.4 mM de  $\text{H}_2\text{PO}_4^-$  y 1 mM de  $\text{Ca}^{2+}$  se observa una saturación en el potencial con un máximo de 140 mV. La fig. 10B presenta un experimento similar adicionando 0.5 mM de  $\text{Mg}^{2+}$ . Se puede observar que la saturación en el  $\Delta\Psi$  se presenta a menores concentraciones de  $\text{H}_2\text{PO}_4^-$  (0.4mM) y  $\text{Ca}^{2+}$  (0.75 mM).

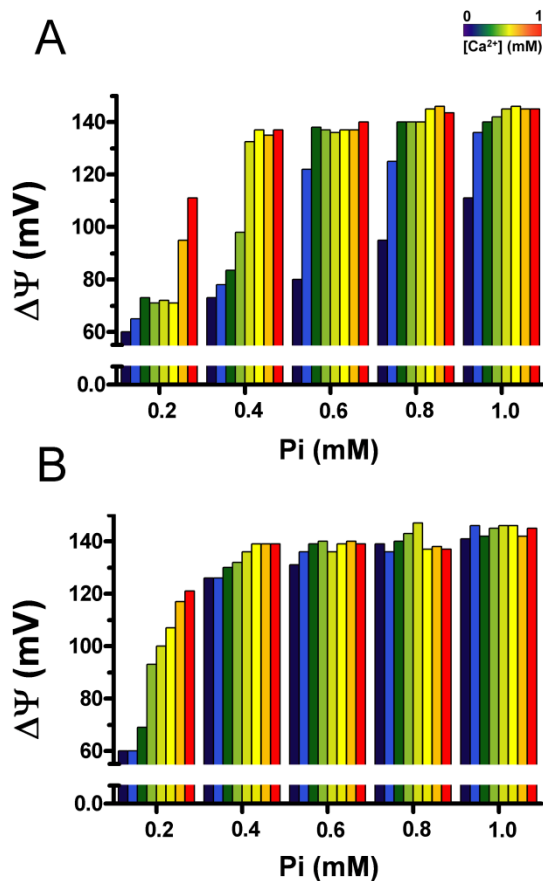


**Figura 10. Efecto Sinérgico de iones sobre el potencial transmembranal.** Los experimentos se realizaron como en la figura 9 adicionando safranina como marcador. La gráfica A corresponde a una titulación con calcio: 0 M (morado), 50 mM (azul), 0.3 mM (verde oscuro), 0.45 mM (verde claro), 0.6 mM (amarillo-verde), 0.75 mM (amarillo brillante), 0.9 mM (naranja), 1 mM (rojo). A diferentes concentraciones de Pi (0.2 mM, 0.4 mM, 0.6 mM, 0.8 mM y 1 M). A la gráfica B se le adicionó además 0.5 mM de  $Mg^{2+}$ .

El efecto del  $Ca^{2+}$ ,  $Mg^{2+}$  y  $H_2PO_4^-$  concuerda con la visión de un mecanismo de regulación mediado por iones al igual que se observó en el consumo de oxígeno.

Otro fenómeno que nos interesaba evaluar del potencial transmembranal era si la apertura del MUC podía estar regulada por  $Ca^{2+}$  y  $Mg^{2+}$  de una forma dinámica (que se

abriera, se cerrara y se volviera a abrir en una misma muestra). Durante mucho tiempo se creyó, ya que el estudio se hacía en mitocondrias de mamíferos, que la PT estaba relacionada con muerte celular accidental (Bernardi y cols., 2006). Hoy en día esta visión ha cambiado y aunque aún no es clara su función, otras propuestas han aparecido (Halestrap, 2009).

Para esto se evaluó en la Fig. 11A el efecto de dos pulsos de  $\text{Ca}^{2+}$  (0.3 mM) a bajas concentraciones de  $\text{H}_2\text{PO}_4^-$  (0.4 mM) seguido por la adición de un agente quelante, en este caso EGTA a 0.3 mM. Se pudo observar que al dar el primer pulso con calcio hay un aumento en el potencial transmembranal, que es abatido al incorporar un pulso de EGTA 0.3 mM (trazo azul). Para comprobar la hipótesis de que el MUC tiene la capacidad de abrir y cerrarse de forma regulada y que su apertura, más que ser accidental, es un mecanismo de regulación de la cadena, se decidió dar un segundo pulso de 0.3 mM de  $\text{Ca}^{2+}$  que ocasionó un restablecimiento del potencial semejante al que se obtuvo en el primer pulso y que es abatible de nuevo con un pulso 0.3 mM de EGTA (trazo azul).

En la Fig. 11B en vez de usar dos pulsos de  $\text{Ca}^{2+}$ , se utilizarón dos pulsos de  $\text{Mg}^{2+}$  (trazo naranja), para ver si éste era un fenómeno en común para los iones divalentes. Como se puede observar, al dar el primer pulso de 0.3 mM de  $\text{Mg}^{2+}$  hay un aumento en los valores del potencial transmembranal que se abaten al incorporar EDTA (a 0.3mM), un agente quelante preferente del  $\text{Mg}^{2+}$ . Al dar el segundo pulso de 0.3 mM de  $\text{Mg}^{2+}$  se vio un restablecimiento parcial del potencial que se abatió de nuevo con 0.3 mM de EDTA (trazo naranja).

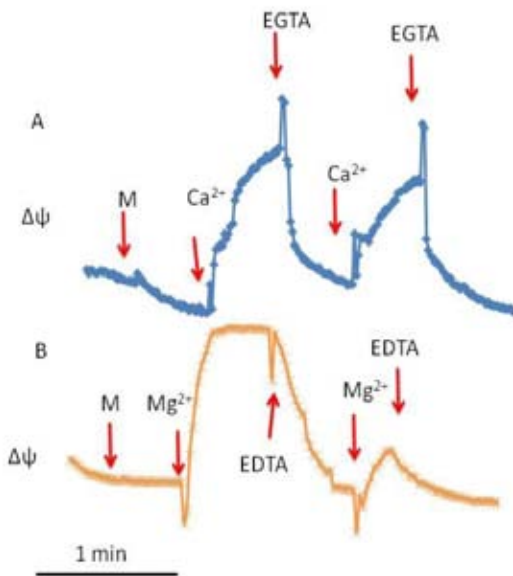


**Figura 11. Apertura dinámica del ScMUC por cationes divalentes.** El potencial transmembranal fue medido como en la figura 10 a 0.4 mM de Pi. En el trazo “A” se utilizó 0.3mM de  $\text{Ca}^{2+}$  y 0.3 mM de EGTA; en la “B” 0.3 mM de  $\text{Mg}^{2+}$  y EDTA.

El  $\text{Mg}^{2+}$  generó un efecto similar al del  $\text{Ca}^{2+}$  durante el primer pulso. En cambio al administrar un segundo pulso había un efecto en el restablecimiento del potencial aunque menor que con el  $\text{Ca}^{2+}$ . Se cree que esto se puede deber a que el  $\text{Mg}^{2+}$  sí se transporta al interior de la mitocondria en *S. cerevisiae* a diferencia del  $\text{Ca}^{2+}$ .

### 6.3 Hinchamiento y recontracción mitocondrial

Otro aspecto que era importante evaluar era el hinchamiento mitocondrial, ya que éste es un marcador de apertura del MUC al generar un desequilibrio osmótico con KCl.

El hinchamiento mitocondrial se midió a bajas concentraciones de Pi (0.4 mM) y fue ocasionado por la adición de 40 mM de KCl. Sin la presencia de algun ión, hay un hinchamiento considerable (Fig. 12, trazo naranja). El hinchamiento disminuye conforme aumentan las concentraciones de ambos iones, como se puede ver en la Fig. 12.

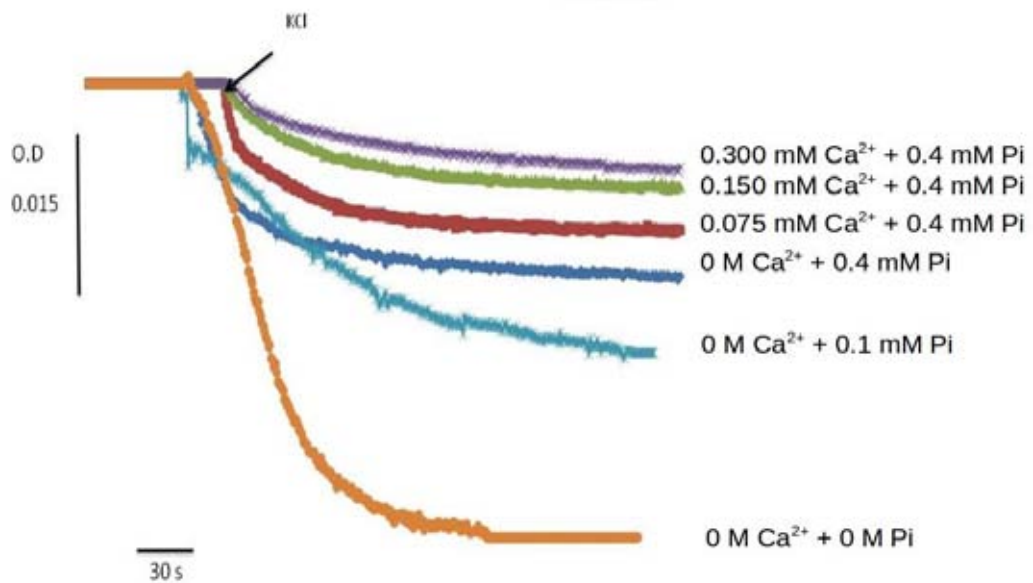


**Figura 12. Hinchamiento mitocondrial como medida de la apertura del ScMUC en respuesta a iones.** El hinchamiento se midió en una solución 5mM de MES, 0.3 M de manitol, 0.4 mM de Pi adicionando KCl donde se indica además Ca<sup>2+</sup> en la siguientes concentraciones: 0.3 mM (morado), 0.15 mM (verde), 0.075 mM (rojo), 0 M (azul oscuro). El trazo azul claro: 0 M Ca<sup>2+</sup>, 0.1 mM Pi; y naranja: 0 M Ca<sup>2+</sup>, 0 M Pi.

Otro fenómeno que nos interesaba explorar era la posibilidad de que el MUC presentara diferentes estados de apertura con diferentes diámetros. En la Fig. 13 se puede ver el hinchamiento en la ausencia de estos iones. La recontracción fue ocasionada con polietilenglicol (PEG) de diferentes pesos moleculares (0.4 KDa, 0.6 KDa, 1 KDa y 1.5 KDa). La Fig. 13 corresponde 0 M  $\text{Ca}^{2+}$ , 0 M Pi; el trazo verde: 1.5 KDa, el rojo: 1 KDa, el azul oscuro: 0.6 KDa, el azul claro: 0.4 KDa.

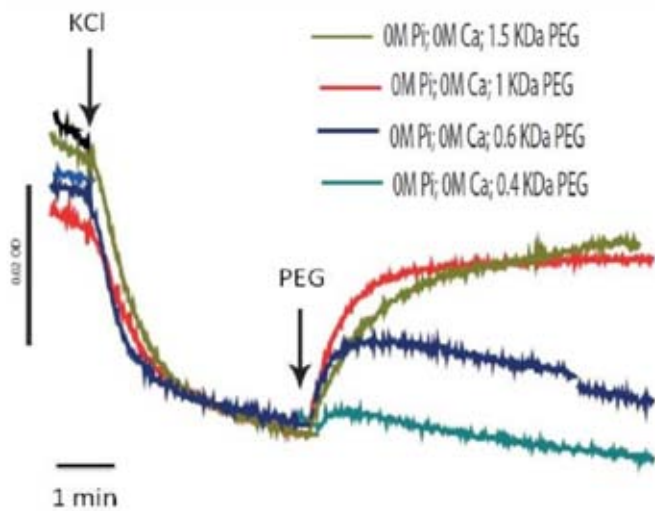
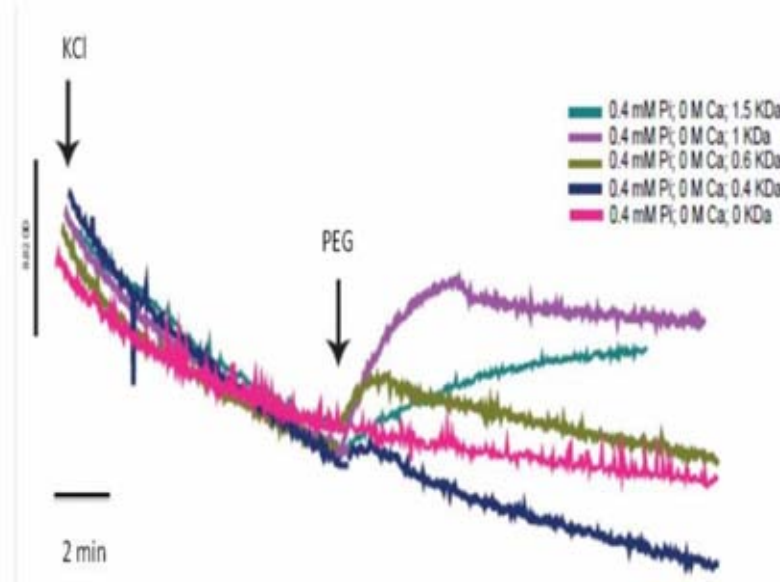


**Figura 13. Hinchamiento-Recontracción I.** Los experimentos se realizaron en las mismas condiciones que en las que se muestran en la Fig. 12 con las concentraciones de  $\text{Ca}^{2+}$  y Pi. El hinchamiento se provocó con KCl y la recontracción con PEG's de distintos tamaños: 0 M  $\text{Ca}^{2+}$ , 0 M Pi: 1.5 KDa (verde), 1 KDa (rojo), 0.6 KDa (azul oscuro), 0.4 KDa (azul).

En la búsqueda de una condición donde la recontracción fuera parcial titulamos con

diferentes concentraciones de  $\text{H}_2\text{PO}_4^-$  y  $\text{Ca}^{2+}$  y se recontrajo con PEG's de diferentes tamaños. La Fig. 14 presenta la condición de 0 M de  $\text{Ca}^{2+}$ , 0.4 mM de Pi. Los trazos



muestran la recontracción ocasionada por PEG. El trazo azul muestra la condición con 1.5 KDa, el morado con 1 KDa, el verde con 0.6 KDa, el azul oscuro con 0.4 KDa, y el rosa con 0 KDa (trazo control).

**Figura 14. Hinchamiento-Recontracción II.** Los experimentos se realizaron en las mismas condiciones que en la Fig. 13. con las concentraciones de  $\text{Ca}^{2+}$  y Pi como se indica en cada gráfica. El hinchamiento se provocó con KCl y la recontracción con PEG's de distintos tamaños. Las condiciones fueron 0 M  $\text{Ca}^{2+}$ , 0.4 mM Pi. 1.0 KDa (azul), 1.0 KDa (morado), 0.6 KDa (verde), 0.4 KDa (azul oscuro), sin PEG (rosa).

La Fig. 15 presenta la condición 0.3 mM  $\text{Ca}^{2+}$ , 0.4 mM Pi. El trazo amarillo se recontrajo con 1.5 KDa, el gris con 1 KDa, el azul con 0.6 KDa, y el naranja con 0.4 KDa.

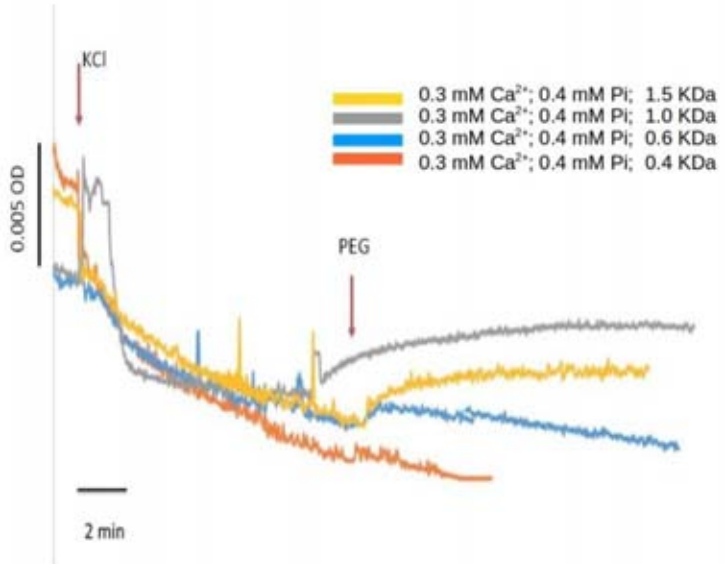


**Figura 15. Hinchamiento-Recontracción III.** Los experimentos se realizaron en las mismas condiciones que en la Fig. 13 con las concentraciones de  $\text{Ca}^{2+}$  y Pi como se indica en cada trazo. El hinchamiento se provocó con KCl y la recontracción con PEG's de distintos tamaños. Las condiciones fueron 0.3 mM  $\text{Ca}^{2+}$ , 0.4 mM Pi. El trazo amarillo muestra la recontracción de mitocondrias en presencia de 1.5 KDa, el gris con 1.0 KDa, el azul con 0.6 KDa, y el naranja con 0.4 KDa.

Como se puede observar en las figuras 13, 14 y 15, el hinchamiento tiene una disminución progresiva a medida que aumenta la concentración de iones, lo que nos lleva a pensar que es un cierre en el ScMUC lo que está evitando un fenómeno de hinchamiento.

A pesar de ver una disminución en el hinchamiento ocasionado por los iones, no se detectó ninguna apertura parcial con los diferentes compuestos de PEG usados (0.4, 0.6, 1, 1.5 KDa). En el único caso en el que hubo una recontracción significativa fue a valores mayores a 1 KDa, con el MUC completamente abierto.

## 6.4 Producción de especies reactivas de oxígeno

Nos interesaba saber si las condiciones en las que el MUC se encontraba cerrado por  $\text{Ca}^{2+}$  y  $\text{H}_2\text{PO}_4^-$ , tenían efectos sobre la producción de ROS. Por esta razón, medimos la producción de especies reactivas de oxígeno en condiciones en las que el MUC se encuentra cerrado y abierto.

En la Fig. 16 se puede ver que no hay una diferencia significativa en la producción de ROS con dos sustratos respiratorios. Para esto se utilizó etanol y NADH. No se observaron diferencias entre las dos condiciones; bajo  $\text{H}_2\text{PO}_4^-$  (0.1 mM, columna azul) y alto (4 mM, columna roja). La siguiente prueba que hicimos fue inhibir el flujo de electrones por la cadena respiratoria con antimicina a, como se puede ver en la Fig. 16 (columna verde y morado), y medimos en condiciones donde el MUC se encuentra abierto (0.1 mM, columna verde) o cerrado (4 mM, columna morada).

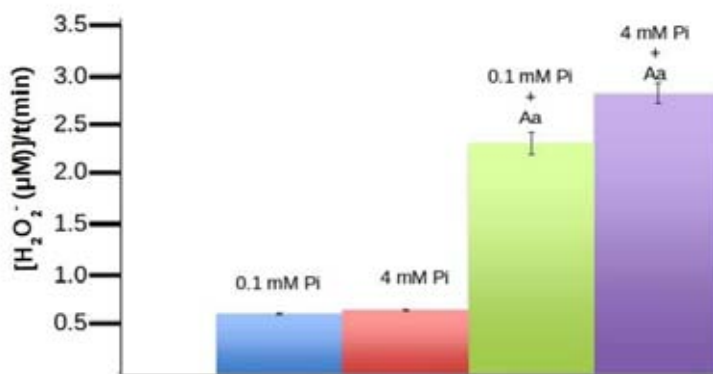


**Figura 16. Producción de ROS.** Los experimentos se realizaron en un medio manitol 0.6 M y 5

mM, y se agregó amplex red y peroxidasa como marcador para la formación de ROS. (Columna azul) 0.1 mM Pi. (Columna roja) 4 mM. (Columna verde) 0.1 mM + Antimicina A (Aa.). (Columna morada) 4 mM de Pi + Aa.

Se puede observar una tendencia a formar una mayor cantidad de ROS en condiciones donde el MUC se encuentra abierto y la cadena de electrones paralizada.



## 7. DISCUSIÓN

En estudios previos el grupo de trabajo había evaluado el papel de distintos iones en diferentes procesos bioenergéticos como son el consumo de oxígeno, la capacidad para establecer y mantener un potencial transmembranal, el hinchamiento como medida de desequilibrio osmótico, síntesis de ATP y la recontracción con PEG como marcadores de la PT y, por ende, de la apertura del MUC. Cabe mencionar el artículo de Castrejón y cols. (2002) en el que se evaluó el efecto de  $K^+$  sobre la mitocondria. Se observó que el KCl ocasionaba un abatimiento del potencial transmembranal sin la necesidad de usar ningún protonóforo. Aunado a esto, también observó que el desacoplamiento ocasionado por el  $K^+$  era inhibido a medida que aumentaba las concentraciones de Pi o  $Mg^{2+}$ . Pérez-Vázquez y cols. (2003) estudiaron el papel del  $Ca^{2+}$  y el  $Mg^{2+}$  sobre el MUC y demostraron que iones como el  $Ca^{2+}$ ,  $Mg^{2+}$  y Pi tienen la capacidad de regular la apertura y cierre del MUC. Para esto, ellos evaluaron diferentes marcadores de la apertura del MUC como: el consumo de oxígeno, el potencial transmembranal y la recontracción con PEG al igual que se hizo en este estudio; mostrando que estos iones, además de tener la capacidad de regular la apertura y cierre del MUC, lo pueden hacer de forma sinérgica teniendo un efecto aditivo. El papel del  $Ca^{2+}$  en la regulación del ciclo de *S. cerevisiae* se ha descrito en diferentes revisiones a las que remitimos al lector (Pringle y Hartwell, 1981). Este ión presenta un aumento en la concentración citoplásmica durante la mitosis, momento de alta demanda energética, lo cual concuerda con la idea de que el  $Ca^{2+}$  cierra el MUC cuando el requerimiento de ATP es elevado. Por el contrario, en circunstancias en las que no se requiere ATP, las concentraciones de calcio bajan y el MUC se abre evitando así la formación de ROS en

levaduras (Murphy, 2009). Aunado a esto, Castrejón y cols. (2002) demostraron que un porcentaje de la síntesis de ATP se mantiene aun cuando se abate el potencial transmembranal, lo que concuerda con modelos en los que existen pozas localizadas de protones que se canalizan de forma específica a la ATP sintasa (Yaguzhinsky y cols., 2006).

Ambos mecanismos; el desacoplamiento por el MUC para evitar una saturación de la cadena respiratoria y la formación de ROS, así como la asociación de complejos respiratorios para la canalización de sustratos son fenómenos que se encuentran regulando de forma muy precisa la fosforilación oxidativa.

Otro artículo que cabe mencionar es el de Gutiérrez-Aguilar y cols. (2010). En éste se estudió el papel de Pi, y su acarreador en la membrana interna, en la apertura del MUC. En este trabajo se observó que al mutar el acarreador del Pi se pierde la sensibilidad a  $H_2PO_4^-$ , además de presentar una disminución en el diámetro del MUC; sugiriendo una posible participación como componente estructural del ScMUC.

Otro fenómeno similar al del  $Ca^{2+}$  ocurre con el  $H_2PO_4^-$  que se acumula en momentos en los que la hidrólisis de ATP es elevada y hay una alta demanda de energía para llevar a cabo las fases del ciclo celular, lo que ocasiona un cierre de MUC que lleva a una mayor eficiencia de la fosforilación oxidativa.

Un problema de los estudios realizados en mitocondrias *in vitro* es que las concentraciones de  $Ca^{2+}$  y/o  $Mg^{2+}$  necesarias para cerrar el MUC se encontraban por encima de las que se encuentran en el ambiente celular, y esto causaba cierto escepticismo de si este fenómeno tendría un papel fisiológico.

Durante mucho tiempo se realizaron estudios en mitocondrias de mamíferos donde el  $Ca^{2+}$  ocasiona la apertura del MUC (Halestrap, 1989; Pfeiffer y Tchen, 1975) mientras

que en *S. cerevisiae*, éste ocasiona un efecto inverso, llevando al cierre y generando un mayor acoplamiento mitocondrial, aumento en el potencial transmembranal e inhibición del hinchamiento (Pérez-Vázquez y cols., 2003). Esta discrepancia llevó a que durante mucho tiempo no se relacionaran estos eventos como un fenómeno en común (Bernardi y cols., 2006; Azzolin y cols., 2010). Hoy en día, la visión sobre la PT y la regulación de MUC ha cambiado y se reconoce que las diferencias en la modulación se deben a divergencias evolutivas y que pueden estar relacionadas con los requerimientos de cambios en la concentración de iones en el medio de las diferentes especies.

Había prevalecido en el estudio del MUC, la idea de que su apertura era irreversible. Esto se debe también a que gran parte de los estudios se hacen en mitocondrias de hígado de ratas, donde al parecer la apertura del MUC parece un proceso irreversible que llevaba a la muerte celular (Jung y cols., 1997). La reversibilidad de este fenómeno se ha cuestionado, ya que eventos patológicos que se han relacionado con la apertura MUC de forma definitiva, como es el caso de la isquemia reperfusión, hoy en día están siendo regulados evitando el daño por un descarga masiva de  $\text{Ca}^{2+}$ , que ocasiona la apertura del MUC de forma irreversible mediante el restablecimiento gradual del flujo sanguíneo en la zona isquémica (Honda y cols., 2005).

Mientras que en levaduras este fenómeno se asumió que ocurría de la misma manera que en mamíferos y que era parte de un programa de muerte celular, al parecer no es así.

Uno de los cuestionamientos de la PT y la apertura del MUC es que deben ser cíclicos a lo largo de la vida de una levadura, debido a los aumentos citoplásmicos de  $\text{Ca}^{2+}$  durante la mitosis; por lo que la idea de un canal irreversible suena algo incongruente con los datos experimentales y con la teoría celular. Esto nos lleva a proponer un mecanismo de

retroalimentación negativa basado en que el  $\text{Ca}^{2+}$ ,  $\text{Mg}^{2+}$  y  $\text{H}_2\text{PO}_4^-$  actúan de forma sinérgica y cíclica, coordinando el ciclo celular con la eficiencia de la fosforilación oxidativa, orquestando el cierre y evitando la PT durante la mitosis.

La regulación en múltiples puntos de una vía es un concepto que cada vez toma mayor importancia para poder entender los procesos bioquímicos, por lo que no es extraño que la respiración celular cuente con diversos mecanismos que le permitan regular la producción de energía, la producción de ROS, el crecimiento celular, etcétera.

En busca de aperturas parciales del MUC indagamos la posibilidad de que presentara alguna apertura en un estado intermedio entre los descritos, abierto y cerrado, y que la pudiéramos detectar por medio de la prueba de recontracción con PEG's de diferente tamaño (Jung y cols., 1997).

El MUC al ser una estructura multiproteica y que permite la salida de diferentes iones y metabolitos de la mitocondria en su estado abierto, creímos interesante evaluar si presentaba diferentes estados entre el abierto y el cerrado que permitieran una salida de algunos de los metabolitos e iones mientras que conservara otros. En relación a esto no podemos concluir nada, nuestros datos no son conclusivos (Fig. 13-15).

## 8. CONCLUSIONES

### 8.1 Efecto sinérgico de $\text{Ca}^{2+}$ , $\text{Mg}^{2+}$ y $\text{H}_2\text{PO}_4^-$

El  $\text{Ca}^{2+}$ ,  $\text{Mg}^{2+}$  y  $\text{H}_2\text{PO}_4^-$  tienen un efecto aditivo sobre el cierre del *ScMUC*.

### 8.2 Regulación dinámica del *ScMUC* por iones

El *ScMUC* tiene una regulación dinámica.

El *ScMUC* tiene la posibilidad de abrirse y cerrarse en respuesta a los cambios en concentraciones de  $\text{Ca}^{2+}$  y  $\text{Mg}^{2+}$ .

### 8.3 En busca de aperturas parciales del *ScMUC*

No podemos concluir nada con respecto a esto.

### 8.4 MUC y ROS

No podemos concluir nada al respecto.



## 9. REFERENCIAS

1. Adams, K. L., & Palmer, J. D. (2003). Evolution of mitochondrial gene content: gene loss and transfer to the nucleus. *Molecular Phylogenetics and Evolution*, 29, 380-395.
2. Åkerman, K. E., & Wikström, M. K. (1976). Safranine as a probe of the mitochondrial membrane potential. *FEBS Letters*, 68(2), 191-197.
3. Alberts, B., Johnson, A., Lewis, J., Martin, R., Roberts, K., & Walter, P. (2009). Introduction to the cell. En B. Alberts, A. Johnson, J. Lewis, R. Martin, K. Roberts & P. Walter (Eds.), *Molecular Biology of the Cell* (5<sup>a</sup> ed.) (pp. 1-125). Nueva York, NY: Garland.
4. Azzolin, L., von Stockum, S., Basso, E., Petronilli, V., Forte, M. A., & Bernardi, P. (2010). The mitochondrial permeability transition from yeast to mammals. *FEBS Letters*, 584, 2504-2509.
5. Baines, C. P., Kaiser, R. A., Purcell, N. H., Blair, N. S., Osinska, H., Hambleton, M. A., Brunskill, E. W., Sayen, M. R., Gottlieb, R. A., Dorn, G. W., Robbins, J., & Molkentin, J. D. (2005). Loss of cyclophilin D reveals a critical role for mitochondrial permeability transition in cell death. *Nature*, 434, 658-662.
6. Baradaran, R., Berrisford, J. M., Minhas, G. S., & Sazanov, L. A. (2013). Crystal structure of the entire respiratory complex I. *Nature*, 494, 443-448.
7. Basso, E., Fante, L., Fowlkes, J., Petronilli, V., Forte, M. A., & Bernardi, P. (2005). Properties of the Permeability Transition Pore in Mitochondria Devoid of Cyclophilin D. *Journal of Biological Chemistry*, 280, 18558-18561.

8. Bernardi, P. (1999). Mitochondrial transport of cations: channels, exchangers and permeability transition. *Physiological Reviews*, 79, 1127-1155.
9. Bernardi, P. & Petronilli, V. (1996). The permeability transition pore as a mitochondrial calcium release channel: a critical appraisal. *Journal of Bioenergetics and Biomembranes*, 28(2), 131-138.
10. Bernardi, P., Krauskopf, A., Basso, E., Petronilli, V., Blachly-Dyson, E., Di Lisa, F., & Forte, M. A. (2006). The mitochondrial permeability transition from in vitro artifact to disease target. *FEBS Journal*, 273, 2077-2099.
11. Boyer, P. D. (1997). The ATP Synthase-A Splendid Molecular Machine. *Annual Reviews of Biochemistry*, 66, 717-749.
12. Brenner, C., & Grimm, S. (2006). The permeability transition pore complex in cancer cell death. *Oncogene*, 25, 4744-4756.
13. Brown, G. C., & Brand, M. D. (1988). Proton/electron stoichiometry of mitochondrial complex I estimated from the equilibrium thermodynamic force ratio. *Biochemical Journal*, 252, 473-479.
14. Cabrera-Orefice, A., Guerrero-Castillo, S., Luévano-Martínez, L. A., Peña, A., & Uribe-Carvajal, S. (2010). Mitochondria from the salt-tolerant yeast Debaryomyces hansenii (halophilic organelles?). *Journal of Bioenergetics and Biomembranes*, 42, 11-19.
15. Cabrera-Orefice, A., Chiquete-Félix, N., Espinasa-Jaramillo, J., Rosas-Lemus, M., Guerrero-Castillo, S., Peña, A., & Uribe-Carvajal, S. (2014). The branched respiratory chain from *Debaryomyces hansenii*: Components and supramolecular organization. *Biochimica et Biophysica acta*, 1837, 73-84.

16. Castrejón V., Peña, A., & Uribe, S. (2002). Closure of the yeast mitochondria unspecific channel (YMUC) unmasks a Mg<sup>2+</sup> and quinine sensitive K<sup>+</sup> uptake pathway in *Saccharomyces cerevisiae*. *Journal of Bioenergetics Biomembranes*, 34, 299-306.
17. Chappell, J. B. (1968). Systems used for the transport of substrates into mitochondria. *British Medical Bulletin*, 24, 150-157.
18. Chateaubodeau, G. A., Guérin, M., & Guérin, B. (1976). Permeability of yeast mitochondrial internal membrane: structure-activity relationship. *Biochemistry*, 58, 601-610.
19. Chen, C., Ko, Y., Delannoy, M., Lutke, S. J., Chiu, W., & Pedersen, P. L. (2004). Mitochondrial ATP Synthasome: Three-dimensional structure by electron microscopy of the ATP synthase in complex formation with carriers for Pi and ADP/ATP. *The Journal of Biological Chemistry*, 279, 31761-31768.
20. Cheng, E. H. Y., Sheiko, T. V., Fisher, J. K., Craigen, W. J., & Korsmeyer, S. J. (2003). VDAC2 inhibits BAK activation and mitochondrial apoptosis. *Science*, 301, 513-17.
21. Colombini, M. (2004). VDAC: The channel at the interface between mitochondria and the cytosol. *Molecular and Cellular Biochemistry*, 256, 107-115.
22. Constanzo, M. C., & Fox, T. D. (1990). Control of Mitochondrial Gene Expression in *Saccharomyces cerevisiae*. *Annual Review of Genetics*, 24, 91-108.
23. Cortés, P., Castrejón, V., Sampedro, J. G., & Uribe, S. (2000). Interactions of arsenate, sulfate and phosphate with yeast mitochondria. *Biochimica et Biophysica Acta (BBA)*, 1456, 67-76.

24. Crompton, M. (1999). The mitochondrial permeability transition pore and its role in cell death. *Biochemical Journal*, 341, 233-249.
25. Crompton, M., & Costi, A. (1988). Kinetic evidence for a heart mitochondrial pore activated by Ca<sup>2+</sup>, inorganic phosphate and oxidative stress. A potential mechanism for mitochondrial dysfunction during cellular Ca<sup>2+</sup> overload. *European Journal of Biochemistry*, 178, 489-501.
26. Davidson, A. M., & Halestrap, A. P. (1990). Partial inhibition by cyclosporin A of the swelling of liver mitochondria in vivo and in vitro induced by sub-micromolar [Ca<sup>2+</sup>], but not by butyrate. Evidence for two distinct swelling mechanisms. *Biochemical Journal*, 268, 147-152.
27. De Klöet, S., van Wermeskerken, R., & Koningsberger, V. V. (1961). Studies on protein synthesis by protoplasts of *Saccharomyces carlsbergensis*. I. The effect of ribonuclease on protein synthesis. *Biochimica Biophysica Acta (BBA)*, 47, 138-143.
28. Dolezal, P., Likic, V., Tachezy, J., & Lithgow, T. (2006). Evolution of the Molecular Machines for Protein Import into Mitochondria. *Science*, 313, 314-318.
29. Estabrook, R. W. (1967). Mitochondrial respiratory control and the polarographic measurement ADP: O ratios. *Methods in Enzymology*, 10, 41-47.
30. García, N., Correa, F., & Chávez, E. (2005). On the Role of the Respiratory Complex I on Membrane Permeability Transition. *Journal of Bioenergetics and Biomembranes*, 37, 17-23.
31. Giorgio, V., von Stockum, S., Antoniel, M., Fabbro, A., Fogolari, F., Forte, M., Glick, G. D., Petronilli, V., Zoratti, M., Szabó, I., Lippe, G., & Bernardi, P. (2013). Dimers of the mitochondrial ATP synthase form the permeability transition pore.

*Proceedings of the National Academy of Sciences (PNAS)*, 100(15), 5887-5892.

32. Gornall A. G., Bardawill, C. J., & David, M. M. (1949). Determination of serum proteins by the means of the Biuret reactions. *Biochemistry*, 177, 751-766.
33. Guérin, B., Bukusoglu, C., Rakotomanana, F., & Wohlrbab, H. (1990). Mitochondrial phosphate transport. N-ethylmaleimide insensitivity correlates with absence of beef heart-like Cys42 from the *Saccharomyces cerevisiae* phosphate transport protein. *Journal of Biological Chemistry*, 265(32), 19736-19741.
34. Guerrero-Castillo, S., Araiza-Olivera, D., Cabrera-Orefice, A., Espinasa-Jaramillo, J., Gutiérrez-Aguilar, M., Luévano-Martínez, L. A., Zepeda-Bastida, A., & Uribe-Carvajal, S. (2011). Physiological uncoupling of mitochondrial oxidative phosphorylation. Studies in different yeast species. *Journal of Bioenergetics and Biomembranes*, 43, 323-331.
35. Guerrero-Castillo, S., Vázquez-Acevedo, M., González-Halphen, D., & Uribe-Carvajal, S. (2009). In *Yarrowia lipolytica* mitochondria, the alternative NADH dehydrogenase interacts specifically with the cytochrome complexes of the classic respiratory pathway. *Biochimica et Biophysica Acta (BBA)*, 1787, 75-85.
36. Gunter, T. E., & Pfeiffer D. R. (1990). Mechanism by which mitochondria transport calcium. *American Journal of Physiology*, 258, C755-C786.
37. Gutiérrez-Aguilar, M., Pérez-Martínez, X., Chávez, E., & Uribe-Carvajal, S. (2010). In *Saccharomyces cerevisiae*, the phosphate carrier is a component of the mitochondrial unselective channel. *Archives of Biochemistry and Biophysics*, 494, 184-191.
38. Halestrap, A. P. (1989). The regulation of the matrix volume of mammalian

- mitochondria in vivo and in vitro and its role in the control of mitochondrial metabolism. *Biochimica et Biophysica Acta (BBA)*, 973, 355-382.
39. Halestrap, A. P. (2009). What is the mitochondrial permeability transition pore? *Journal of Molecular and Cellular Cardiology*, 46, 821-831.
40. Handschumacher, R. E., Harding, M. W., Rice, J., Drugge, R. J., & Speicher, D. W. (1984). Cyclophilin: a specific cytosolic binding protein for cyclosporin A. *Science*, 226, 544-547.
41. Haworth, R. A., & Hunter, D. R. (2000). Control of the Mitochondrial Permeability Transition Pore by High-Affinity ADP Binding at the ADP/ATP Translocase in Permeabilized Mitochondria. *Journal of Bioenergetics and Biomembranes*, 32, 91-96.
42. Honda, H. M., Korge, P., & Weiss, J. N. (2005). Mitochondria and Ischemia/Reperfusion Injury. *Annals of the New York Academy of Sciences*, 1047, 248-258.
43. Horton, H. R., Moran, L. A., Scrimgeour, K. G., Perry, M. D., & Rawn, J. D. (2008). *Principios de Bioquímica*. México: Pearson Educación.
44. Hunter, D.R. & Haworth, R.A. (1979). The  $\text{Ca}^{2+}$  -induced membrane transition in mitochondria. II. Nature of the  $\text{Ca}^{2+}$  trigger site. *Arch Biochem Biophys*, 195, 460-467.
45. Jung, D. W., Bradshaw, P. C., & Pfeiffer, D. R. (1997). Properties of a cyclosporin-insensitive transition pore in yeast mitochondria. *Journal of Biological Chemistry*, 272, 21104-21112.
46. Kaasik, A., Safiulina, D., Zharkovsky, A., & Veksler, V. (2007). Regulation of

- mitochondrial matrix volume. *American Journal of Physiology-Cell Physiology*, 292, C157-C163.
47. Kokoszka, J. E., Waymire, K. G., Levy, S. E., Sligh, J. E., Cai, J., Jones, D. P., MacGregor, G. R., & Wallace, D. C. (2004). The ADP/ATP translocator is not essential for the mitochondrial permeability transition pore. *Nature*, 427, 461-465.
48. Kowaltowski, A. J., Vercesi, A. E., Rhee, S. G., & Netto, L. E. (2000). Catalases and thioredoxin peroxidase protect *Saccharomyces cerevisiae* against Ca(2+) induced mitochondrial membrane permeabilization and cell death. *FEBS Letters*, 473, 177-182.
49. Kroemer, G., & Reed, J. C. (2000). Mitochondrial control of cell death. *Nature Medicine*, 6, 513-519.
50. Kunji, E. R. S. (2004). The role and structure of mitochondrial carriers. *FEBS Letters*, 564, 239-244.
51. Leung, A. W., Varanyuwatana, P., & Halestrap, A. P. (2008). The mitochondrial phosphate carrier interacts with cyclophilin D and may play a key role in the permeability transition. *Journal of Biological Chemistry*, 283, 26312-26323.
52. Michel, H., Behr, J., Harrenga, A., & Kannt, A. (1998). Cytochrome c oxidase: structure and spectroscopy. *Annual Review of Biophysics and Biomolecular Structure*, 27, 329-356.
53. Mitchell, P. (1966). Chemiosmotic coupling in oxidative and photosynthetic phosphorylation. *Biological Reviews*, 41, 445-501.
54. Murphy, M. P. (1989). Slip and leak in mitochondrial oxidative phosphorylation. *Biochimica et Biophysica Acta (BBA)*, 977, 123-141.

55. Murphy, M. P. (2009). How Mitochondria produce reactive oxygen species. *Biochemical Journal*, 417, 1-13.
56. Nicholls, D. G., & Ferguson, S. J. (2002). *Bioenergetics 3*. EUA: Academic Press.
57. Nicolli, A., Petronilli, V., & Bernardi, P. (1993). Modulation of the Mitochondrial Cyclosporin A-Sensitive Permeability Transition Pore by Matrix pH. Evidence that the Pore Open-Closed Probability Is Regulated by Reversible Histidine Protonation. *Biochemistry*, 32, 4461-4465.
58. Overkamp, K. M., Bakker, B. M., Kötter, P., van Tuijl, A., de Vries, S., van Dijken, J. P., & Pronk, J. T. (2000). In vivo analysis of the mechanisms for oxidation of cytosolic NADH by *Saccharomyces cerevisiae* mitochondria. *Journal of Bacteriology*, 182(10), 2823-2830.
59. Palou, A., Picó, C., Bonet, M. L., & Oliver, P. (1998). The uncoupling protein, thermogenin. *International Journal of Biochemistry and Cell Biology*, 30, 7-11.
60. Paumard, P., Vaillier, J., Coulary, B., Schaeffer J., Soubannier V., Mueller, D. M., Brèthes, D., di Rago, J. P., & Velours, J. (2002). The ATP synthase is involved in generating mitochondrial cristae morphology. *The EMBO Journal*, 21, 221-230.
61. Pebay-Peyroula, E., Dahout-Gonzalez, C., Kahn, R., Trézéguit, V., Lauquin, G. J. M., & Brandolin, G. (2003). Structure of mitochondrial ADP/ATP carrier in complex with carboxyatractyloside. *Nature*, 426, 39-44.
62. Peña, A., Piña, M. Z., Escamilla, E., & Piña, E. (1977). A novel method for the rapid preparation of coupled yeast mitochondria. *FEBS Letters*, 80, 209-213.
63. Pérez-Vázquez, V., Saavedra-Molina, A., & Uribe, S. (2003). In *Saccharomyces cerevisiae*, Cations Control The Fate of the Energy Derived From Oxidative

- Metabolism Through the Opening and Closing of the Yeast Mitochondrial Unselective Channel. *Journal of Bioenergetics and Biomembranes*, 35, 231-241.
64. Pfeiffer, D. R., & Tchen, T. T. (1975). The activation of adrenal cortex mitochondrial malic enzyme by Ca<sup>2+</sup> and Mg<sup>2+</sup>. *Biochemistry*, 14, 89-96.
65. Pringle, J. R., & Hartwell, L. H. (1981). The *Saccharomyces cerevisiae* Cell Cycle. En J. N. Strathern, E. W. Jones & J. R. Broach (Eds.), *The Molecular Biology of the Yeast Saccharomyces: Life Cycle and Inheritance* (pp. 97-142). New York: Cold Spring Harbor Monograph Archive.
66. Reszka, K. J., Wagner, B. A., Burns, C. P., & Britigan, B. E. (2005). Effects of peroxidase substrates on the Amplex red/peroxidase assay: Antioxidant properties of anthracyclines. *Analytical Biochemistry*, 342, 327-337.
67. Sagan, L. (1967). On the Origin of Mitosing Cells. *Journal of Theoretical Biology*, 4, 225-274.
68. Saint-Georges, Y., Hamel, P., Lemaire, C., & Dujardin, G. (2001). Role of positively charged transmembrane segments in the insertion and assembly of mitochondrial inner-membrane proteins. *Proceedings of the National Academy of Sciences (PNAS)*, 98, 13814-13819.
69. Schultheiss, H. P., & Klingenberg, M. (1984). Immunochemical characterization of the adenine nucleotide translocator. Organ specificity and conformation specificity. *European Journal of Biochemistry*, 143, 599-605.
70. Scott, I., & Youle, R. J. (2010). Mitochondrial fission and fusion. *Essays in Biochemistry*, 47, 85-98.
71. Sheldon, K. L., Maldonado, E. N., Lemasters, J. J., Rostovtseva, T. K., & Bezrukov,

- S. M. (2011). Phosphorylation of voltage-dependent anion channel by serine/threonine kinases governs its interaction with tubulin. *PLoS One*, 6(10), e25539.
72. Sherman, F. (2002). Getting started with yeast. *Methods in Enzymology*, 350, 3-41.
73. Singer, T. P., Kearney, E. B., & Kenney, W. C. (1973). Succinate Dehydrogenase. En A. Meister (Ed.), *Advances in Enzymology and Related Areas of Molecular Biology* (pp.189-270). EUA: Interscience.
74. Slater, E. C. (1953). Mechanism of Phosphorylation in the Respiratory Chain. *Nature*, 172, 975-978.
75. Stappen, R., & Krämer, R. (1994). Kinetic mechanism of phosphate/phosphate and phosphate/OH<sup>-</sup> antiports catalyzed by reconstituted phosphate carrier from beef heart mitochondria. *Journal of Biological Chemistry*, 269, 11240-11246.
76. Stock, D., Leslie, A. G. W., & Walker, J. E. (1999). Molecular Architecture of the Rotary Motor in ATP Synthase. *Science*, 286, 1700-1705.
77. Sun, F., Huo, X., Zhai, Y., Wang, A., Xu, J., Su, D., Bartlam, M., & Rao, Z. (2005). Crystal Structure of Mitochondrial Respiratory Membrane Protein Complex II. *Cell Press*, 121, 1043-1057.
78. Szabó, I., Bernardi, P., & Zoratti, M. (1992). Modulation of the mitochondrial megachannel by divalent cations and protons. *Journal of Biological Chemistry*, 267, 2940-2946.
79. Szabó, I., De Pinto, V., & Zoratti M. (1993). The mitochondrial permeability transition pore may comprise VDAC molecules. II. The electrophysiological properties of VDAC are compatible with those of the mitochondrial megachannel.

*FEBS Letters*, 330, 206-210.

80. Szabó, I., & Zoratti, M. (1992). The Mitochondrial Megachannel is the Permeability Transition Pore. *Journal of Bioenergetics and Biomembranes*, 24, 111-117.
81. Trumper, B. L. (1990). Cytochrome bc<sub>1</sub> Complexes of Microorganisms. *Microbiological Reviews*, 54, 101-129.
82. Uribe-Carvajal, S., Luévano-Martínez, L. A., Guerrero-Castillo, S., Cabrera-Orefice, A., Corona-de-la-Peña, N. A., & Gutiérrez-Aguilar, M. (2011). Mitochondrial Unselective Channels throughout the eukaryotic domain. *Mitochondrion*, 11, 382-390.
83. Wikström, M. K. F. (1977). Proton pump coupled to cytochrome c oxidase in mitochondria. *Nature*, 266, 271-273.
84. Wittig, I., & Schägger, H. (2009). Supramolecular organization of ATP synthase and respiratory chain in mitochondrial membranes. *Biochimica et Biophysica Acta (BBA)*, 1787, 672-680.
85. Xia, D., Yu, C., Kim, H., Xia, J., Kachurin, A. M., Zhang, L., Yu, L., & Deisenhofer, J. (1997). Crystal Structure of the Cytochrome bc<sub>1</sub> Complex from Bovine Heart Mitochondria. *Science*, 277, 60-66.
86. Yaguzhinsky, L. S., Yurkov, V. I., & Krasinskaya, I. P. (2006). On the localized coupling of respiration and phosphorylation in mitochondria. *Biochimica et Biophysica Acta (BBA)*, 1757, 408-414.

#### Citas de páginas web

1. Scitable Nature. Essentials of Cell Biology:

<<http://www.nature.com/scitable/topicpage/mitochondria-14053590>>

2. Uniprot:

[◇](#).

## 10. AGRADECIMIENTOS

Mientras escribía estos agradecimientos se me ocurrió un montón de gente a quien agradecerle y seguro se me fueron algunos... así que ahí les voy:

Los primeros por razones obvias y a quien está dedicada esta tesis, es a mis papás, Ana María y José María, por el apoyo incondicional que me brindan, y por motivarme en los momentos más difíciles.

Otro personaje que es fundamental en mi recorrido por la UNAM es el Dr. Salvador Uribe que siempre fue una guía y un apoyo. Además de las incontables cosas que aprendí mientras estuve en el laboratorio 305 oriente, tanto en el ámbito académico como personal. Le agradezco también por no dejar que claudicara con la misión de terminar la tesis y titularme.

Le doy las gracias a Andrea por ayudarme corrigiendo esta tesis, que cuando llegó a sus manos por primera vez era un cúmulo de faltas de ortografía y por ser una persona increíble.

Mientras estuve en el laboratorio pasaron muchas personalidades que fueron importantes para mí. Cabe mencionar a Sergio y a Manuel por ser los que me enseñaron a obtener mis primeras mitocondrias acopladas, medir el potencial transmembranal y romper mis primeros geles nativos. A Alfredo y a Mona por ser amigos, compañeros y maestros en el laboratorio, y por enseñarme a calibrar el oxímetro y muchos de los aparatejos que no lograba hacer funcionar. A Natalia por tener siempre todo para que el lab funcionará, estar al pendiente de los cumpleaños de todos, y de procurar que constantemente disfrutáramos de comidas deliciosas. Y a Ramón, que si llegábamos muy temprano lo encontrábamos

dedicado a labores de limpieza y después desaparecía por gran parte del día, mientras volvíamos a ensuciar todo.

También agradezco a los miembros del jurado que leyeron y corrigieron esta tesis, al laboratorio 306 Ote. por dejarme usar la autoclave y el espectrofotómetro. A la Facultad de Medicina, al Instituto de Investigaciones Biomédicas, al Instituto de Fisiología y a la UNAM por brindarme la oportunidad de estudiar en la mejor institución de México.

Por último, me gustaría recordar a mi generación por los momentos y las clases que compartimos (las aburridísimas horas de las sesiones de inmunología, o las discusiones acaloradas con el Dr. Zentella). Recuerdo las anécdotas que me pasaron con Diego, Mauricio, Itzel y Rodrigo que fueron mis compañeros más cercanos y a quienes les tengo un gran cariño.

## 11. LISTA DE ABREVIATURAS

<b>Abreviatura</b>	<b>Definición</b>
Å	Amstrongs
ADP	Adenosin difosfato
ANT	Transportador de adenin nucleótidos
AOX	Oxidasa alterna
ATP	Adenosin trifosfato
CCCP	Carbonil cianide <i>m</i> -clorofenyl hidrazone
CR	Cociente Respiratorio
CsA	Ciclosporina A
CyP-D	Ciclofilina D
DNA	Ácido desoxirribonucleico
EDTA	Ácido dietil-diamino tetra-acético
EGTA	Ácido etilen-glicol tetra-acético
EI	Espacio intermembranal
F	Constante de Faraday
FCCP	Carbonil cyanide-4-(trifluorometoxi)fenylhydrazone
IMM	Membrana interna mitocondrial
J	Flujo de electrones
J <sub>H</sub>	Flujo de protones
KDa	Kilo Daltons
NADH	Nitoconiamida adenin dinucleotido
NDH2e	NADH deshidrogenasa tipo II externa
Ndep1	NADH deshidrogenasa tipo II externa de <i>S. cerevisiae</i>
Ndep2	NADH deshidrogenasa tipo II externa de <i>S. cerevisiae</i>
Ndip	NADH deshidrogenasa tipo II interna de <i>S. cerevisiae</i>
nS	Nano Siemens
M	Matriz
MCF	Familia de acarreadores mitocondriales
MES	Ácido 2-( <i>N</i> -morpholino)etano-sulfónico
Mg	Miligramos
MIM	Membrana interna mitocondrial
mL	Militros
Mm	Milimetros
mM	Mili-molar
MMC	Canal mega mitocondrial
mMUC	Canal inespecífico mitocondrial de mamíferos
MOM	Membrana externa mitocondrial
MUC	Cana Inespecífico Mitocondrial
mV	Mili-Volts
Ng	nanogramos
OXPHOS	Fosforilación oxidativa

PEG	Polietilén glicol
pH	Potencial de hidrógeno
Pi	Fosfato inorgánico
PiC	Transportador de fosfato
Ppif	Gen de la ciclofilina D
PT	Transición de la permeabilidad
ROS	Especies Reactivas de Oxígeno
Rpm	Revoluciones por minuto
ScMUC	Canal inespecífico mitocondrial de <i>S. cerevisiae</i>
TEA	Trietanolamina
UCP	Proteína desacoplante
UCP3	Isoforma 3 de la proteína desacoplante de mamíferos
U/4	Estado desacoplado entre estado 4
VDAC	Canal aniónico dependiente de voltaje
W/V	Masa entre volumen
$\mu\text{L}$	Microlitro
$\Delta P$	Fuerza protón-motriz
$\Delta \text{pH}$	Diferencia de pH
$\Delta \Psi$	Potencial transmembranal
$\Delta \mu\text{H}^+$	Diferencia en la concentración de protones

## 12. ANEXOS



# The branched mitochondrial respiratory chain from *Debaryomyces hansenii*: Components and supramolecular organization

Alfredo Cabrera-Orefice, Natalia Chiquete-Félix, Juan Espinasa-Jaramillo, Mónica Rosas-Lemus,  
Sergio Guerrero-Castillo, Antonio Peña, Salvador Uribe-Carvajal \*

*Dept. of Molecular Genetics, Instituto de Fisiología Celular, Universidad Nacional Autónoma de México, Mexico City, Mexico*



## ARTICLE INFO

### Article history:

Received 12 June 2013

Received in revised form 23 July 2013

Accepted 25 July 2013

Available online 7 August 2013

### Keywords:

Respiratory chain

*Debaryomyces hansenii*

Alternative oxidase

Alternative NADH dehydrogenase

Glycerol-phosphate dehydrogenase

Supercomplexes

## ABSTRACT

The branched respiratory chain in mitochondria from the halotolerant yeast *Debaryomyces hansenii* contains the classical complexes I, II, III and IV plus a cyanide-insensitive, AMP-activated, alternative-oxidase (AOX). Two additional alternative oxidoreductases were found in this organism: an alternative NADH dehydrogenase (NDH2e) and a mitochondrial isoform of glycerol-phosphate dehydrogenase (<sub>Mit</sub>GPDH). These monomeric enzymes lack proton pump activity. They are located on the outer face of the inner mitochondrial membrane. NDH2e oxidizes exogenous NADH in a rotenone-insensitive, flavone-sensitive, process. AOX seems to be constitutive; nonetheless, most electrons are transferred to the cytochrome pathway. Respiratory supercomplexes containing complexes I, III and IV in different stoichiometries were detected. Dimeric complex V was also detected. In-gel activity of NADH dehydrogenase, mass spectrometry, and cytochrome c oxidase and ATPase activities led to determine the composition of the putative supercomplexes. Molecular weights were estimated by comparison with those from the yeast *Y. lipolytica* and they were IV<sub>2</sub>, I–IV, III<sub>2</sub>–IV<sub>4</sub>, V<sub>2</sub>, I–III<sub>2</sub>, I–III<sub>2</sub>–IV, I–III<sub>2</sub>–IV<sub>2</sub>, I–III<sub>2</sub>–IV<sub>3</sub> and I–III<sub>2</sub>–IV<sub>4</sub>. Binding of the alternative enzymes to supercomplexes was not detected. This is the first report on the structure and organization of the mitochondrial respiratory chain from *D. hansenii*.

© 2013 Elsevier B.V. All rights reserved.

## 1. Introduction

The halotolerant, non-pathogenic, oleaginous yeast *Debaryomyces hansenii* is found in the sea and other hyperosmotic habitats [1,2]. *D. hansenii* grows in various environmental conditions including different salt concentrations [3–5], low temperatures [3] and different pHs [3,6]. In addition, *D. hansenii* assimilates many different carbon sources [7–9]. The ability of this yeast to synthesize and store lipids is used in biotechnology to make products of commercial interest, such as cheese [2,10].

*D. hansenii* has high aerobic metabolism and low fermentative activity which are enhanced by high extracellular NaCl or KCl [11–13]. Isolated *D. hansenii* mitochondria undergo permeability transition due to the opening of a mitochondrial unspecific channel (MUC) [14]. Both, the MUCs from *D. hansenii* (<sub>Dh</sub>MUC) and *S. cerevisiae* (<sub>Sc</sub>MUC) are

regulated by effectors such as phosphate, Mg<sup>2+</sup> or Ca<sup>2+</sup> [14–19]. The <sub>Dh</sub>MUC is the only MUC reported to date that is closed by Na<sup>+</sup> or K<sup>+</sup> [14] probably accounting for the monovalent cation coupling effects observed in whole yeast [12,13].

The mammalian oxidative phosphorylation system contains the four “orthodox” respiratory complexes (I, II, III and IV) plus the F<sub>1</sub>F<sub>0</sub>-ATP synthase (complex V) [20]. In addition to the above, mitochondria from plants, fungi, protozoa and some animals may contain “alternative” redox enzymes that substitute or coexist with the classical complexes; e.g. alternative NADH dehydrogenases and oxidases [21–25]. In fungi a mammalian-like respiratory complex may be substituted by an alternative enzyme, e.g. in *S. cerevisiae* complex I the oxidoreductase activity was substituted by an internal alternative NADH dehydrogenase [26,27].

The fungal alternative oxidases (AOXs) are single subunit proteins bound to the matrix side of the inner mitochondrial membrane (IMM) [28–31]. The cyanide-resistant AOX transfers electrons from ubiquinol to oxygen. AOX is inhibited by hydroxamic acids and by n-alkyl-gallates [29,32]. The presence of AOX constitutes an uncoupled branch of the respiratory chain probably designed to prevent substrate overload and overproduction of reactive oxygen species (ROS) [25,28,33–36].

Alternative type II NADH dehydrogenases (NDH2s) transfer electrons from NADH to ubiquinone without pumping protons [37]. NDH2s are monomeric proteins bound to the inner (NDH2i) or the outer (NDH2e) face of IMM [21,37]. NDH2s are not sensitive to rotenone, but instead are specifically inhibited by flavone [38].

*Abbreviations:* ADP, adenosine diphosphate; AMP, adenosine monophosphate; AOX, alternative oxidase; BN, blue-native; COX, cytochrome c oxidase; CRR, cyanide-resistant respiration; Dig, digitonin; IMM, inner mitochondrial membrane; LC-MS, liquid chromatography mass spectrometry; LM, laurylmaltoside; <sub>Mit</sub>GPDH, glycerol-phosphate dehydrogenase (mitochondrial isoform); MUC, mitochondrial unspecific channel; MW, molecular weight; NDH, NADH dehydrogenase activity; NDH2e, alternative external NADH dehydrogenase; PAGE, polyacrylamide-gel electrophoresis; PG, propyl-gallate; ROS, reactive oxygen species; SDS, sodium dodecyl sulfate; 2D, second dimension

\* Corresponding author at: Departamento de Genética Molecular, Instituto de Fisiología Celular, Universidad Nacional Autónoma de México, Ciudad Universitaria, Apdo. Postal 70-242, Mexico City, Mexico. Tel.: +52 55 5622 5632; fax: +52 55 5622 5630.

E-mail address: [suribe@ifc.unam.mx](mailto:suribe@ifc.unam.mx) (S. Uribe-Carvajal).

The mitochondrial isoform of glycerol-phosphate dehydrogenase ( $M_{\text{Mit}}\text{GPDH}$ ) is another component of branched respiratory chains [39,40].  $M_{\text{Mit}}\text{GPDH}$  oxidizes glycerol-phosphate to dihydroxyacetone-phosphate and reduces ubiquinone. Also, this protein is located on the outer face of the IMM [41]. The peripheral proteins NDH2s,  $M_{\text{Mit}}\text{GPDH}$  and AOX are not proton pumps [21,29,40].

Two major models describe the structure/function relationship of the respiratory chain. The *fluid* or *random collision* model proposes that respiratory complexes float freely within the IMM and electron transport occurs through the diffusible carriers ubiquinone and cytochrome c [42]. On the other hand, the *solid* model proposes that respiratory complexes are organized into stable hetero-oligomers (supercomplexes or “respirasomes”) that channel electrons between them [43–46]. There are data that support each model [47]. Kinetic studies show that each respiratory complex can be purified individually, retaining activity [42]. By contrast, blue native gel polyacrylamide electrophoresis (BN-PAGE) reveals the existence of supercomplexes composed of several respiratory complexes [48]. Respiratory supercomplexes can be observed when solubilizing mitochondrial membranes with small amounts of mild detergents such as digitonin [44]. The presence of respiratory supercomplexes has been well documented in mammals [48,49], plants [43,46,50] and different yeast species [51–54]. Additionally, a third model has been proposed: the *plasticity* model, where respiratory complexes undergo a dynamic association-dissociation process and isolated supercomplexes transfer electrons from NADH to oxygen [55]. The plasticity model suggests that complex association/dissociation regulates oxidative phosphorylation [55,56].

Here, the mitochondrial respiratory chain of *D. hansenii*, which has been reported to contain all four mammalian-like respiratory complexes [57] plus a putative stationary-phase-inducible AOX, was characterized [58,59]. This branched respiratory chain contains all the complexes reported [59] plus an external NDH2 and a glycerol-phosphate dehydrogenase. In addition, association of these complexes in different supercomplexes was observed.

## 2. Materials and methods

### 2.1. Chemicals

All chemicals were reagent grade. D-sorbitol, D-mannitol, D-glucose, D-galactose, glycerol, Trizma® base (Tris), malic acid, pyruvic acid, citric acid, maleic acid, DL- $\alpha$ -glycerophosphate, NADH, ATP, ADP, rotenone, flavone, antimycin A, propyl-gallate, digitonin, *n*-dodecyl  $\beta$ -D-maltoside (laurylmaltoside), Nitrotetrazolium blue chloride and antifoam A were from Sigma Chem Co. (St Louis, MO). Bovine serum albumin (Probulmin™) was from Millipore. Yeast extract and bacto-peptone were from BD Bioxon. DL-lactic acid,  $H_3PO_4$ , NaCN, KCl,  $MgCl_2$  and ethanol were from J.T. Baker. 3,3'-Diaminobenzidine tetrahydrochloride hydrate was from Fluka. Coomassie Blue G was from SERVA (Heidelberg, Germany). Coomassie® brilliant blue G-250 and electrophoresis reagents were from BIO-RAD (Richmond, CA).

### 2.2. Biologicals

*D. hansenii* Y7426 strain (US Dept. of Agriculture) was used throughout this work. The strain was maintained in YPGal-NaCl (1% yeast extract, 2% bacto-peptone, 2% D-galactose, 1 M NaCl and 2% bacto agar) plate cultures. *Yarrowia lipolytica* E150 strain was also used. This strain was maintained in YD (1% yeast extract and 2% D-glucose and 2% bacto agar) plate cultures.

### 2.3. Yeast culture and isolation of coupled mitochondria

*D. hansenii* cells were grown as follows: pre-cultures were prepared inoculating 100 mL of YPLac-NaCl medium (1% yeast extract, 2% bacto-peptone, 2% lactic acid, pH 5.5 adjusted with NaOH and adding NaCl to

reach 0.6 M  $Na^+$ ) containing antifoam A emulsion 50  $\mu$ L/L. Pre-cultures were grown for 36 h under continuous agitation in an orbital shaker at 250 rpm at 29 °C. Then, each pre-culture was used to inoculate a 750 mL flask with the same medium. Incubation was continued for 24 h (i.e. medium to late logarithmic phase). *D. hansenii* mitochondria were isolated as reported previously [14]. Mitochondria from *Y. lipolytica* were isolated as in [51].

### 2.4. Protein quantification

Mitochondrial protein was measured by the Biuret method [60]. Absorbance was determined at 540 nm in a Beckman DU-50 spectrophotometer. Bovine serum albumin was used as a standard.

### 2.5. Oxygen consumption

The rate of oxygen consumption was measured in a YSI-5300 Oxygraph equipped with a Clark-Type electrode (Yellow Springs Instruments Inc., OH) interfaced to a chart recorder. The sample was placed in a water-jacketed chamber at 30 °C. The phosphorylating state (III) was induced with 0.5 mM ADP. The reaction mixture was 1 M sorbitol, 10 mM maleate (pH was adjusted to 6.8 with Tris), 10 mM Tris-phosphate (Pi), 0.5 mM  $MgCl_2$  and 75 mM KCl. Mitochondrial protein (Prot) was 0.5 mg/mL; final volume was 1.5 mL. The concentrations of different respiratory substrates and inhibitors are indicated in the legends to the figures.

### 2.6. Blue native (BN) and 2D SDS-Tricine electrophoresis

BN-PAGE was performed as described in the literature [49]. The mitochondrial pellet was suspended in sample buffer (750 mM aminocaproic acid, 25 mM imidazole (pH 7.0)) and solubilized with 2.0 mg *n*-dodecyl- $\beta$ -D-maltoside (laurylmaltoside, LM)/mg Prot, or 4.0 mg digitonin (Dig)/mg Prot at 4 °C for 1 h and centrifuged at 33,000 rpm at 4 °C for 25 min. The supernatants were loaded on 4–12% (w/v) polyacrylamide gradient gels. Protein, 0.25 or 0.5 mg per lane was added to 8.5 × 6 cm or 17 × 12 cm gel sizes, respectively. The stacking gel contained 4% (w/v) polyacrylamide. Also, 0.025% digitonin was added to the gel preparation to improve protein band definition [61]. For 2D SDS-Tricine-PAGE, complete lanes from the BN-gels were loaded on 12% polyacrylamide gels to resolve the subunits that constitute each complex. 2D-gels were subjected to Coomassie-staining [61] and silver-staining [62,63]. Apparent molecular weights were estimated using Benchmark Protein (Invitrogen, CA) and Precision Plus Protein™ (BIO-RAD, Richmond, CA) standards.

### 2.7. In-gel enzymatic activities

In-gel NADH/nitrotetrazolium blue chloride (NTB) oxidoreductase activity was determined incubating native gels in a mixture of 10 mM Tris (pH 7.0), 0.5 mg NTB/mL and 1 mM NADH [64]. Inhibitors such as rotenone and flavone were not able to act on their target enzymes in the gel assays, probably due to dilution into the BN-gel incubation medium, their hydrophobicity or their specific inhibition sites on the protein i.e. the indicator (NTB) seems to receive electrons from flavin prosthetic groups [65], far from the inhibitor blocking sites (near the ubiquinone site) [66,67] (result not shown). In-gel cytochrome c oxidase (COX) activity was determined using diaminobenzidine and cytochrome c [68]. Cyanide was useful to inhibit COX (Result not shown), but cannot be used to unveil the alternative oxidase because there is no method available to measure AOX in-gel activity. In-gel ATPase activity was measured as in [61]. Oligomycin was not able to inhibit this activity (Result not shown) as previously reported in [68].

**Table 1**

Rates of oxygen consumption in isolated mitochondria from *D. hansenii* in the presence of different respiratory substrates and inhibitors.

Substrate and other additions	Rate of oxygen consumption (natgO · (min · mg Prot) <sup>-1</sup> )	Respiratory control (III/IV)
Pyruvate (10 mM) + malate (10 mM)	123 ± 10*	2.36 ± 0.07
+ ADP (500 µM)	290 ± 7**	
+ Rotenone (50 µM)	8 ± 1	
+ Flavone (500 µM)	114 ± 5	
+ Antimycin-A (5 µM)	32 ± 3	
+ NaCN (500 µM)	33 ± 2	
+ Propyl-gallate (100 µM)	108 ± 6	
Citrate (10 mM) + malate (10 mM)	138 ± 10*	2.17 ± 0.05
+ ADP (500 µM)	299 ± 12**	
+ Rotenone (50 µM)	11 ± 2	
+ Flavone (500 µM)	135 ± 5	
+ Antimycin-A (5 µM)	41 ± 3	
+ NaCN (500 µM)	39 ± 2	
+ Propyl-gallate (100 µM)	128 ± 6	
Succinate (10 mM)	143 ± 11*	1.64 ± 0.08
+ ADP (500 µM)	235 ± 14**	
+ Rotenone (50 µM)	144 ± 9	
+ Flavone (500 µM)	143 ± 11	
+ Antimycin-A (5 µM)	38 ± 3	
+ NaCN (500 µM)	39 ± 5	
+ Propyl-gallate (100 µM)	117 ± 4	
NADH (1 mM)	258 ± 9*	1.23 ± 0.05
+ ADP (500 µM)	317 ± 12**	
+ Rotenone (50 µM)	243 ± 10	
+ Flavone (500 µM)	28 ± 14	
+ Antimycin-A (5 µM)	65 ± 3	
+ NaCN (500 µM)	65 ± 4	
+ Propyl-gallate (100 µM)	204 ± 4	
Glycerol-phosphate (10 mM)	216 ± 10*	1.28 ± 0.03
+ ADP (500 µM)	276 ± 11**	
+ Rotenone (50 µM)	216 ± 10	
+ Flavone (500 µM)	216 ± 10	
+ Antimycin-A (5 µM)	39 ± 3	
+ NaCN (500 µM)	37 ± 3	
+ Propyl-gallate (100 µM)	188 ± 7	

The rates of oxygen consumption were measured in resting state (IV)\* and phosphorylating state (III)\*\*. The phosphorylating state was induced with ADP. Rates of oxygen consumption in the presence of inhibitors were measured after a steady state was reached. Reaction mixture: 1 M sorbitol, 75 mM KCl, 10 mM Tris-phosphate, 1 mM MgCl<sub>2</sub> and 10 mM maleic acid, pH 6.8 (Tris). Mitochondria 0.5 mg Prot · (mL)<sup>-1</sup> were added in each assay. Temperature 30 °C. Final volume 1.5 mL. Data from five independent experiments are expressed as the mean ± SD.

## 2.8. Protein search, alignment and sequence analysis

We used the BLAST website and the NCBI database to search and compare protein sequences from alternative respiratory enzymes. We used the known protein sequences from other yeasts [69–71] to search for possible NDH2s, AOXs and/or MitGPDHs in the *D. hansenii* NCBI database. The identified *D. hansenii* sequences were aligned against those from *S. cerevisiae*, *Y. lipolytica* and/or *C. albicans* using Clustal W 2.0 [72]. The BLAST analysis also indicated the percentages of identity and similarity between amino acid sequences.

## 2.9. Western blotting

Mitochondrial samples were diluted in 0.5 mL sample buffer (500 mM Tris pH 6.8, 10% glycerol, 10% SDS, 0.05% 2-β-mercaptoethanol and 0.01% bromophenol blue) and boiled for 5 min [73]. SDS-Tricine-PAGE was performed in a 10% polyacrylamide gel. Proteins were electrotransferred to PVDF membranes for immunoblotting using 25 mM potassium phosphate, 25 mM sodium phosphate, 12 mM Tris, 192 mM glycine and 20% methanol, pH 7.0 [74]. Membranes

were blocked with 0.5% albumin in TBS/T (50 mM Tris, 100 mM NaCl, pH 7.6, and 0.1% Tween 20) for 1 h and incubated overnight at 4 °C with the primary antibody (monoclonal mouse antibody against the AOX from the higher plant *Sauvormatum guttatum* [75]). Then, membranes were washed with TBS/T and incubated at room temperature for 1 h with the horseradish peroxidase (HRP)-conjugated secondary antibody (HRP anti-mouse-IgG). Antibodies were diluted in TBS/T. Once the membranes were washed, the bands were developed by chemiluminescence (ECL kit [76].

## 2.10. Mass spectrometry

From the BN-gels or 2D SDS-Tricine gels, the indicated bands were excised and sent for protein sequence identification by LC-MS to the University Proteomics Laboratory of the Instituto de Biotecnología, UNAM (Cuernavaca, Morelos, Mexico). Peptides were analyzed in a LC-MS system constituted by an Accela microflux liquid chromatographer (Thermo-Fisher Co., San Jose, CA, USA) with a splitter (1/20), a LTQ Orbitrap Velos mass spectrometer (Thermo-Fisher Co., San Jose, CA, USA) and a nano-electrospray ionization (ESI) system. After tryptic digestion, samples were analyzed in a tandem high-resolution mass spectrometer. Mascot and Protein-Prospector algorithms were used to search all spectrometric results against the NCBI database. Protein sequence coverage (%) is shown in Tables 3 and 5.

## 3. Results

### 3.1. *D. hansenii* contains a branched mitochondrial respiratory chain

To define the composition of the respiratory chain from *D. hansenii*, we measured the rate of oxygen consumption in isolated mitochondria using different substrates and inhibitors. To prevent the mitochondrial permeability transition (PT), 10 mM phosphate and 75 mM KCl were added (Table 1). As expected [58,59], citrate-malate and pyruvate-malate were efficiently oxidized in a rotenone-sensitive fashion by complex I while succinate was oxidized by complex II. In addition, the complex III inhibitor antimycin-A and the complex IV inhibitor NaCN partially inhibited oxygen consumption. Partial inhibitions indicated the presence of an alternative pathway for oxygen consumption [59]. The presence of an active AOX was confirmed by the partial sensitivity of the rate of oxygen consumption to propyl-gallate (PG). PG was preferred over salicylhydroxamic acid (SHAM) because full inhibition was achieved with 100 µM PG while a higher 500 µM SHAM was needed (Result not shown). Full inhibition of oxygen consumption was achieved by adding NaCN and PG together (Table 1).

The above results confirm the presence of a branched mitochondrial respiratory chain in *D. hansenii* that contains at least all four multi-subunit complexes plus an alternative AOX [55,56]. The presence of additional external alternative dehydrogenases was suggested when NADH and glycerol-phosphate were oxidized at high rates (Table 1). Oxidation of these substrates was partially sensitive to both, NaCN or PG, indicating that electrons coming from these substrates could reach either the cytochrome pathway or AOX. The external NADH dehydrogenase (NDH2e) activity was sensitive to flavone, a specific inhibitor of type II NADH dehydrogenases, but it was not sensitive to rotenone. Also, the glycerol-phosphate dehydrogenase (MitGPDH) activity was not sensitive to either rotenone or flavone. Thus, it is suggested that *D. hansenii* contains a branched mitochondrial respiratory chain composed by the four canonical complexes, alternative dehydrogenases (at least NDH2 and MitGPDH) and an AOX.

The substrates predicted to yield a higher number of protons-pumped per electron consumed in the respiratory chain ( $H^+ / e^-$ ) exhibited a higher respiratory control (RC = phosphorylating state (III)/resting state (IV)) than those with a low  $H^+ / e^-$  (Table 1), i.e., the highest respiratory controls were obtained using pyruvate-malate, RC = 2.35 ± 0.07 or citrate-malate, RC = 2.17 ± 0.05. By contrast,

with succinate a low  $RC = 1.64 \pm 0.08$  was observed, while with glycerol-phosphate  $RC = 1.28 \pm 0.03$  and with NADH  $RC = 1.23 \pm 0.05$ .

### 3.2. The putative mitochondrial NDH2e from *D. hansenii* is inhibited by flavone and exhibits a high homology with NDH2s from other sources

To confirm the presence of external NDH2(s) in *D. hansenii* the rate of oxygen consumption was titrated with rotenone to inhibit complex I or flavone to inhibit any NDH2 activity present [38]. The rate of oxygen consumption in the absence of inhibitors was taken as 100%. In the presence of pyruvate-malate, respiration was inhibited by rotenone, but it was insensitive to flavone (Fig. 1A). At 5  $\mu$ M rotenone 50% inhibition was obtained while maximum inhibition of the pyruvate-malate-supported oxygen consumption was reached at 50  $\mu$ M rotenone (Fig. 1A, full circles). By contrast, with NADH, flavone inhibited oxygen consumption while rotenone exhibited little effect (Fig. 1B). In the presence of NADH, 500  $\mu$ M flavone led to maximal inhibition (Fig. 1B, empty circles).

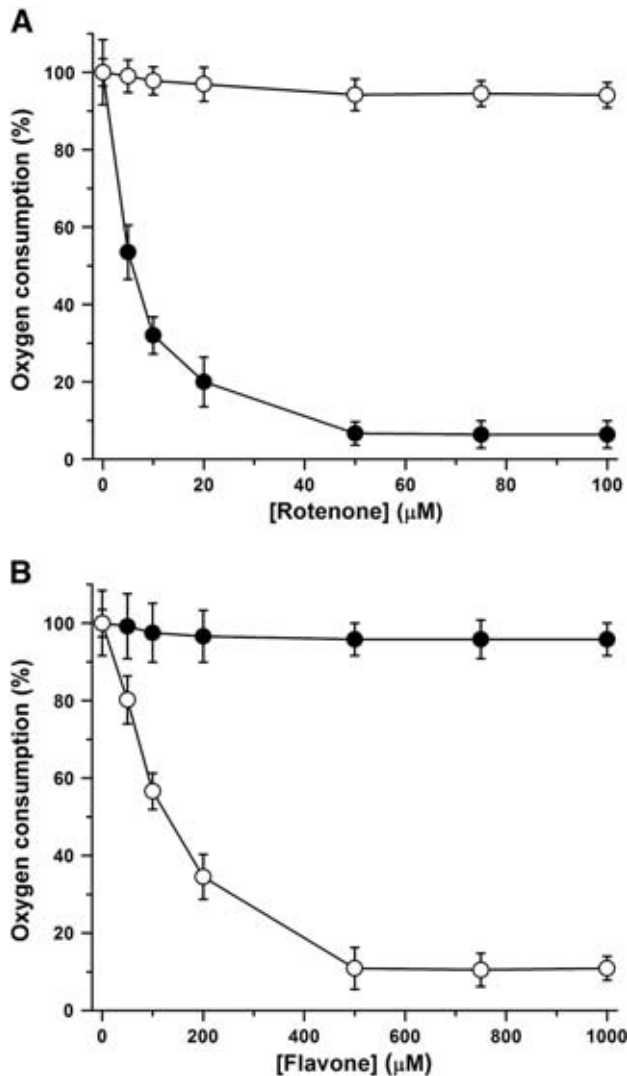


**Fig. 1.** Inhibition of oxygen consumption in isolated mitochondria from *D. hansenii* with rotenone (A) or flavone (B). The substrate was either 10 mM pyruvate-malate (●) or 1 mM NADH (○). Oxygen measurements were made in the resting state (IV). The reaction mixture was as in Table 1. Data from five independent experiments are expressed as the mean  $\pm$  SD.

Yeast species may contain different alternative dehydrogenases, e.g. *S. cerevisiae* contains three mitochondrial NDH2 isoforms plus an external MitGPDH [21,40]. To detect possible alternative dehydrogenases in the NCBI database, the genome of *D. hansenii* was analyzed for sequences homologous to those encoding for NDH2s and MitGPDHs in *Y. lipolytica* and *S. cerevisiae*. For NDH2s, the BLAST analysis unveiled a protein sequence with high homology to type II NADH dehydrogenases. This is the hypothetical protein DEHA2D07568p, a 568 amino acid (MW = 63 kDa) precursor. DEHA2D07568p was aligned against the NDH2e sequence from *Y. lipolytica* (YALI0F25135p) and the NDH2s from *S. cerevisiae*, i.e. NDI (YML120c), NDE1 (YMR145c) and NDE2 (YDL085w) (Table 2), exhibiting high sequence similarity. In addition, DEHA2D07568p closely resembles external NDH2s from several fungi and plants (Result not shown). Furthermore, when the conserved motifs described for the NDH2e from *Y. lipolytica* [77] were compared with the DEHA2D07568p, both proteins exhibited highly matching dinucleotide binding sites (for NADH or FAD) and hydrophobic regions (Fig. 2). These results plus the flavone sensitivity strongly suggest that DEHA2D07568p is an NDH2e. In addition, there is a 98.9% probability that this protein is imported into mitochondria as predicted by the MitoProt II-v1.101 program [78]. Analysis of the *D. hansenii* genome did not detect other genes coding for NDH2s.

### 3.3. *D. hansenii* has a mitochondrial glycerol-phosphate dehydrogenase (MitGPDH)

Isolated mitochondria from *D. hansenii* oxidized glycerol-phosphate at a high rate (Table 1), suggesting the presence of a mitochondrial GPDH as predicted by Adler and co-workers [79]. Thus, to look for orthologues the *D. hansenii* sequences were aligned against the corresponding genes from *S. cerevisiae* (Gut2p) and *Y. lipolytica* (YALI0B13970p). The analysis unveiled only one candidate sequence, annotated as hypothetical protein DEHA2E08624p; a 652 amino-acid precursor, MW = 72.5 kDa with a 65.9% probability of being imported by mitochondria [78]. DEHA2E08624p sequence is similar to MitGPDHs from other yeast species (Table 2) and with other MitGPDHs stored in the NCBI database. Thus, our data suggest that DEHA2E08624p is a mitochondrial GPDH.

### 3.4. The AOX in *D. hansenii* mitochondria is sensitive to AMP

In isolated mitochondria from *D. hansenii* cyanide-resistant respiration (CRR) was ~20–25% of the total. In different organisms this percentage can vary depending on different molecules or environmental

**Table 2**

*D. hansenii* putative alternative oxidoreductase sequences. Percentage of identity and similarity with those from other yeast sources.

Sequences	Identity (%)	Similarity (%)
<b>a) NDH2s</b>		
• DEHA2D07568p vs. YALI0F25135p (Y <sub>l</sub> NDH2e)	50	65
• DEHA2D07568p vs. YML120c (ScNDE1)	45	64
• DEHA2D07568p vs. YMR145c (ScNDE2)	52	69
• DEHA2D07568p vs. YDL085w (ScNDI)	50	69
<b>b) MitGPDHs</b>		
• DEHA2E08624p vs. YALI0B13970p (Y <sub>l</sub> MitGPDH)	49	64
• DEHA2E08624p vs. Gut2p (ScMitGPDH)	58	73
<b>c) AOXs</b>		
• DEHA2C03828p vs. AAQ08895 (YAOX1)	54	69
• DEHA2C03828p vs. AAQ08896 (YAOX2)	50	66
• DEHA2C03828p vs. XP_723460 (CaAOX1)	63	73
• DEHA2C03828p vs. XP_723269 (CaAOX2)	65	79

Protein sequences are shown accordingly with their NCBI definition or accession nomenclature.

Abbreviations: Sc: *S. cerevisiae*; Yl: *Y. lipolytica*; Ca: *C. albicans*; NDH2e/NDE: external alternative NADH dehydrogenase; NDI: internal alternative NADH dehydrogenase; AOX1: alternative oxidase isoform 1; AOX2: alternative oxidase isoform 2; Mit: mitochondrial isoform.

### Dinucleotide binding motif I

<i>D. hansenii</i>	90	QKKKTLVILGSGWGSISLLKNLDTLYNVVVSPR	124
<i>Y. lipolytica</i>	110	PSKKTLVVLGSGWGSVSFLKKLDTSNYNVIVVSPR	144
	.	:	:

### Hydrophobic motif I

<i>D. hansenii</i>	126	YFLFTPPLLPS	135
<i>Y. lipolytica</i>	146	YFLFTPPLLPS	155

### Hydrophobic motif II

<i>D. hansenii</i>	214	SLNYDYLVVGVAQPSTFGIPGVAEHSTFLKEV	246
<i>Y. lipolytica</i>	215	EIPFDYLVVGAMSTSFGIPGVQENACFLKEI	247
	.	:	:

### Dinucleotide binding motif II

<i>D. hansenii</i>	278	SIVVCGGGPTGVEVAGELQDYIDQDLKKWMPEVASELKVIIVEA	321
<i>Y. lipolytica</i>	278	HTVVVGGGPTGVEFAELQDFFEDLRLKWIPIRDDFKVTLVEA	321
	*	:	:

**Fig. 2.** Alignment of the conserved motifs of DEHA2D07568p and *Y. lipolytica* NDH2e amino acid sequences. (:) Conserved substitutions; (.) semi-conserved substitutions. Identical residues in both sequences are shown in gray. Numbers indicate amino acids in the linear sequence of each protein.

conditions, e.g.  $\alpha$ -ketoacids, AMP, salts, temperature and mitochondrial-matrix redox state [80–82]. In addition, many plants and microorganisms express AOX in response to ROS or cytochromic pathway inhibitors [83,84]. AOXs from yeast or from *Ustilago maydis* are activated by AMP and possibly by the redox state, but not by  $\alpha$ -ketoacids [85]. To test some of the properties of the *D. hansenii* AOX (*DhAOX*); it was decided to explore the sensitivity to AMP or pyruvate. To measure only CRR, these experiments were conducted in the presence of 500  $\mu$ M NaCN. Full oxygen consumption inhibition was achieved with 500  $\mu$ M NaCN plus 100  $\mu$ M propyl-gallate. It was observed that AMP increased CRR (~15%) while pyruvate had no effects (Fig. 3), i.e. the AOX from *D. hansenii* shares the sensitivity to AMP from other fungi AOXs.

Further analysis of AOX was conducted by comparing the *DhAOX* hypothetical protein sequence with the constitutive and inducible AOX isoforms (1 and 2, respectively) from *Yarrowia lipolytica* and *Candida albicans*. The BLAST analysis unveiled only one candidate, annotated as hypothetical protein DEHA2C03828p. This sequence corresponds to a 338 amino-acid precursor with a theoretical MW of 39.4 kDa. There is a 97.1% probability that this protein is imported by mitochondria [78]. The DEHA2C03828p sequence has high similarity to the AOXs from both yeast species (Table 2). With the above results, it may be concluded that *D. hansenii* mitochondria contain a branched respiratory chain composed by all four canonical complexes plus three alternative oxidoreductases, namely an NDH2e, a  $\text{Mit}_\text{GPDH}$  and the *DhAOX* already reported [59]. Alternative enzymes were analyzed using SDS-Tricine PAGE, western blotting and mass spectrometry (see below).

*albicans*. The BLAST analysis unveiled only one candidate, annotated as hypothetical protein DEHA2C03828p. This sequence corresponds to a 338 amino-acid precursor with a theoretical MW of 39.4 kDa. There is a 97.1% probability that this protein is imported by mitochondria [78]. The DEHA2C03828p sequence has high similarity to the AOXs from both yeast species (Table 2). With the above results, it may be concluded that *D. hansenii* mitochondria contain a branched respiratory chain composed by all four canonical complexes plus three alternative oxidoreductases, namely an NDH2e, a  $\text{Mit}_\text{GPDH}$  and the *DhAOX* already reported [59]. Alternative enzymes were analyzed using SDS-Tricine PAGE, western blotting and mass spectrometry (see below).

### 3.5. In *D. hansenii* mitochondria, respiratory complexes organize into supercomplexes

After detection of the different components of the mitochondrial respiratory chain from *D. hansenii*, it was decided to define whether the respiratory complexes were organized into supercomplexes as described for many other species [48,50,51]. Both *D. hansenii* and *Y. lipolytica* are closely related [69,70], so we decided to use *Y. lipolytica* mitochondrial respiratory complexes and supercomplexes as standards to estimate the MW of those from *D. hansenii*. For BN-PAGE, mitochondrial membranes were solubilized with either laurylmaltoside (LM) or digitonin (Dig). Digitonin was used expecting to preserve associations between respiratory complexes, while laurylmaltoside was expected to allow isolation of the individual complexes. The BN-PAGE results are shown for solubilized mitochondria from *Y. lipolytica* (Fig. 4A) and from *D. hansenii* (Fig. 4B). In LM-solubilized mitochondria, the individual complexes from either *Y. lipolytica* or *D. hansenii* were observed at different migration distances. Migration distances for complexes I, IV and V were reasonably near in both species. By contrast, the complex III band from *D. hansenii* was hardly detectable by BN-PAGE (Fig. 4B lane LM). In fact, the location of complex III was detected only in the 2D Tricine-SDS-PAGE (see below). In digitonin-solubilized mitochondria from both *Y. lipolytica* (Fig. 4A) and *D. hansenii* (Fig. 4B) several high MW bands corresponding to putative respiratory supercomplexes were revealed.

To further characterize the location and composition of each complex and supercomplex, the in-gel enzymatic activities of NADH dehydrogenase (NDH), ATPase and cytochrome c oxidase (COX) were assayed in BN-gels (Fig. 4C to E). In the LM solubilized sample, NDH activity

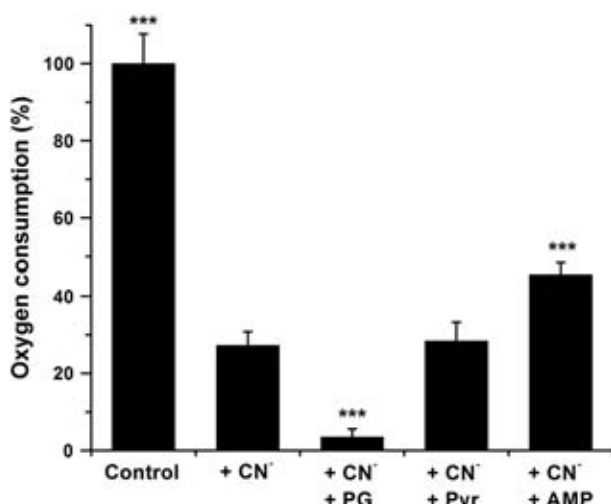


**Fig. 3.** Activation of the *D. hansenii* AOX by AMP but not by pyruvate (Pyr). Oxygen consumption was measured in state IV with 10 mM succinate as respiratory substrate. 50  $\mu$ M rotenone was added to inhibit complex I. Cytochrome-dependent oxygen consumption was inhibited with 500  $\mu$ M NaCN (CN<sup>-</sup>). 100  $\mu$ M propylgallate (PG), 10 mM pyruvate (Pyr) or 1 mM AMP was used as indicated. n = 3  $\pm$  SD. One-way ANOVA (Dunnett's multiple comparison test) \*P < 0.05 compared to the cyanide-treated sample (second bar).

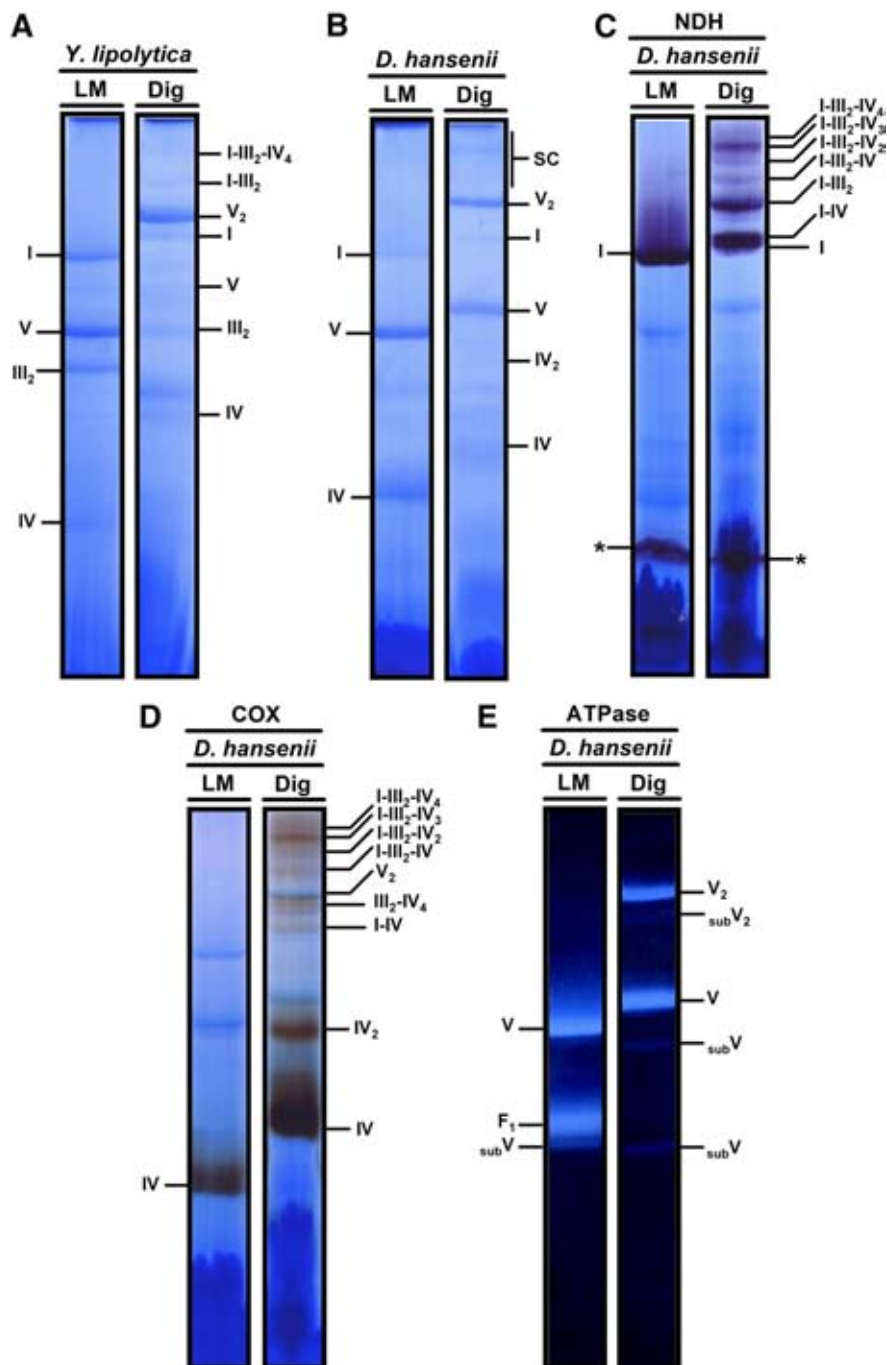


**Fig. 4.** Respiratory complexes and supercomplexes found in solubilized *D. hansenii* mitochondria. Isolated mitochondria were solubilized with laurylmaltoside (LM) 2.0 mg/mg Prot or digitonin 4.0 mg/mg Prot. (A) *Y. lipolytica* solubilizates were resolved by BN-PAGE in a 4–12% polyacrylamide gradient gel and were used as MWs standards. (B) LM- and Dig-solubilizates from *D. hansenii* mitochondria resolved by BN-PAGE. (C) In-gel NADH-dehydrogenase activity (NDH); 1 mM NADH and 0.5 mg/mL nitrotetrazolium blue chloride (NTB). (D) In-gel cytochrome c oxidase activity (COX); 0.04% diaminobenzidine and 0.02% cytochrome c. (E) In-gel ATPase activity performed in BN-gel; 35 mM Tris, 270 mM glycine, 0.2% Pb(NO<sub>3</sub>)<sub>2</sub>, 14 mM MgSO<sub>4</sub> and 8 mM ATP (pH 8.4). I, III<sub>2</sub>, IV and V are the mitochondrial mammalian-like complexes. (\*) Putative NDH2e. *D. hansenii* supercomplexes (SC) were: I-IV, I-III<sub>2</sub>, I-III<sub>2</sub>-IV, I-III<sub>2</sub>-IV<sub>2</sub>, I-III<sub>2</sub>-IV<sub>3</sub> and I-III<sub>2</sub>-IV<sub>4</sub> where stoichiometries are indicated as sub-indexes. IV<sub>2</sub>: complex IV dimer; F<sub>1</sub>: soluble domain of complex V; V<sub>2</sub>: complex V dimer; subV: complex V sub-complexes.

exhibited two purple bands corresponding to complex I and presumably to the NDH2e (Fig. 4C lane LM). When solubilized with digitonin, higher MW purple bands were detected (Fig. 4C lane Dig). These bands were assigned as supercomplexes containing complex I plus different amounts of either complex III or complex IV (see below). Also, the NDH activity seemed more intense in three bands than in all others, suggesting that complex I-containing supercomplexes were concentrated in these bands. These bands had MWs compatible with their assignment as the

complex I band running alone; as a I-IV supercomplex; a I-III<sub>2</sub> supercomplex and a I-III<sub>2</sub>-IV<sub>3</sub> supercomplex (Fig. 4C lane Dig; also see Fig. 4D which is described below).

When COX activity was measured, a single brown band was observed in the LM-solubilized lane (Fig. 4D lane LM). It is suggested that this activity is the product of monomeric complex IV. The digitonin lane revealed several brown bands corresponding to monomeric complex IV and to a number of supercomplexes containing complexes I, III<sub>2</sub>

and IV (Fig. 4D lane Dig). Supercomplex I-III<sub>2</sub>-IV<sub>3</sub> exhibited the highest activity. Also, a faint band, probably corresponding to I-IV supercomplex was detected near complex I.

In regard to in-gel ATPase activity, LM treatment revealed three activity bands that were respectively assigned as the monomeric complex V, the F<sub>1</sub> subunit and a F<sub>1</sub> subcomplex (Fig. 4E lane LM). In the first two bands the ATPase activity was much higher than the activity detected in the subcomplex, indicating that this may be at low concentrations or exhibit less activity. In the digitonin solubilized samples ATPase activity was detected in four bands (Fig. 4E lane Dig). The ATPase activity was more intense in the bands assigned as the complex V dimer and monomer, while the lower intensity bands probably were the F<sub>1</sub> subunit and an F<sub>1</sub>F<sub>0</sub>-ATP synthase sub-complex. Dimers of complex V have also been detected previously in mitochondria from beef heart, *S. cerevisiae*, *Polytomella* sp. and from other sources by digitonin solubilization or using lower LM/protein ratios [51].

To determine the location of each respiratory complex, including complex III which was not observed in the BN gels, and also whether any given complex was part of a putative supercomplex, complete BN-PAGE lanes from LM- and Dig-solubilized mitochondria were resolved by second dimension denaturing gels (2D Tricine-SDS-PAGE) and subjected to Coomassie-staining (Fig. 5) or silver-staining (Fig. 6), respectively. The second dimension gel from LM-solubilized mitochondria contains the individual subunit signatures [49] from each respiratory complex (Fig. 5). In order to confirm the assignments for complexes I, III, IV and V different bands were excised and sent to protein identification by LC-MS. The 75-kDa subunit from NADH dehydrogenase (I), the core proteins 1 and 2 from the bc<sub>1</sub> complex (III), the COX subunit 2 from cytochrome c oxidase (IV) and the gamma ( $\gamma$ ) subunit from F<sub>1</sub>F<sub>0</sub>-ATP synthase (V) were identified with a high sequence coverage (Table 3). In all cases, identified subunits were located at the lane that was previously predicted for a specific respiratory complex. Complex III, which was difficult to see before (Fig. 4B, lane LM), could be located next to the complex V monomer (Fig. 5).

In the 2D-gel obtained from digitonin-solubilized mitochondria, the subunit pattern of individual complexes was found also at high MWs indicating the presence of supercomplexes (Fig. 6). The MWs suggested that these supercomplexes contained complexes I, III and IV. In addition, a pattern corresponding to a complex V dimer (V<sub>2</sub>) was identified. It is suggested that the supercomplexes detected by BN-gels (Fig. 4) and

2D SDS-Tricine-gels (Figs. 5 and 6) were: IV<sub>2</sub>, I-IV, III<sub>2</sub>-IV<sub>4</sub>, V<sub>2</sub>, I-III<sub>2</sub>(S<sub>0</sub>), I-III<sub>2</sub>-IV(S<sub>1</sub>), I-III<sub>2</sub>-IV<sub>2</sub>(S<sub>2</sub>), I-III<sub>2</sub>-IV<sub>3</sub>(S<sub>3</sub>) and I-III<sub>2</sub>-IV<sub>4</sub>(S<sub>4</sub>).

To determine the stoichiometry and the theoretical MWs of these supercomplexes, the MWs of each complex/supercomplex were estimated by measuring the migration distance of the corresponding bands in BN-PAGE of the digitonin solubilizates from *D. hansenii* and interpolating them by linear regression in a log MW vs. migration distance plot from the solubilized mitochondrial respiratory complexes from *Y. lipolytica* that we used as MW standards (Fig. 7). The estimated MWs are shown in Table 4. The composition of each supercomplex was determined by correlating the MW estimates and the presence of NDH, COX and/or ATPase activity in each band. The calculated MWs for complex I, IV and V monomers and complex III dimer were very similar to those from *Y. lipolytica* (Fig. 7). The *D. hansenii* MWs of the supercomplexes were similar to those reported for *Y. lipolytica* [51]. By contrast, the complex V dimers from *D. hansenii* were heavier than expected (Table 4).

In mammalian systems, large supercomplexes containing I<sub>1</sub>-III<sub>2</sub>-IV<sub>4</sub> and III<sub>2</sub>-IV<sub>4</sub> have been detected in BN-gels [49]. Also, mammalian supercomplexes seem to be associated into larger “respiratory strings” [86]. In *D. hansenii*, it seems that complexes I, III<sub>2</sub> and IV organize into supercomplexes suggesting that these mitochondria also possess “respiratory strings” where chain units of the I-III<sub>2</sub>-IV<sub>3</sub> supercomplex would attach to each other. In contrast to *Y. lipolytica* [87], NDH2e seems to be detached from the cytochrome-complexes; i.e. in digitonin-treated samples in-gel NADH dehydrogenase activity was absent at the sites where cytochrome complexes migrated (Fig. 4C lane Dig).

At this point, we can conclude that the branched respiratory chain from *D. hansenii* contains a large amount of canonical respiratory complexes (I, III and IV), which may be associated in supercomplexes (Fig. 4). Alternative enzymes probably are independent from the respiratory supercomplexes (at least the NDH2e (Fig. 4C lane Dig)). Nevertheless alternative enzyme distribution needs to be explored further.

### 3.6. Identification of the alternative respiratory enzymes from *D. hansenii*

NDH2e has already been proposed to correspond to the lower NADH dehydrogenase activity band detected in a BN-gel (Fig. 4C); when this band was subjected to 2D-SDS-Tricine-PAGE different proteins were separated (Fig. 8). Three spots were selected for identification; the

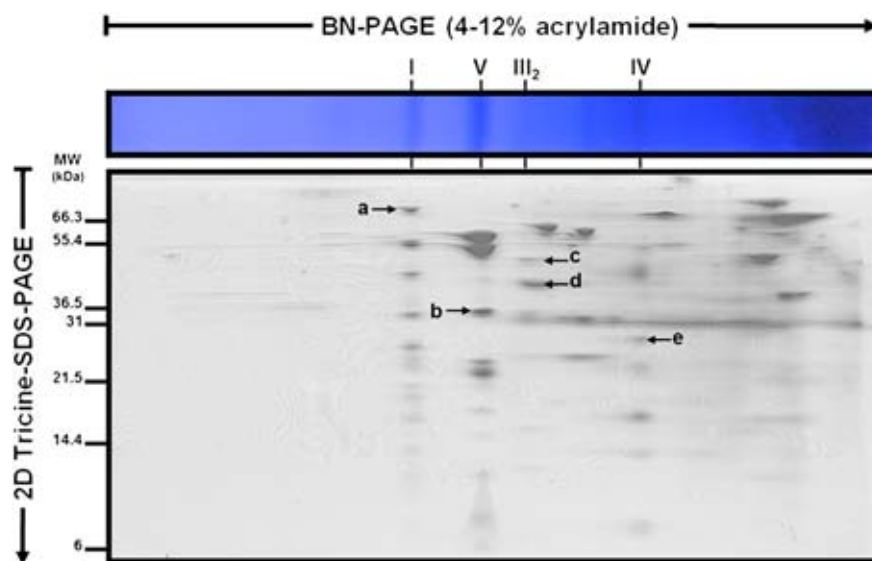


**Fig. 5.** 2D SDS-Tricine-PAGE of *D. hansenii* mitochondrial respiratory complexes. From the BN-PAGE, the lane containing the laurylmaltoside (LM) solubilized proteins was excised and subjected to 2D SDS-Tricine-PAGE. Bands that appear labeled were cut and sent for protein identification by LC-MS. These results are shown in Table 3. All SDS-Tricine-gels showed were stained with Coomassie® brilliant blue G-250. Respiratory complexes are tagged as in Fig. 4.

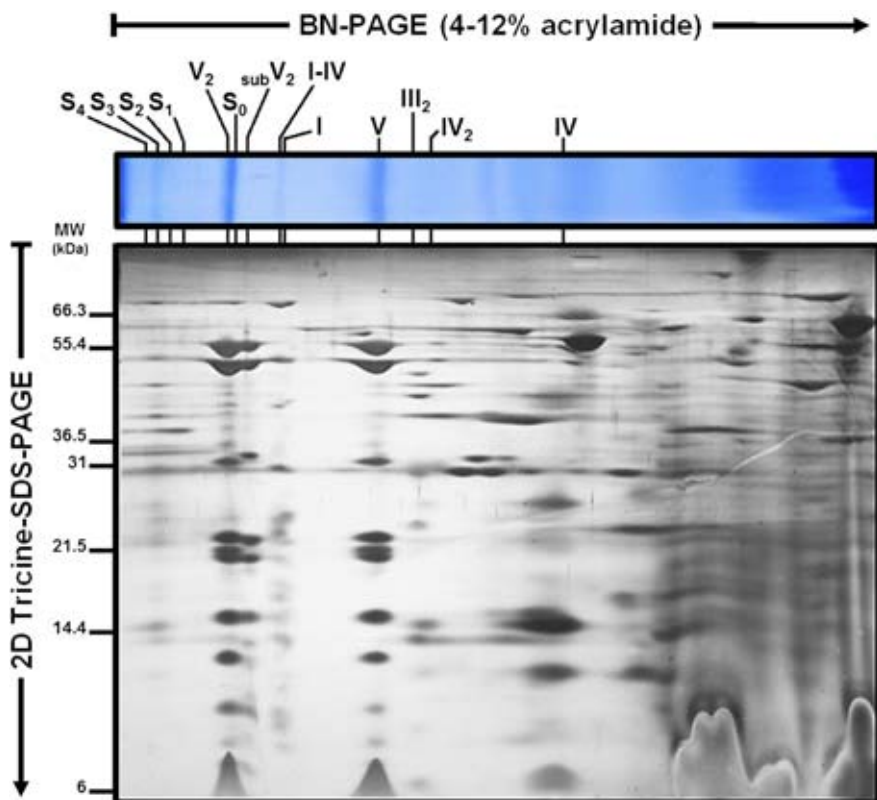


**Fig. 6.** 2D SDS-Tricine-PAGE of *D. hansenii* mitochondrial supercomplexes. After BN-PAGE, the lane containing the digitonin-solubilized proteins was excised and subjected to 2D-SDS-Tricine-PAGE followed by silver staining. Respiratory complexes are tagged as in Fig. 4. Supercomplex nomenclature: S<sub>0</sub>: I–III<sub>2</sub>, S<sub>1</sub>: I–III<sub>2</sub>–IV, S<sub>2</sub>: I–III<sub>2</sub>–IV<sub>2</sub>, S<sub>3</sub>: I–III<sub>2</sub>–IV<sub>3</sub> and S<sub>4</sub>: I–III<sub>2</sub>–IV<sub>4</sub>.

first corresponded to the hypothetical MW of NDH2e; i.e. 63 kDa (Fig. 8, f) and the other two were chosen due to their high concentration (Fig. 8, bands g and h). The spots were analyzed by LC-MS/MS and the results are shown in Table 5. The first band (f) was reported as the NDH2e hypothetical sequence (DEHA2D07568p) but surprisingly, it also contained the putative <sub>Mit</sub>GPDH (DEHA2E08624p), in spite that the predicted MWs were widely different (63 vs. 72.5 kDa, respectively) (Table 5), i.e. they were in the same spot in the 2D SDS-Tricine-gel (Fig. 8). The presence of both proteins in the asterisked band (excised from the BN-gel, Fig. 4) might reflect a physiological interaction of these alternative dehydrogenases. A similar interaction has been described in *S. cerevisiae* as part of a mitochondrial dehydrogenase membrane complex, which contains different external peripheral alternative dehydrogenases, part of the Krebs cycle enzymes (including complex II), the NDI and other NADH producing enzymes that were not defined [88]. Also, in *D. hansenii* dihydrolipoamide dehydrogenase was identified next to NDH2e and <sub>Mit</sub>GPDH (Fig. 8, g). This protein is part of the pyruvate dehydrogenase and the  $\alpha$ -ketoglutarate dehydrogenase complexes [20]. The lower band contained three proteins: the ATP/

ADP carrier (ANC); the mitochondrial porin (VDAC) and the phosphate carrier (Fig. 8, h). These proteins are involved in metabolite fluxes and have been proposed to be part of the mitochondrial unspecific channel in other yeast species [89].

In *S. cerevisiae* <sub>Mit</sub>GPDH (Gut2p) has a predicted MW = 72.4 kDa, while the mature form of this protein has a MW = 68.4 kDa [88]. This MW is close to the mature *S. cerevisiae* NDE2 with a MW = 61.7 kDa [88]. In *D. hansenii*, NDH2e exhibited an approximate MW = 60 kDa (Fig. 8) and <sub>Mit</sub>GPDH migrated very near that weight. In silico data and estimated MWs suggested that *D. hansenii* <sub>Mit</sub>GPDH contains a longer signal-sequence than the NDH2e. When both proteins mature, their MWs become similar and their electrophoretic migration coincides. As a result, both dehydrogenases appeared in the same 2D-gel spot (Fig. 8, f; Table 5).

AOX was identified by mass spectrometry (Fig. 9, upper panel) and by western blotting (WB) (Fig. 9, lower panel). For the western blot, an antibody against AOX from *S. guttatum* was used. Two bands were detected by this procedure (Fig. 9, lower panel). To determine which of these bands contains AOX, they were excised from the gel and sent

**Table 3**

Proteins identified by LC-MS analysis contained in the indicated bands from the 2D SDS-Tricine-gel (Fig. 5).

Band	Protein name	Accession no.	gl protein	Length <sup>a</sup>	Cov <sup>b</sup> (%)	MW <sup>c</sup> (kDa)
a	NADH-quinone oxidoreductase 75-kDa subunit	DEHA2G06050p	199433960	722	26.7	79
b	F <sub>1</sub> F <sub>0</sub> -ATP synthase gamma subunit	DEHA2F20658p	202953475	286	36.7	31.3
c	Ubiquinol-cytochrome c reductase core protein 1	DEHA2D13640p	199431718	445	31.7	48
d	Ubiquinol-cytochrome c reductase core protein 2	DEHA2E09834p	49655402	376	75	39.4
	IDH2 subunit of mitochondrial NAD(+) -dependent isocitrate dehydrogenase	DEHA2G05786p	49657467	365	22.2	39.5
	IDH1 subunit of mitochondrial NAD(+) -dependent isocitrate dehydrogenase	DEHA2C10758p	199430720	359	19.2	38.6
e	Cytochrome c oxidase subunit 2	YP_001621413.1	162951843	246	11.7	28.4

<sup>a</sup> Number of amino acids.

<sup>b</sup> Protein sequence coverage.

<sup>c</sup> Predicted molecular weights from the *D. hansenii* NCBI database sequences.

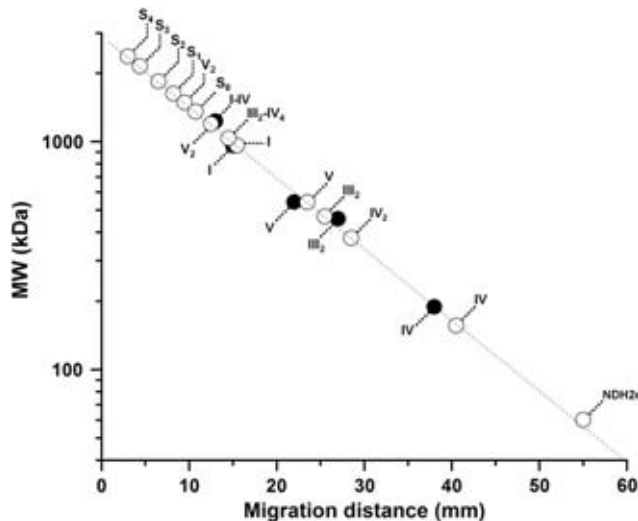


**Fig. 7.** Molecular weight (MW) estimates of the *D. hansenii* complexes and supercomplexes. The previously characterized molecular masses of *Y. lipolytica* mitochondrial complexes were plotted against their migration distance in BN-PAGE (●). Then, the migration distances of the *D. hansenii* respiratory complexes and supercomplexes (○) were interpolated and their corresponding molecular masses inferred (see values in Table 4). MW values from *Y. lipolytica* complexes I, III<sub>2</sub>, IV, V and complex V dimer (V<sub>2</sub>) were taken from the previous report by Guerrero-Castillo and co-workers [51]. (\*) Putative NDH2e. Note that y-axis is in log-scale. Nomenclature for complexes and supercomplexes is as in Figs. 4 and 6.

to LC-MS/MS analysis. AOX was the “i” band (Fig. 9, upper panel) while the “j” band contained the ANC and VDAC (Fig. 9, upper panel). Results are shown in Table 5.

Experimental evidence supports the presence of a branched mitochondrial respiratory chain in *D. hansenii*. This chain contains the multi-subunit complexes I, II, III and IV; there is also a mitochondrial F<sub>1</sub>F<sub>0</sub>-ATP synthase (complex V), which tends to be a dimer and is detached from the respiratory supercomplexes (Fig. 4E). Three alternative enzymes: NDH2e, MitGPDH and *Dh*AOX were detected as additional components of the branched respiratory chain. Preliminary evidence presented here suggests that multiprotein associations containing the alternative dehydrogenases plus at least two enzymes from the Krebs cycle do exist. Such associations have been described in *S. cerevisiae* [88].

**Table 4**  
Estimated molecular weights (MWs) of the *D. hansenii* complexes and supercomplexes by BN-PAGE.

Complex/supercomplex	Calculated MW <sup>a</sup> (kDa)	Expected MW <sup>b</sup> (kDa)
I	963 ± 49	–
III <sub>2</sub>	469 ± 24	–
IV	156 ± 12	–
V	541 ± 28	–
IV <sub>2</sub>	377 ± 19	312
I-IV	1035 ± 53	1119
III <sub>2</sub> -IV <sub>4</sub>	1196 ± 61	1223
I-III <sub>2</sub> (S <sub>0</sub> )	1356 ± 35	1432
V <sub>2</sub>	1484 ± 76	1082
I-III <sub>2</sub> -IV (S <sub>1</sub> )	1630 ± 87	1588
I-III <sub>2</sub> -IV <sub>2</sub> (S <sub>2</sub> )	1842 ± 51	1744
I-III <sub>2</sub> -IV <sub>3</sub> (S <sub>3</sub> )	2143 ± 59	1900
I-III <sub>2</sub> -IV <sub>4</sub> (S <sub>4</sub> )	2370 ± 135	2056

Complex and supercomplex nomenclature as in Figs. 4–6.

<sup>a</sup> Calculated MW of the *D. hansenii* complexes and supercomplexes correspond to the mean ± SD from three independent experiments.

<sup>b</sup> Supercomplexes expected MWs correspond to the sum of the individual MW of each respiratory complex according to their stoichiometries (subscript numbers).

#### 4. Discussion

The structure of the branched mitochondrial respiratory chain from *D. hansenii* was analyzed in isolated mitochondria. In addition, we characterized the association pattern of respiratory complexes into respiratory supercomplexes [44,48,49,86]. In agreement with Veiga and co-workers [59], we found that the *D. hansenii* respiratory chain contains all four canonical respiratory complexes I, II, III and IV plus an AOX. In addition, we detected two additional components, namely, an external type II NADH dehydrogenase (NDH2e) and a mitochondrial glycerol-phosphate dehydrogenase (<sub>Mit</sub>GPDH).

AOX activity is resistant to cyanide [58,80]; electrons reach it directly from the ubiquinone pool, as indicated by the resistance of oxygen consumption activity to the complex III inhibitor antimycin-A (Table 1, Fig. 3). Cyanide-resistant, AOX-supported respiration is found in many yeast species, including *D. hansenii* and it has been proposed that AOX regulates energy production in response to different physiological conditions [57–59]. Regulation is the result of a decrease in the electron flux to the cytochromic pathway with the concomitant increase in electron flux to AOX [34–36,87]. Here, it was observed that *D. hansenii* alternative oxidase (*Dh*AOX) is activated by AMP while it is insensitive to α-ketoacids, such as pyruvate. AMP activation is widely reported for AOXs from different yeasts and fungi [21,80,85]. It was suggested that *Dh*AOX activity is induced at the stationary growth phase [59]. In this view, the presence of the AOX could be helpful to diminish the electron flux through the cytochromic pathway and reduce the ATP/O ratio in this physiological condition. In contrast to Veiga and co-workers [59], in our hands *Dh*AOX activity was detected in isolated mitochondria from mid-exponential growth phase cultures. This is probably due to the differences in growth conditions, as we used a non-fermentable carbon source (lactate, see Materials and methods) [14]. This result suggests that *Dh*AOX is active in early growth phases and not only at the stationary phase where it probably acts as an energy sink [35,87]. In cells grown in lactate, *Dh*AOX was detected regardless of the addition of AMP (Table 1, Fig. 3). The role of *Dh*AOX in different growth phases requires further studies.

Two other alternative enzymes, a glycerol-phosphate dehydrogenase and an alternative NADH dehydrogenase were both bound to the external face of the IMM. Electrons were fed to <sub>Mit</sub>GPDH and NDH2e by external glycerol-phosphate or NADH, respectively. These electrons were used to reduce oxygen. From the BLAST analysis of the genomes, we concluded that there is a single gene codifying for each of these

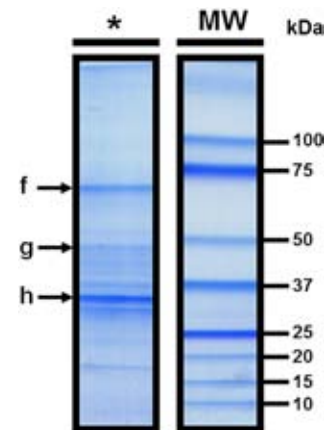


**Fig. 8.** Identification of the *D. hansenii* alternative NADH dehydrogenase (NDH2e) and the mitochondrial glycerol-phosphate dehydrogenase (<sub>Mit</sub>GPDH) by 2D SDS-Tricine-PAGE and LC-MS. (\*) NADH dehydrogenase activity band from the BN gel, which was excised and subjected to 2D SDS-Tricine-PAGE in order to separate components. SDS-Tricine-gel was stained with Coomassie® brilliant blue G-250. Both *D. hansenii*. Bands contained f: NDH2e and MitGPDH, g: dihydrolipoamide dehydrogenase (subunit from pyruvate dehydrogenase and α-keto glutarate dehydrogenase) and h: ANC, PiC and VDAC (Table 5).

**Table 5**

Proteins identified by LC-MS analysis contained in the indicated bands from the SDS-Tricine-gels (Figs. 8 and 9).

Band	Protein name	Accession no.	gi protein	Length <sup>a</sup>	Cov <sup>b</sup> (%)	MW <sup>c</sup> (kDa)
f	Glycerol-3-phosphate dehydrogenase ( <i>Mit</i> GPDH) precursor	DEHA2E08624p	49655350	652	25.3	72.5
	Mitochondrial external alternative NADH dehydrogenase (NDH2e) precursor	DEHA2D07568p	199431532	568	38.2	63
g	Dihydrolipoamide dehydrogenase	CBS767	49653406	495	58	53.2
	Major ADP/ATP carrier (ANC) of the mitochondrial inner membrane	DEHA2E12276p	49655508	301	41.5	33
h	Voltage-dependent anion channel (VDAC) of the outer mitochondrial membrane	DEHA2D16456p	49654868	282	65.6	29.9
	Mitochondrial phosphate carrier (PiC)	DEHA2B12188p	49653149	307	33.6	32.4
i	Alternative oxidase (AOX) precursor	DEHA2C03828p	199430515	338	36.7	39.4
j	Major ADP/ATP carrier (ANC) of the mitochondrial inner membrane	DEHA2E12276p	49655508	301	38.5	33
	Voltage-dependent anion channel (VDAC) of the outer mitochondrial membrane	DEHA2D16456p	49654868	282	52.1	29.9

<sup>a</sup> Amino acid sequence length.

<sup>b</sup> Protein sequence coverage.

<sup>c</sup> Predicted molecular weights from the *D. hansenii* NCBI database sequences.

proteins and we assigned DEHA2E08624p and DEHA2D07568p as the *Mit*GPDH and the NDH2e, respectively. These sequences were highly homologous to those from *Y. lipolytica* [77] and *S. cerevisiae* [90] (Fig. 2, Table 2).

NDH2e from *D. hansenii* was insensitive to rotenone while it was inhibited specifically by flavone. In isolated mitochondria from *D. hansenii*, 500 μM flavone promoted maximum inhibition of oxygen consumption (Fig. 1B, empty circles), which is similar to the concentrations reported for other organisms, e.g. in isolated mitochondria from *Plasmodium yoelii yoelii* [91] or *Paracoccidioides brasiliensis* [92] exogenous NADH-supported oxygen uptake is inhibited at similar flavone concentrations. In isolated mitochondria from *U. maydis*, complete inhibition is obtained at 250 μM flavone [85]. The flavone-mediated inhibition of the NADH:Q<sub>5</sub> oxidoreductase from *S. cerevisiae* exhibited an IC<sub>50</sub> = 95 μM, although in the presence of 300 μM flavone, activity was still at 20% [38].

NDH2e has been proposed to compensate for the absence of an aspartate-malate shuttle in ascomycetous fungi [85]. Here, we observed a high rate of exogenous NADH oxidation in isolated mitochondria from *D. hansenii*. Mitochondrial NADH oxidation probably occurs in the intact cell, establishing a NADH/NAD<sup>+</sup> recirculation cycle with the cytosol. Furthermore, probably *Mit*GPDH also constitutes an important mitochondrial sink of redox equivalents [93].

In *D. hansenii* active synthesis and accumulation of glycerol and lipids occur during growth; remarkably, these activities are stimulated by high salt concentrations [79] and *Mit*GPDH seems to participate in both processes. In addition, in *S. cerevisiae*, glycerol-phosphate dehydrogenase is finely regulated by the activity of NDHs, i.e. at saturating NADH, alternative NADH dehydrogenases physically attached to the *Mit*GPDH inhibit the use of glycerol-phosphate and transfer only

electrons that come from external NDH [39]. In fact, the presence of both enzymes, whether associated or not, causes competition for the entrance of electrons into the respiratory chain [94].

In *Y. lipolytica* growing in the exponential phase, electrons entering the respiratory chain at NDH2e are channeled to the cytochrome pathway [87]. This reflects the presence of an NDH2e-III<sub>2</sub>-IV supercomplex. By contrast, electrons coming from pyruvate-malate (Complex I) or succinate (Complex II) can reach either the cytochrome or the alternative pathways both in *Y. lipolytica* and in *D. hansenii*. The presence of unattached non proton-pumping alternative oxidoreductases (NDH2e, *Mit*GPDH, and *Dh*AOX) probably constitutes a physiological mitochondrial uncoupling mechanism [35]. This is interesting, as *Y. lipolytica* seems to lack the ability to undergo a permeability transition [51,95] while *D. hansenii* does possess a mitochondrial unspecific channel [14]. Electron transfer from the alternative oxidoreductases to AOX constitutes a futile oxygen consumption pathway that needs to be tightly regulated [89]. The presence of this pathway in *D. hansenii* during the exponential growth phase is puzzling, although it may be suggested that it participates in the modulation of ROS production as has been proposed in other branched respiratory chains [35].

In *D. hansenii*, the mammalian-like mitochondrial respiratory complexes I, III and IV are associated in supercomplexes. Supramolecular organization of the respiratory chain has been proposed to promote electron channeling, stabilization of labile multi-subunit complexes and sequestration of free radicals [48]. Consistent association patterns of supercomplexes observed by BN-PAGE, strongly suggest the existence of larger structures such as "respiratory strings" [86] or "respiratory patches" [54]. In *Y. lipolytica* supercomplexes I-III<sub>2</sub>, I-III<sub>2</sub>-IV<sub>4</sub>, I-IV, III<sub>2</sub>-IV and III<sub>2</sub>-IV<sub>2</sub> and a complex V dimer have been described [51]. In *S. cerevisiae* mitochondria a supercomplex III<sub>2</sub>-IV<sub>2</sub> has been detected [96]. In *D. hansenii* respiratory supercomplexes involving complexes I, III and IV were similar to those found in *Y. lipolytica*. Supercomplexes I-III<sub>2</sub>, I-III<sub>2</sub>-IV<sub>3</sub> and III<sub>2</sub>-IV<sub>4</sub> from *D. hansenii* contained the higher NADH dehydrogenase and COX activities as measured in BN-gels (Fig. 4C and D, lanes Dig). These supercomplexes were better observed in the activity staining experiments. In addition, the complex V dimer was easily observed both in the BN-gel and by ATPase activity staining (Fig. 4B and E, lane Dig). The *D. hansenii* F<sub>1</sub>F<sub>0</sub>-ATP synthase dimer was heavier than the V<sub>2</sub> from *Y. lipolytica*. This is probably due to stronger interactions between the subunits of complex V in these mitochondria than in other yeasts. Another explanation to this observation could be that V<sub>2</sub> may be associated to, and stabilized by the ATP/ADP carrier (ANC) and the phosphate carrier (PiC) in a structure known as the "synthasome" [97]. Molecular weights from the other respiratory complexes were similar to those from *Y. lipolytica*. Moreover, a big difference was observed between the single classical complexes from both *D. hansenii* and *Y. lipolytica* (Fig. 4A and B, lanes LM). In *D. hansenii* respiratory complexes were observed in smaller concentration than complex V. In fact, complex III was not observed in the BN-gels; it was only located by its subunit pattern in the 2D-SDS-Tricine-gels (Fig. 5) and by the identification of the core proteins 1 and 2 by mass

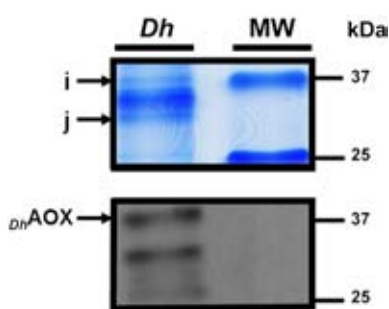


**Fig. 9.** Identification of the *D. hansenii* alternative oxidase (AOX) by SDS-Tricine-PAGE, western blotting and LC-MS. Total mitochondrial protein extract was subjected to SDS-Tricine-PAGE. SDS-Tricine-gel was stained with Coomassie® brilliant blue G-250 (upper panel). The SDS-Tricine-gel was electrotransferred onto PVDF membrane for western blotting. The membrane was decorated with a monoclonal mouse antibody against the AOX from the higher plant *S. guttatum* (lower panel). The two bands that were resulted immunoreactive in panel A (labeled as "i" and "j") were excised and subjected to identification by LC-MS. These results are shown in Table 5. At the upper panel, *D. hansenii* AOX corresponds to the "i" band. *DhAOX*: *Debaryomyces hansenii* alternative oxidase.

spectrometry (Table 3). Cytochromic complexes III and IV are postulated to be the scaffold of the “respiratory string” [86]. In this case, our observation is unclear, as complex III does not seem to be present in the same amount as complex IV (Fig. 4B, lane LM). These results are not clearly understood and need to be explored further. Still, the electrophoretic migration of respiratory supercomplexes, their putative MWs, their enzymatic activities and the LC-MS identification of some of their subunits indicate that the mitochondrial respiratory chain from *D. hansenii* associates into supercomplexes which are very similar to those detected in organisms studied before such as mammals [44,48,68], plants [43,45,46,50] and other yeasts such as *S. cerevisiae* [44,53] and *Y. lipolytica* [51].

This is the first description of the complete structure of the branched respiratory chain from *D. hansenii*. In addition, we analyzed the supramolecular organization of the classical respiratory complexes in *D. hansenii* mitochondria. Alternative redox enzymes from this yeast do not seem to be attached to supercomplexes at least under our experimental conditions (mid-exponential phase, non-fermentable carbon source), which suggests that the *D. hansenii* alternative oxidoreductases dynamically associate/dissociate with supercomplexes. This would be in agreement with a dynamic plasticity model of the oxidative phosphorylation [55], i.e. respiratory components alternate between association in supercomplexes and free forms.

## Acknowledgements

Technical assistance was received from Martha Calahorra, Ramón Méndez-Franco and Norma Sánchez. We thank Dr Juan Pablo Pardo for the gift of the AOX antibody. Partially funded by the PAPIIT program and DGAPA/UNAM (grant IN202612). ACO, SGC and MRL are CONACYT fellows enrolled in the Biochemistry Graduate Program at UNAM. This is a partial requirement for the obtention of the PhD degree by ACO.

## References

- [1] J.C. Gonzalez-Hernandez, C.A. Cardenas-Monroy, A. Pena, Sodium and potassium transport in the halophilic yeast *Debaryomyces hansenii*, Yeast 21 (2004) 403–412.
- [2] U. Breuer, H. Harms, *Debaryomyces hansenii*—an extremophilic yeast with biotechnological potential, Yeast 23 (2006) 415–427.
- [3] B. Norkrans, Studies on marine occurring yeasts: growth related to pH, NaCl concentration and temperature, Arch. Mikrobiol. 54 (1966) 374–392.
- [4] B. Norkrans, A. Kylin, Regulation of the potassium to sodium ratio and of the osmotic potential in relation to salt tolerance in yeasts, J. Bacteriol. 100 (1969) 836–845.
- [5] C. Prista, M.C. Loureiro-Dias, V. Montiel, R. Garcia, J. Ramos, Mechanisms underlying the halotolerant way of *Debaryomyces hansenii*, FEMS Yeast Res. 5 (2005) 693–701.
- [6] J.A. Hobot, D.H. Jennings, Growth of *Debaryomyces hansenii* and *Saccharomyces cerevisiae* in relation to pH and salinity, Exp. Mycol. 5 (1981) 217–228.
- [7] H. Seiler, M. Busse, The yeasts of cheese brines, Int. J. Food Microbiol. 11 (1990) 289–303.
- [8] T. Nakase, M. Suzuki, Taxonomic studies on *Debaryomyces hansenii* (Zopf) Lodder et Kreger-Van Rij and related species. II. Practical discrimination and nomenclature, J. Gen. Appl. Microbiol. 31 (1985) 71–86.
- [9] T.v.d. Tempel, M. Jakobsen, The technological characteristics of *Debaryomyces hansenii* and *Yarrowia lipolytica* and their potential as starter cultures for production of Danablu, Int. Dairy J. 10 (2000) 263–270.
- [10] M.E. Fadda, V. Mossa, M.B. Pisano, M. Deplano, S. Cosentino, Occurrence and characterization of yeasts isolated from artisanal Fiore Sardo cheese, Int. J. Food Microbiol. 95 (2004) 51–59.
- [11] N.S. Sanchez, M. Calahorra, J.C. Gonzalez-Hernandez, A. Pena, Glycolytic sequence and respiration of *Debaryomyces hansenii* as compared to *Saccharomyces cerevisiae*, Yeast 23 (2006) 361–374.
- [12] N.S. Sanchez, R. Arreguin, M. Calahorra, A. Pena, Effects of salts on aerobic metabolism of *Debaryomyces hansenii*, FEMS Yeast Res. 8 (2008) 1303–1312.
- [13] M. Calahorra, N.S. Sanchez, A. Pena, Activation of fermentation by salts in *Debaryomyces hansenii*, FEMS Yeast Res. 9 (2009) 1293–1301.
- [14] A. Cabrera-Orefice, S. Guerrero-Castillo, L.A. Luevano-Martinez, A. Pena, S. Uribe-Carvaljal, Mitochondria from the salt-tolerant yeast *Debaryomyces hansenii* (halophilic organelles?), J. Bioenerg. Biomembr. 42 (2010) 11–19.
- [15] M. Gutierrez-Aguilar, X. Perez-Martinez, E. Chavez, S. Uribe-Carvaljal, In *Saccharomyces cerevisiae*, the phosphate carrier is a component of the mitochondrial unselective channel, Arch. Biochem. Biophys. 494 (2010) 184–191.
- [16] B. Guerin, O. Bunoust, V. Rouqueys, M. Rigoulet, ATP-induced unspecific channel in yeast mitochondria, J. Biol. Chem. 269 (1994) 25406–25410.
- [17] S. Manon, M. Guerin, Investigation of the yeast mitochondrial unselective channel in intact and permeabilized spheroplasts, Biochem. Mol. Biol. Int. 44 (1998) 565–575.
- [18] V. Perez-Vazquez, A. Saavedra-Molina, S. Uribe, In *Saccharomyces cerevisiae*, cations control the fate of the energy derived from oxidative metabolism through the opening and closing of the yeast mitochondrial unselective channel, J. Bioenerg. Biomembr. 35 (2003) 231–241.
- [19] M. Gutierrez-Aguilar, V. Perez-Vazquez, O. Bunoust, S. Manon, M. Rigoulet, S. Uribe, In yeast, Ca<sup>2+</sup> and octylguanidine interact with porin (VDAC) preventing the mitochondrial permeability transition, Biochim. Biophys. Acta 1767 (2007) 1245–1251.
- [20] D.G. Nicholls, S.J. Ferguson, Bioenergetics 3, Academic Press, London, 2002.
- [21] T. Joseph-Horne, D.W. Hollomon, P.M. Wood, Fungal respiration: a fusion of standard and alternative components, Biochim. Biophys. Acta 1504 (2001) 179–195.
- [22] I.M. Juszczuk, A.M. Rychter, Alternative oxidase in higher plants, Acta Biochim. Pol. 50 (2003) 1257–1271.
- [23] N. Sen, H.K. Majumder, Mitochondrion of protozoan parasite emerges as potent therapeutic target: exciting drugs are on the horizon, Curr. Pharm. Des. 14 (2008) 839–846.
- [24] A. McDonald, G. Vanlerberghe, Branched mitochondrial electron transport in the Animalia: presence of alternative oxidase in several animal phyla, IUBMB Life 56 (2004) 333–341.
- [25] D. Munro, N. Pichaud, F. Paquin, V. Kemeid, P.U. Blier, Low hydrogen peroxide production in mitochondria of the long-lived *Arctica islandica*: underlying mechanisms for slow aging, Aging cell 12 (2013) 584–592.
- [26] R. Buschges, G. Bahrenberg, M. Zimmermann, K. Wolf, NADH: ubiquinone oxidoreductase in obligate aerobic yeasts, Yeast 10 (1994) 475–479.
- [27] J. Nosek, H. Fukuhara, NADH dehydrogenase subunit genes in the mitochondrial DNA of yeasts, J. Bacteriol. 176 (1994) 5622–5630.
- [28] D.A. Berthold, M.E. Andersson, P. Nordlund, New insight into the structure and function of the alternative oxidase, Biochim. Biophys. Acta 1460 (2000) 241–254.
- [29] M.S. Albury, C. Affourtit, P.G. Crichton, A.L. Moore, Structure of the plant alternative oxidase, Site-directed mutagenesis provides new information on the active site and membrane topology, J. Biol. Chem. 277 (2002) 1190–1194.
- [30] M.E. Andersson, P. Nordlund, A revised model of the active site of alternative oxidase, FEBS Lett. 449 (1999) 17–22.
- [31] A.L. Moore, J.N. Siedow, The regulation and nature of the cyanide-resistant alternative oxidase of plant mitochondria, Biochim. Biophys. Acta 1059 (1991) 121–140.
- [32] H. Lambers, The physiological significance of the cyanide-resistant respiration in higher plants, Plant Cell Environ. 3 (1980) 293–302.
- [33] D.A. Day, J.T. Wiskich, Regulation of alternative oxidase activity in higher plants, J. Bioenerg. Biomembr. 27 (1995) 379–385.
- [34] D.P. Maxwell, Y. Wang, L. McIntosh, The alternative oxidase lowers mitochondrial reactive oxygen production in plant cells, Proc. Natl. Acad. Sci. U. S. A. 96 (1999) 8271–8276.
- [35] S. Guerrero-Castillo, D. Araiza-Olivera, A. Cabrera-Orefice, J. Espinasa-Jaramillo, M. Gutierrez-Aguilar, L.A. Luevano-Martinez, A. Zepeda-Bastida, S. Uribe-Carvaljal, Physiological uncoupling of mitochondrial oxidative phosphorylation. Studies in different yeast species, J. Bioenerg. Biomembr. 43 (2011) 323–331.
- [36] R. El-Khoury, E. Dufour, M. Rak, N. Ramanantsoa, N. Grandchamp, Z. Csaba, B. Duvillie, P. Benit, J. Gallego, P. Gressens, C. Sarkis, H.T. Jacobs, P. Rustin, Alternative oxidase expression in the mouse enables bypassing cytochrome c oxidase blockade and limits mitochondrial ROS overproduction, PLoS Genet. 9 (2013) e1003182.
- [37] S. Kerscher, S. Drose, V. Zickermann, U. Brandt, The three families of respiratory NADH dehydrogenases, Results Probl. Cell Differ. 45 (2008) 185–222.
- [38] S. de Vries, L.A. Grivell, Purification and characterization of a rotenone-insensitive NADH:Q6 oxidoreductase from mitochondria of *Saccharomyces cerevisiae*, Eur. J. Biochem. 176 (1988) 377–384.
- [39] I.L. Pahlman, C. Larsson, N. Averet, O. Bunoust, S. Boubeker, L. Gustafsson, M. Rigoulet, Kinetic regulation of the mitochondrial glycerol-3-phosphate dehydrogenase by the external NADH dehydrogenase in *Saccharomyces cerevisiae*, J. Biol. Chem. 277 (2002) 27991–27995.
- [40] M. Rigoulet, A. Mourier, A. Galinier, L. Casteilla, A. Devin, Electron competition process in respiratory chain: regulatory mechanisms and physiological functions, Biochim. Biophys. Acta 1797 (2010) 671–677.
- [41] B. Ronnow, M.C. Kielland-Brandt, GUT2, a gene for mitochondrial glycerol 3-phosphate dehydrogenase of *Saccharomyces cerevisiae*, Yeast 9 (1993) 1121–1130.
- [42] C.R. Hackenbrock, B. Chazotte, S.S. Gupte, The random collision model and a critical assessment of diffusion and collision in mitochondrial electron transport, J. Bioenerg. Biomembr. 18 (1986) 331–368.
- [43] H. Eubel, J. Heinemeyer, H.P. Braun, Identification and characterization of respirasomes in potato mitochondria, Plant Physiol. 134 (2004) 1450–1459.
- [44] H. Schagger, K. Pfeiffer, Supercomplexes in the respiratory chains of yeast and mammalian mitochondria, EMBO J. 19 (2000) 1777–1783.
- [45] F. Krause, N.H. Reischneider, D. Vocke, H. Seelert, S. Rexroth, N.A. Dencher, “Respirasome”-like supercomplexes in green leaf mitochondria of spinach, J. Biol. Chem. 279 (2004) 48369–48375.
- [46] H. Eubel, L. Jansch, H.P. Braun, New insights into the respiratory chain of plant mitochondria. Supercomplexes and a unique composition of complex II, Plant Physiol. 133 (2003) 274–286.
- [47] G. Lenaz, M.L. Genova, Kinetics of integrated electron transfer in the mitochondrial respiratory chain: random collisions vs. solid state electron channeling, Am. J. Physiol. Cell Physiol. 292 (2007) C1221–C1239.
- [48] H. Schagger, Respiratory chain supercomplexes of mitochondria and bacteria, Biochim. Biophys. Acta 1555 (2002) 154–159.
- [49] H. Schagger, Respiratory chain supercomplexes, IUBMB Life 52 (2001) 119–128.
- [50] N.V. Dudkina, J. Heinemeyer, S. Sunderhaus, E.J. Boekema, H.P. Braun, Respiratory chain supercomplexes in the plant mitochondrial membrane, Trends Plant Sci. 11 (2006) 232–240.

- [51] S. Guerrero-Castillo, M. Vazquez-Acevedo, D. Gonzalez-Halphen, S. Uribe-Carvajal, In *Yarrowia lipolytica* mitochondria, the alternative NADH dehydrogenase interacts specifically with the cytochrome complexes of the classic respiratory pathway, *Biochim. Biophys. Acta* 1787 (2009) 75–85.
- [52] H. Boumans, L.A. Grivell, J.A. Berden, The respiratory chain in yeast behaves as a single functional unit, *J. Biol. Chem.* 273 (1998) 4872–4877.
- [53] R.A. Stuart, Supercomplex organization of the oxidative phosphorylation enzymes in yeast mitochondria, *J. Bioenerg. Biomembr.* 40 (2008) 411–417.
- [54] E. Nubel, I. Wittig, S. Kerscher, U. Brandt, H. Schagger, Two-dimensional native electrophoretic analysis of respiratory supercomplexes from *Yarrowia lipolytica*, *Proteomics* 9 (2009) 2408–2418.
- [55] R. Acin-Perez, P. Fernandez-Silva, M.L. Peleato, A. Perez-Martos, J.A. Enriquez, Respiratory active mitochondrial supercomplexes, *Mol. Cell* 32 (2008) 529–539.
- [56] E.J. Boekema, H.P. Braun, Supramolecular structure of the mitochondrial oxidative phosphorylation system, *J. Biol. Chem.* 282 (2007) 1–4.
- [57] A. Veiga, J.D. Arrabaca, M.C. Loureiro-Dias, Cyanide-resistant respiration is frequent, but confined to yeasts incapable of aerobic fermentation, *FEMS Microbiol. Lett.* 190 (2000) 93–97.
- [58] A. Veiga, J.D. Arrabaca, M.C. Loureiro-Dias, Cyanide-resistant respiration, a very frequent metabolic pathway in yeasts, *FEMS Yeast Res.* 3 (2003) 239–245.
- [59] A. Veiga, J.D. Arrabaca, F. Sansonetty, P. Ludovico, M. Corte-Real, M.C. Loureiro-Dias, Energy conversion coupled to cyanide-resistant respiration in the yeasts *Pichia membranifaciens* and *Debaryomyces hansenii*, *FEMS Yeast Res.* 3 (2003) 141–148.
- [60] A.G. Gornall, C.J. Bardawill, M.M. David, Determination of serum proteins by means of the biuret reaction, *J. Biol. Chem.* 177 (1949) 751–766.
- [61] I. Wittig, H. Schagger, Advantages and limitations of clear-native PAGE, *Proteomics* 5 (2005) 4338–4346.
- [62] B.R. Oakley, D.R. Kirsch, N.R. Morris, A simplified ultrasensitive silver stain for detecting proteins in polyacrylamide gels, *Anal. Biochem.* 105 (1980) 361–363.
- [63] W. Wray, T. Boulikas, V.P. Wray, R. Hancock, Silver staining of proteins in polyacrylamide gels, *Anal. Biochem.* 118 (1981) 197–203.
- [64] E. Zerbetto, L. Vergani, F. Dabbeni-Sala, Quantification of muscle mitochondrial oxidative phosphorylation enzymes via histochemical staining of blue native polyacrylamide gels, *Electrophoresis* 18 (1997) 2059–2064.
- [65] M.S. Johnson, S.A. Kuby, Studies on NADH (NADPH)-cytochrome c reductase (FMN-containing) from yeast. Isolation and physicochemical properties of the enzyme from top-fermenting ale yeast, *J. Biol. Chem.* 260 (1985) 12341–12350.
- [66] U. Brandt, A two-state stabilization-change mechanism for proton-pumping complex I, *Biochim. Biophys. Acta* 1807 (2011) 1364–1369.
- [67] M. Iwata, Y. Lee, T. Yamashita, T. Yagi, S. Iwata, A.D. Cameron, M.J. Maher, The structure of the yeast NADH dehydrogenase (Ndi1) reveals overlapping binding sites for water- and lipid-soluble substrates, *Proc. Natl. Acad. Sci. U. S. A.* 109 (2012) 15247–15252.
- [68] I. Wittig, M. Karas, H. Schagger, High resolution clear native electrophoresis for in-gel functional assays and fluorescence studies of membrane protein complexes, *Mol. Cell. Proteomics* 6 (2007) 1215–1225.
- [69] B. Dujon, D. Sherman, G. Fischer, P. Durrens, S. Casaregola, I. Lafontaine, J. De Montigny, C. Marche, C. Neveuville, E. Talla, N. Goffard, L. Frangeul, M. Aigle, V. Anthouard, A. Babour, V. Barbe, S. Barnay, S. Blanchin, J.M. Beckerich, E. Beyne, C. Bleykasten, A. Boisrame, J. Boyer, L. Cattolico, F. Confaniolieri, A. De Daruvar, L. Despons, E. Fabre, C. Fairhead, H. Ferry-Dumazet, A. Groppi, F. Hantraye, C. Hennequin, N. Jauniaux, P. Joyet, R. Kachouri, A. Kerrest, R. Koszul, M. Lemaire, I. Lesur, L. Ma, H. Muller, J.M. Nicaud, M. Nikolski, S. Oztas, O. Ozier-Kalogeropoulos, S. Pellenz, S. Potier, G.F. Richard, M.L. Straub, A. Suleau, D. Swennen, F. Tekaia, M. Wesolowski-Louvel, E. Westhof, B. Wirth, M. Zeniou-Meyer, I. Zivanovic, M. Bolotin-Fukuhara, A. Thierry, C. Bouchier, B. Caudron, C. Scarpelli, C. Gaillardin, J. Weissenbach, P. Wincker, J.L. Souciet, Genome evolution in yeasts, *Nature* 430 (2004) 35–44.
- [70] D.J. Sherman, T. Martin, M. Nikolski, C. Cayla, J.L. Souciet, P. Durrens, Genolevures: protein families and synteny among complete hemiascomycetous yeast proteomes and genomes, *Nucleic Acids Res.* 37 (2009) D550–D554.
- [71] W.K. Huh, S.O. Kang, Characterization of the gene family encoding alternative oxidase from *Candida albicans*, *Biochem. J.* 356 (2001) 595–604.
- [72] M.A. Larkin, G. Blackshields, N.P. Brown, R. Chenna, P.A. McGettigan, H. McWilliam, F. Valentin, I.M. Wallace, A. Wilm, R. Lopez, J.D. Thompson, T.J. Gibson, D.G. Higgins, Clustal W and Clustal X version 2.0, *Bioinformatics* 23 (2007) 2947–2948.
- [73] U.K. Laemmli, Cleavage of structural proteins during the assembly of the head of bacteriophage T4, *Nature* 227 (1970) 680–685.
- [74] H. Towbin, T. Staehelin, J. Gordon, Electrophoretic transfer of proteins from polyacrylamide gels to nitrocellulose sheets: procedure and some applications, *Proc. Natl. Acad. Sci. U. S. A.* 76 (1979) 4350–4354.
- [75] T.E. Elthon, R.L. Nickels, L. McIntosh, Monoclonal antibodies to the alternative oxidase of higher plant mitochondria, *Plant Physiol.* 89 (1989) 1311–1317.
- [76] N. Chiquete-Felix, J.M. Hernandez, J.A. Mendez, A. Zepeda-Bastida, A. Chagolla-Lopez, A. Mujica, In guinea pig sperm, aldolase A forms a complex with actin, WASP, and Arp2/3 that plays a role in actin polymerization, *Reproduction* 137 (2009) 669–678.
- [77] S.J. Kerscher, J.G. Okun, U. Brandt, A single external enzyme confers alternative NADH:ubiquinone oxidoreductase activity in *Yarrowia lipolytica*, *J. Cell Sci.* 112 (Pt 14) (1999) 2347–2354.
- [78] M.G. Claros, P. Vincens, Computational method to predict mitochondrially imported proteins and their targeting sequences, *Eur. J. Biochem.* 241 (1996) 779–786.
- [79] L. Adler, A. Blomberg, A. Nilsson, Glycerol metabolism and osmoregulation in the salt-tolerant yeast *Debaryomyces hansenii*, *J. Bacteriol.* 162 (1985) 300–306.
- [80] A.L. Umbach, J.N. Siedow, The cyanide-resistant alternative oxidases from the fungi *Pichia stipitis* and *Neurospora crassa* are monomeric and lack regulatory features of the plant enzyme, *Arch. Biochem. Biophys.* 378 (2000) 234–245.
- [81] C. Affourtit, K. Krab, A.L. Moore, Control of plant mitochondrial respiration, *Biochim. Biophys. Acta* 1504 (2001) 58–69.
- [82] C.A. Smith, V.J. Melino, C. Sweetman, K.L. Soole, Manipulation of alternative oxidase can influence salt tolerance in *Arabidopsis thaliana*, *Physiol. Plant.* 137 (2009) 459–472.
- [83] S. Sakajo, N. Minagawa, T. Komiyama, A. Yoshimoto, Characterization of cyanide-resistant respiration and appearance of a 36 kDa protein in mitochondria isolated from antimycin A-treated *Hansenula anomala*, *J. Biochem.* 108 (1990) 166–168.
- [84] X. Huang, U. von Rad, J. Durner, Nitric oxide induces transcriptional activation of the nitric oxide-tolerant alternative oxidase in *Arabidopsis* suspension cells, *Planta* 215 (2002) 914–923.
- [85] O. Juarez, G. Guerra, F. Martinez, J.P. Pardo, The mitochondrial respiratory chain of *Ustilago maydis*, *Biochim. Biophys. Acta* 1658 (2004) 244–251.
- [86] I. Wittig, R. Carrozzo, F.M. Santorelli, H. Schagger, Supercomplexes and subcomplexes of mitochondrial oxidative phosphorylation, *Biochim. Biophys. Acta* 1757 (2006) 1066–1072.
- [87] S. Guerrero-Castillo, A. Cabrera-Orefice, M. Vazquez-Acevedo, D. Gonzalez-Halphen, S. Uribe-Carvajal, During the stationary growth phase, *Yarrowia lipolytica* prevents the overproduction of reactive oxygen species by activating an uncoupled mitochondrial respiratory pathway, *Biochim. Biophys. Acta* 1817 (2012) 353–362.
- [88] X. Grandier-Vazeille, K. Bathany, S. Chaignepain, N. Camougrand, S. Manon, J.M. Schmitter, Yeast mitochondrial dehydrogenases are associated in a supramolecular complex, *Biochemistry* 40 (2001) 9758–9769.
- [89] S. Uribe-Carvajal, L.A. Luevano-Martinez, S. Guerrero-Castillo, A. Cabrera-Orefice, N.A. Corona-de-la-Pena, M. Gutierrez-Aguilar, Mitochondrial unselective channels throughout the eukaryotic domain, *Mitochondrion* 11 (2011) 382–390.
- [90] S.J. Kerscher, Diversity and origin of alternative NADH:ubiquinone oxidoreductases, *Biochim. Biophys. Acta* 1459 (2000) 274–283.
- [91] S.A. Uyemura, S. Luo, M. Vieira, S.N. Moreno, R. Docampo, Oxidative phosphorylation and rotenone-insensitive malate- and NADH-quinone oxidoreductases in *Plasmodium yoelii yoelii* mitochondria in situ, *J. Biol. Chem.* 279 (2004) 385–393.
- [92] V.P. Martins, F.M. Soriano, T. Magnani, V.G. Tudela, G.H. Goldman, C. Curti, S.A. Uyemura, Mitochondrial function in the yeast form of the pathogenic fungus *Paracoccidioides brasiliensis*, *J. Bioenerg. Biomembr.* 40 (2008) 297–305.
- [93] M. Klingenberg, Localization of the glycerol-phosphate dehydrogenase in the outer phase of the mitochondrial inner membrane, *Eur. J. Biochem.* 13 (1970) 247–252.
- [94] O. Bunoust, A. Devin, N. Averet, N. Camougrand, M. Rigoulet, Competition of electrons to enter the respiratory chain: a new regulatory mechanism of oxidative metabolism in *Saccharomyces cerevisiae*, *J. Biol. Chem.* 280 (2005) 3407–3413.
- [95] M.V. Kovaleva, E.I. Sukhanova, T.A. Trendeleva, M.V. Zyl'kova, L.A. Ural'skaya, K.M. Popova, N.E. Saris, R.A. Zvyagilskaya, Induction of a non-specific permeability transition in mitochondria from *Yarrowia lipolytica* and *Dipodascus (Endomyces) magnusii* yeasts, *J. Bioenerg. Biomembr.* 41 (2009) 239–249.
- [96] J. Heinemeyer, H.P. Braun, E.J. Boekema, R. Kouril, A structural model of the cytochrome C reductase/oxidase supercomplex from yeast mitochondria, *J. Biol. Chem.* 282 (2007) 12240–12248.
- [97] C. Chen, Y. Ko, M. Delannoy, S.J. Ludtke, W. Chiu, P.L. Pedersen, Mitochondrial ATP synthosome: three-dimensional structure by electron microscopy of the ATP synthase in complex formation with carriers for Pi and ADP/ATP, *J. Biol. Chem.* 279 (2004) 31761–31768.

# Physiological uncoupling of mitochondrial oxidative phosphorylation. Studies in different yeast species

Sergio Guerrero-Castillo · Daniela Araiza-Olivera · Alfredo Cabrera-Orefice ·  
Juan Espinasa-Jaramillo · Manuel Gutiérrez-Aguilar · Luís A. Luévano-Martínez ·  
Armando Zepeda-Bastida · Salvador Uribe-Carvajal

Published online: 10 May 2011  
© Springer Science+Business Media, LLC 2011

**Abstract** Under non-phosphorylating conditions a high proton transmembrane gradient inhibits the rate of oxygen consumption mediated by the mitochondrial respiratory chain (state IV). Slow electron transit leads to production of reactive oxygen species (ROS) capable of participating in deleterious side reactions. In order to avoid overproducing ROS, mitochondria maintain a high rate of O<sub>2</sub> consumption by activating different exquisitely controlled uncoupling pathways. Different yeast species possess one or more uncoupling systems that work through one of two possible mechanisms: i) Proton sinks and ii) Non-pumping redox enzymes. Proton sinks are exemplified by mitochondrial unspecific channels (MUC) and by uncoupling proteins (UCP). *Saccharomyces cerevisiae* and *Debaryomyces hansenii* express highly regulated MUCs. Also, a UCP was described in *Yarrowia lipolytica* which promotes uncoupled O<sub>2</sub> consumption. Non-pumping alternative oxido-reductases may substitute for a pump, as in *S. cerevisiae* or may coexist with a complete set of pumps as in the branched respiratory chains from *Y. lipolytica* or *D. hansenii*. In addition, pumps may suffer intrinsic uncoupling (slipping). Promising models for study are unicellular parasites which can turn off their aerobic metabolism completely. The variety of energy dissipating systems in eukaryote species is probably designed to control ROS production in the different environments where each species lives.

**Keywords** Uncoupling · Permeability transition · Uncoupling protein · Branched respiratory chain · *Saccharomyces cerevisiae* · *Yarrowia lipolytica* · *Debaryomyces hansenii*

## Introduction

In mitochondria, oxidative phosphorylation results from the coupling between the redox-primary proton pumps in the respiratory chain and the F<sub>1</sub>F<sub>0</sub>-ATP synthase. The redox H<sup>+</sup> pumps create a pH gradient ( $\Delta\text{pH}$ ) used by the F<sub>1</sub>F<sub>0</sub>-ATP synthase to phosphorylate ADP. The efficiency of this system varies when electrons enter or exit the respiratory chain at different enzymes or when the H<sup>+</sup> gradient is used by secondary pumps for the active transport of proteins, ions and metabolites (Nicholls and Ferguson 2002) (Fig. 1).

Three of the four respiratory complexes in an orthodox respiratory chain are proton pumps. These enzymes oxidize substrates, transferring electron(s) to the next acceptor in the chain and expelling H<sup>+</sup>(s) to the intermembrane space. Recycling of the electron within a given pump often results in H<sup>+</sup>/e<sup>−</sup> stoichiometries higher than 1 (Brandt 2006; Hosler et al. 2006; Trumppower 1990). This high efficiency comes at a price, as redox reactions involve several steps where incomplete reductions transiently convert coenzymes into reactive free radicals (Drose and Brandt 2008; Kushnareva et al. 2002). Therefore, when the mitochondrial ADP concentration drops, the rate of electron flux through the respiratory chain decreases (State IV respiration) and mitochondria become an important source of superoxide and other reactive oxygen species (ROS) (Chen et al. 2003). ROS production has diverse functions, such as signaling and apoptosis (Forman et al. 2010; Perrone et al. 2008).

S. Guerrero-Castillo · D. Araiza-Olivera · A. Cabrera-Orefice ·  
J. Espinasa-Jaramillo · M. Gutiérrez-Aguilar ·  
L. A. Luévano-Martínez · A. Zepeda-Bastida ·  
S. Uribe-Carvajal (✉)  
Departamento de Genética Molecular, Instituto de Fisiología  
Celular, Universidad Nacional Autónoma de México,  
Ciudad Universitaria, Apdo. Postal 70–242, Mexico City, México  
DF, Mexico  
e-mail: suribe@ifc.unam.mx

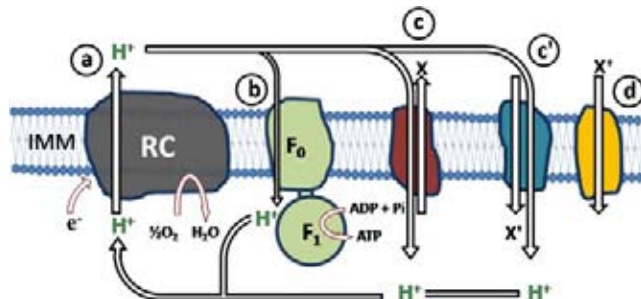


**Fig. 1** Oxidative phosphorylation efficiency variations due to different systems that use protons. The proton gradient generated by the respiratory chain may be used by (a) the  $F_1F_0$ -ATP synthase ( $F_0F_1$ ) for ADP phosphorylation (b) the transport of ions or metabolites across the inner mitochondrial membrane (IMM) either as (c) antiporter or (c') symporter. (d) ion uniport. RC, respiratory chain

However, overproduction of ROS may lead to ageing and disease (Drakulic et al. 2005; Wilhelm et al. 2006).

The labile nature of the superoxide radical has made difficult the identification of all its mitochondrial sources. Still, it is known that the ubiquinone and flavin oxidoreduction centers produce ROS (Chen et al. 2003; Starkov et al. 2004; Zundorf et al. 2009). During the redox ubiquinone/ubiquinol reaction, oxidized ubiquinone is partially reduced by one electron in the Qo site of the  $bc_1$  complex becoming a potential superoxide source (Drose and Brandt 2008). At a high mitochondrial transmembrane potential, semiquinone accumulates participating in a side reactions that produce ROS (Koshkin et al. 2003; Rottenberg et al. 2009).

In cells and mitochondria there are different enzymes that eliminate ROS, such as  $Mn^{2+}$  SOD-dismutases, catalase and glutathione peroxidases. However, ROS overproduction may overwhelm these systems and thus different energy-dissipating uncoupling mechanisms may be activated to prevent such overproduction. These “physiological uncoupling” mechanisms would prevent ROS over-accumulation by inducing increased electron flux (Czarna and Jarmuszkiewicz 2005; Maxwell et al. 1999).

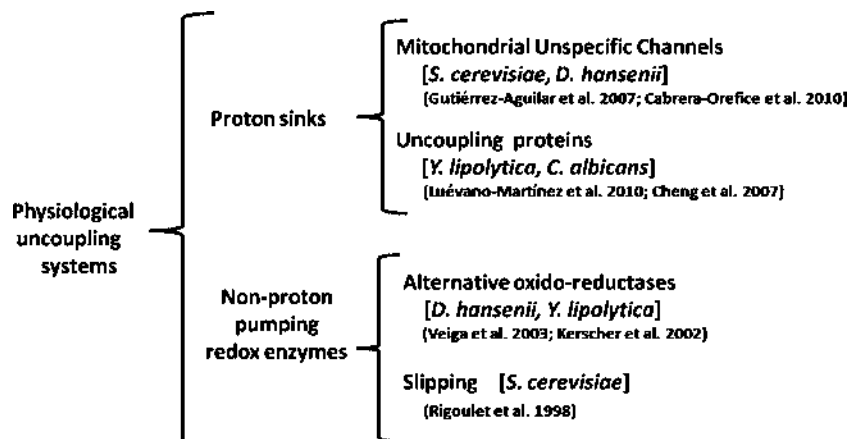
**Fig. 2** Physiological uncoupling systems in yeast mitochondria. The rate of oxygen consumption may be accelerated independently of the synthesis of ATP by either depleting the transmembrane pH gradient or by reducing oxygen without contributing to the proton gradient. These mechanisms are present in different yeast species

Among plants, yeast and fungi, there are different strategies aimed at preventing ROS overproduction (Kowaltowski et al. 1998; Magnani et al. 2008). In different yeast species it has been observed that oxidative phosphorylation can be uncoupled by different mechanisms (Fig. 2). Oxidative phosphorylation may be uncoupled through dissipation of the  $H^+$  gradient through proton sinks, also termed extrinsic uncouplers (Kadenbach 2003): these may be channels or transporters and are represented by two well studied systems. These are the yeast mitochondrial unspecific channel (MUC) (Manon et al. 1998), which in mammals is known as the permeability transition pore (PTP) (Haworth and Hunter 1979), and the uncoupling proteins (UCP) (Nicholls and Rial 1999) that specifically dissipate  $H^+$  gradients (Fig. 3). The second respiratory chain uncoupling mechanism, also termed intrinsic uncoupling (Kadenbach 2003) is the catalysis of redox reactions without pumping protons. Non-pumping redox enzymes are widely represented in the branched mitochondrial respiratory chains observed in plants and unicellular organisms (Rasmussen et al. 2004; Umbach and Siedow 2000; Wagner and Moore 1997). Among these enzymes, there are type-II NADH dehydrogenases (NDH2) and alternative oxidases (AOX). In addition, the variations in  $H^+/e^-$  stoichiometry (slipping) are another source of uncoupling.

### Proton dissipating pathways

#### The mitochondrial unselective channel

Mitochondrial unspecific channels (MUCs) have been detected in yeast such as *Saccharomyces cerevisiae* (*S.c*MUC) (Guerin et al. 1994; Prieto et al. 1992) and *Debaryomyces hansenii* (*Dh*MUC) (Cabrera-Orefice et al. 2010). MUC opening results in a mitochondrial permeability transition (PT) similar to that described in mammals, i.e. a large



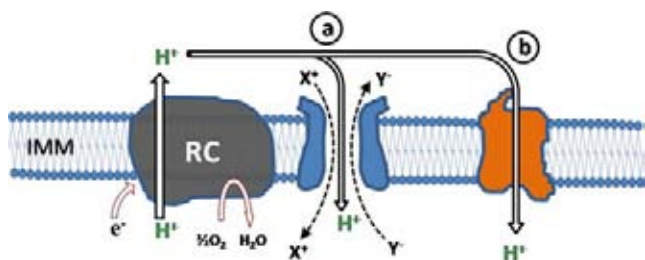


**Fig. 3** Proton Sinks. Two proton sink systems are exemplified. Once the (a) Respiratory chain establishes a proton gradient, protons may be returned to the matrix through (b) unspecific channels or through (c) uncoupling proteins that are specific protonophores

increase in conductivity that depletes electrochemical gradients (Azzolin et al. 2010).

The *Sc*MUC has been thoroughly characterized. *Sc*MUC opens in response to ATP, while it is closed by Pi or ADP (Prieto et al. 1995). This suggests that *Sc*MUC is controlled by the phosphorylation potential (Wallace et al. 1994). In addition, both the *Sc*MUC (Perez-Vazquez et al. 2003) and the *Dh*MUC (Cabreria-Orefice et al. 2010) are closed by Mg<sup>2+</sup> and by Ca<sup>2+</sup>. Furthermore, the *Sc*MUC seems to be controlled cooperatively by Ca<sup>2+</sup>, Mg<sup>2+</sup> and Pi [to be published]. In *S. cerevisiae*, a rise in cytoplasmic [Ca<sup>2+</sup>] precedes processes such as division, mating (Nakajima-Shimada et al. 2000; Ohya et al. 1991); or even a death program resembling apoptosis (Nakajima-Shimada et al. 2000; Ohya et al. 1991; Pozniakovskiy et al. 2005). That is, a rise in [Ca<sup>2+</sup>]<sub>cyt</sub> indicates that the cell is about to spend a large amount of energy (Anraku et al. 1991; Manon and Guerin 1998). Both the *Sc*MUC and the *Dh*MUC close in response to low [ATP] or high [Pi] while in contrast, when there is a surplus of ATP and no signals this indicates an oncoming need for energy, yeast MUCs open, dissipating the transmembrane potential and thus allowing the rate of oxygen consumption to increase (Prieto et al. 1992) and the production of ROS to decrease (Korshunov et al. 1997).

In *S. cerevisiae*, Ca<sup>2+</sup> closes MUC, probably through its interaction with the voltage-dependent anionic channel (VDAC) (Gutierrez-Aguilar et al. 2007). The Ca<sup>2+</sup>-VDAC interaction has also been proposed for vertebrates (Gincel et al. 2001). In both cases, the possibility that VDAC is a regulatory pore component has been suggested (Baines et al. 2007; Gutierrez-Aguilar et al. 2007). In regard to the possible component of MUC in the IMM, in *S. cerevisiae* it has long been evident that Pi is a strong MUC regulator (Azzolin et al. 2010; Cortes et al. 2000; Jung et al. 1997; Manon and Guerin 1997; Prieto et al. 1992; Velours et al. 1977). From this, it should not be surprising that recent evidence suggests that the mitochondrial phosphate carrier (PiC) is a constituent of the *Sc*MUC: in the absence of PiC, *Sc*MUC changes its solute size exclusion size and Pi sensitivity (Gutierrez-Aguilar et al. 2010). In mammals,

PiC has also been proposed to be part of this channel (Leung et al. 2008).

Different modulators of MUCs have been reported depending on the species, strain or even tissue under study (Berman et al. 2000; Fortes et al. 2001; Friberg et al. 1999; Manon et al. 1998), suggesting that MUCs have evolved in response to selective pressure, e.g. in *D. hansenii*, the MUC is closed by monovalent cations (Cabrera-Orefice et al. 2010). This closure probably results in higher production of ATP, as it correlates with increased growth rate and mass yield (Gonzalez-Hernandez et al. 2004) and probably constitutes an adaptation to the high Na<sup>+</sup> contents of sea water (Gustafsson and Norkrans 1976).

Adding to the ongoing debate on the physiological role of MUCs, it is suggested that their role as physiological uncouplers should be considered; i.e. MUCs probably are highly regulated energy dissipative systems that decrease mitochondrial gradients when the demand for energy is low.

PT does not seem to be universal. *Yarrowia lipolytica* and *Endomyces magnusii* undergo PT only upon forced conditions which include incubation with the Ca<sup>2+</sup> ionophore ETH129 (Kovaleva et al. 2009; Yamada et al. 2009). If MUC-mediated uncoupling is important to inhibit ROS production, and *Y. lipolytica* and *E. magnusii* seem to lack such a structure, then these yeast species should possess alternative uncoupling systems. Indeed, in *Y. lipolytica* mitochondria there are two such systems that might function as uncouplers: an uncoupling protein (Luevano-Martinez et al. 2010) and a branched respiratory chain (Guerrero-Castillo et al. 2009; Kerscher et al. 2002).

#### Uncoupling proteins

Uncoupling protein (UCP)-like activities have been detected in mitochondria from unicellular organisms, higher eukaryotes and plants (Jarmuszkiewicz et al. 2010). The physiological role of UCPs in unicellular organisms is still debated: the small size of unicellular eukaryotes makes a thermogenic role unlikely, as it is impossible to form a temperature gradient between the cell and the environment although, in *Acanthamoeba castellanii* UCP expression does increase in cells growing at 4 °C (Jarmuszkiewicz et al. 2004). Here, it is proposed that unicellular UCPs are capable of decreasing the mitochondrial  $\Delta\Psi$  with the aim of decreasing production of ROS. Also, in unicellular organisms resistance to exogenous ROS is enhanced by UCP activity (Kowaltowski et al. 1998; Ricquier 2005), probably because UCP decreases endogenous ROS production (Krauss et al. 2005) and thus detoxifying enzymes are free to deal with the exogenous species: e.g. strains of *Candida albicans* devoid of UCP are less invasive than the wild type (Cavalheiro et al. 2004; Cheng et al. 2007).

In addition to the available functional evidence, recently a protein exhibiting UCP-like activity was identified in *Y. lipolytica* (Luevano-Martinez et al. 2010). The UCP activity was regulated similarly to the UCP1 from brown adipose tissue. After an extensive phylogenetic search for a UCP ortholog in this yeast, it was demonstrated that the mitochondrial oxaloacetate carrier (OAC) from *Y. lipolytica* is a *bona fide* UCP. The *Y. lipolytica* OAC displayed both, a sulfate/oxaloacetate transport and a UCP behavior. It is noteworthy that in the unicellular organisms where UCP activity has been reported, the green algae *Chlamydomonas reinhardtii*, the amoeba *Dictyostelium discoideum* (DictyBase) and the yeast *Candida albicans* (Cavalheiro et al. 2004; Jarmuszkiewicz et al. 2002) the only UCP-like proteins seem to be the mitochondrial oxaloacetate carriers (results not published). In regard to whether a UCP might prevent ROS overproduction, in *Y. lipolytica*, it has been demonstrated that this protein is over-expressed in the stationary phase, where a degree of uncoupling would be needed to maintain a high rate of oxygen consumption in the absence of ATP synthesis (Luevano-Martinez et al. 2010).

## Redox enzymes that do not pump protons

### Branched mitochondrial respiratory chains

Redox enzymes lacking pumping activity are constituted by a single protein subunit. These enzymes probably appeared early in the reducing world, before the appearance of oxidative phosphorylation, fulfilling the need to detoxify oxygen from the vicinity of enzymes and membranes. Some prokaryotes still use oxidoreductase-mediated detoxification of oxygen to protect their fragile nitrogen reducing enzymes (Flores-Encarnacion et al. 1999).

Alternative redox enzymes do not contribute to the proton gradient. Branched mitochondrial respiratory chains may contain a number of different enzymes that donate electrons to the quinone pool including complex I (the only proton pump), succinate dehydrogenase, glycerol phosphate dehydrogenase, dihydroorotate dehydrogenase and internal or external type II NADH dehydrogenases. Then the electrons in reduced ubiquinol follow two possible pathways reaching either the cytochrome pathway (complexes III and IV), or the alternative oxidase (AOX). In these respiratory chains, different electron pathways may be envisioned that bypass energy-conserving respiratory complexes I, III and/or IV, i.e. branched chains seem to be able to reduce oxygen while using 0, 1, 2 or 3 proton pumps (Fig. 4).

In mitochondria, the most widely distributed mono-subunit redox enzymes are type II NADH dehydrogenases

(NDH2) and alternative oxidases (AOX). NDH2s may be located on either surface of the IMM. External NDH2s (NDH2e) oxidize cytosolic NADH, while internal NDH2s (NDH2i) oxidize NADH from the matrix in a rotenone-insensitive reaction. The structure (Fisher et al. 2007; Fisher et al. 2009; Gonzalez-Meler et al. 1999; Kerscher 2000; Melo et al. 2004; Schmid and Gerloff 2004) and kinetics (Fisher et al. 2009; Velazquez and Pardo 2001) of NDH2s from different organisms have been reported. AOX is a single subunit enzyme (Albury et al. 2002; Andersson and Nordlund 1999; Berthold et al. 2000; Moore and Siedow 1991). AOX activity is regulated by nucleotides, by dimerization and/or by  $\alpha$ -ketoacids (Hoefnagel et al. 1995; Millar et al. 1993; Millenaar et al. 1998). Some yeast species contain two AOX isoforms, one being constitutively expressed and a second one induced by stress (Siedow and Umbach 2000). It is noteworthy that AOX is present only in fungi that express complex I, possibly because in a respiratory chain without Complex I, any electron reaching AOX would be totally unproductive (Joseph-Horne et al. 2001).

In mitochondria with alternative components, the pathway that electrons follow has to be strictly controlled. A direct reaction between NDH2, ubiquinone and AOX would result in a non-productive, uncoupled pathway, i.e. no protons would be pumped. Furthermore, at the external face of the inner membrane, NDH2 receives the hydride from NADH and takes one  $H^+$ , transferring both hydrogen atoms to ubiquinone. Then ubiquinone is regenerated by AOX which in turn transfers its hydrogen atoms to oxygen producing water. This sequence of reactions results in the dissipation of a  $H^+$ , i.e. it has a  $H^+/e^-$  pumping stoichiometry of -0.5. Therefore, when energy is required, alternative redox enzymes need to be isolated from each other, probably by binding to the proton-pumping complexes. In contrast, when phosphorylation is not active, as in the stationary phase, the non-producing electron transfer between NDH2 and AOX would be useful to maintain a high rate of oxygen consumption at a high transmembrane potential, preventing semiquinone accumulation and decreasing ROS formation (Joseph-Horne et al. 2001).

### Proton/electron stoichiometry variations. Slipping

Non-branched respiratory chains seem to use other mechanisms to regulate the efficiency of oxidative phosphorylation (van Dam et al. 1990). Uncoupling may result from increased proton conductance at the lipid bilayer (Luvisetto and Azzone 1989; Luvisetto et al. 1991). A second mechanism would be the decrease in the efficiency of a respiratory pump (slipping) (Pietrobon et al. 1981; Pietrobon et al. 1983). Intrinsic uncoupling or slipping is defined as a decrease in the efficiency of a

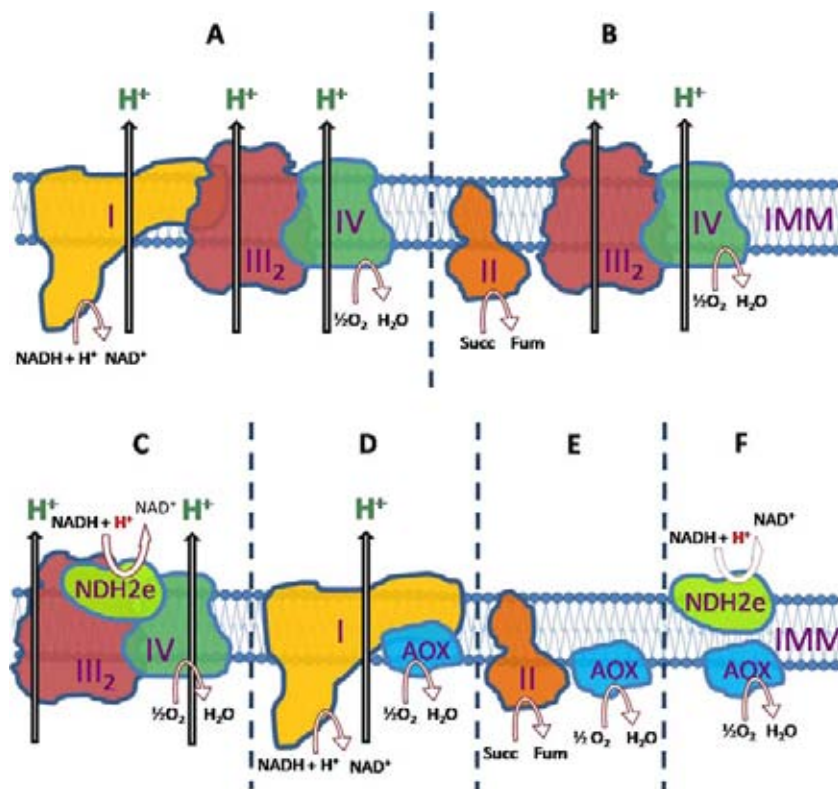


**Fig. 4** In a branched respiratory chain the number of proton pumps participating in electron transfer may vary from three to zero. In branched respiratory chains electrons may follow different routes to reach oxygen. Thus the number of proton pumps involved may change: **a** complexes I, III and IV: three proton pumps are involved. **b** from succinate dehydrogenase through the cytochrome pathway, two proton pumps. **c** from NDH2e through complexes III-IV; two proton pumps, although H<sup>+</sup>/e<sup>-</sup> is 2.5 instead of 3 as in (b). **d** from complex I though AOX; one pump. **e** from succinate dehydrogenase through AOX; No proton pumps

proton pump (decrease of the H<sup>+</sup>/e or H<sup>+</sup>/ATP stoichiometry) resulting in a diminished P/O ratio (Kadenbach 2003).

Slipping has been reported in cytochrome c oxidase (Azzone et al. 1985; Frank and Kadenbach 1996). The F<sub>1</sub>F<sub>0</sub>-synthase can also undergo slipping, hydrolyzing ATP without pumping protons (Feniouk et al. 2005). In addition, protons can reenter the matrix through the pumps without moving electrons backwards or making ATP (Pietrobon et al. 1983).

Slipping accelerates the rate of oxygen consumption as more electrons are needed to maintain a high ΔpH. Normally in the proton pump the chemical reaction and the transport of protons are tightly coupled, while during slipping both processes become independent (Mourier et al. 2010). Upon slipping, the rate of electron flux increases while the proton motive force remains constant and energy is dissipated as heat (Kadenbach 2003).

In *S. cerevisiae* mitochondria, a remarkable change in the stoichiometry of proton pumping has been described. Feeding the respiratory chain with substrates for different quinone reductases leads to an increase in the rate of

participate. **f** NDH2e through AOX; zero proton pumps participate and in addition, the combined activity of NDH2e with AOX would consume a H<sup>+</sup> from the intermembrane space, yielding a negative stoichiometry of  $-0.5 \text{ H}^+/\text{e}^-$ . Numbers I, II, III<sub>2</sub> and IV represent each of the four respiratory complexes; NDH2e, external NADH dehydrogenase; AOX, alternative oxidase; IMM, inner mitochondrial membrane. Protons in red are used for ubiquinone reduction in the intermembrane side of the IMM, i.e. they do not contribute (c) or contribute negatively to the H<sup>+</sup>/e<sup>-</sup> stoichiometry (f)

oxygen consumption without increasing the rate of ATP phosphorylation (Mourier et al. 2010). This phenomenon has been termed active leak and is probably due to slipping of an oxidative phosphorylation pump, although an increase in the proton conductance of the bilayer has not been ruled out.

#### Interactions between the cytoplasm and mitochondria regulate the efficiency of oxidative phosphorylation

At any given moment the cell's energy needs determine which metabolic pathways are activated or inhibited (Devin and Rigoulet 2007). The catabolism/anabolism activity ratio is determined by metabolic fluxes (Cascante et al. 1994; Moreno-Sánchez et al. 2010; Ovadi and Saks 2004; Srere 1987). Upon oxygenation, the rate of glycolysis decreases. This may be explained by the allosteric regulation of glycolytic enzymes by ATP and fructose 2,6-bisphosphate and by the competition for ADP and for reducing equivalents observed between glycolysis and

oxidative phosphorylation (Beauvoit et al. 1993; Gosalvez et al. 1974).

In *Saccharomyces cerevisiae*, glycolysis is the main source of ATP; however, in the presence of non-fermentable substrates oxidative phosphorylation becomes the main energy source. During fermentation the genes that encode for oxidative metabolism enzymes stop their expression (Takeda 1981), e.g. glucose addition inhibits the expression of cytochrome c (Thevelein 1994; Zitomer and Nichols 1978), while glycolytic intermediates are accumulated to induce the expression of glycolytic enzymes (Boles et al. 1993).

In *S. cerevisiae* the addition of glucose induces the transition to fermentative metabolism, where glycolysis is increased and oxidative phosphorylation is decreased (den Hollander et al. 1986). This is the Crabtree effect. There are both Crabtree-positive and negative yeast species. Recent studies indicate that fructose1,6-bisphosphate inhibits oxygen consumption through an interaction with complexes III and IV. In contrast, physiological concentrations of glucose 6-phosphate and fructose 6-phosphate stimulate the respiratory flux, possibly inducing slipping (Diaz-Ruiz et al. 2008).

### Unicellular organisms other than yeast

Protists make up the bulk of the eukaryotes, while vertebrates and fungi represent only a small fraction. Protists present a wide variety of physiological properties. There are very few bioenergetics studies on these organisms. *Giardia lamblia* (Hashimoto et al. 1994) and *Entamoeba histolytica* (Tovar et al. 1999) have lost their mitochondria. Other protists, such as some Trichomonadidae and ciliates, have organelles called hydrogenosomes, which are related to mitochondria (de Souza et al. 2009; Mather and Vaidya 2008).

Unicellular parasites have evolved to adapt their metabolism for survival within the host. Depending on the environment and stage in their life cycle, *Plasmodium*, *Trypanosoma* and *Leishmania* can make a complete switch from a glycolytic to an aerobic metabolism and back, such that in *Plasmodium falciparum* the activities of complex III, IV and dihydroorotate dehydrogenase, are 10 times higher in the sexual than in the asexual stage (Monzote and Gille 2010). Likewise, mitochondria have adapted to the metabolic conditions found within the host, e.g. in the mosquito, *Plasmodium* gametocytes are aerobic and mitochondria are typical. In contrast, in the vertebrate host, sporozoites and merozoites are adapted to microaerophilia and contain few, underdeveloped mitochondria (Segura and Blair 2003).

Throughout the trypanosomatid life cycle, mitochondrial activity varies widely (Schneider 2001). In the bloodstream,

these protozoans are anaerobic while in the gut of the insect they perform oxidative phosphorylation. In *Toxoplasma* most energy is obtained from glycolysis, although the mitochondrial DNA sequence of these parasites shows significant differences from the mammalian host, suggesting possible drug targets (Monzote and Gille 2010). Remarkably, the mitochondrial DNAs from trypanosomatids and Apicomplexa lack genes for transfer RNA (Mather and Vaidya 2008).

### Concluding remarks

Aerobic metabolism is at the same time highly efficient and very dangerous. The reactive oxygen species produced by the respiratory chain can react with, and damage different components of the cell. Diverse mechanisms have evolved to prevent the deleterious effect of ROS. There are many detoxifying enzymes such as glutathione reductase, superoxide dismutase or catalase. In addition, upriver from these reactions, there are diverse mitochondrial systems designed to prevent ROS overproduction. These systems promote physiological uncoupling to ensure that the redox enzymes in the respiratory chain work at a fast rate, thus preventing reactive intermediates from participating in collateral reactions.

There are two mitochondrial uncoupling mechanisms: a) Those that dissipate the pH gradient and b) Non-productive redox reactions. Both mechanisms are widely spread in nature. Physiological proton sinks are the uncoupling proteins and the mitochondrial unspecific channels, while non productive redox reactions are catalyzed by redox/non-pumping alternative dehydrogenases and by orthodox complexes that undergo slipping.

The relationship between the cytoplasmic and the mitochondrial metabolic pathways needs to be better understood. The ability of some products from glycolysis to regulate oxidative phosphorylation is illustrative. The comparison between Crabtree positive and Crabtree negative yeast species may help understand the mechanisms and consequences of these interactions.

Understanding the mechanisms underlying the control and production of ROS may help to select more resistant organisms for biotechnological applications. Also, various ROS-related diseases have to be understood in order to design better treatments. In this light, it seems useful to know that uncoupling prevents ROS production.

During evolution, each eukaryote species preserved one or more ROS overproduction-prevention mechanism(s). Yeast species are ideal to study each mechanism. Other unicellular organisms may be helpful to understand their ability to shut down aerobic metabolism without being overwhelmed by ROS production.

**Acknowledgements** Partially funded by grants from CONACYT 79989 and by DGAPA/UNAM, IN217109. SGC, DAO, ACO, MGA and LALM are CONACYT fellows enrolled in the Biochemistry Graduate Program at UNAM. JEJ has a SNI-III aid fellowship. The assistance of Dr Natalia Chiquete-Félix is acknowledged. We thank Dr Soledad Funes-Argüello for critically reading the manuscript.

## References

- Albury MS, Affourtit C, Crichton PG, Moore AL (2002) Structure of the plant alternative oxidase. Site-directed mutagenesis provides new information on the active site and membrane topology. *J Biol Chem* 277:1190–1194
- Andersson ME, Nordlund P (1999) A revised model of the active site of alternative oxidase. *FEBS Lett* 449:17–22
- Anraku Y, Ohya Y, Iida H (1991) Cell cycle control by calcium and calmodulin in *Saccharomyces cerevisiae*. *Biochim Biophys Acta* 1093:169–177
- Azzolin L, von Stockum S, Basso E, Petronilli V, Forte MA, Bernardi P (2010) The mitochondrial permeability transition from yeast to mammals. *FEBS Lett* 584:2504–2509
- Azzone GF, Zoratti M, Petronilli V, Pietrobon D (1985) The stoichiometry of  $H^+$  pumping in cytochrome oxidase and the mechanism of uncoupling. *J Inorg Biochem* 23:349–356
- Baines CP, Kaiser RA, Sheiko T, Craigen WJ, Molkentin JD (2007) Voltage-dependent anion channels are dispensable for mitochondrial-dependent cell death. *Nat Cell Biol* 9:550–555
- Beauvoit B, Rigoulet M, Bunoust O, Raffard G, Canioni P, Guerin B (1993) Interactions between glucose metabolism and oxidative phosphorylations on respiratory-competent *Saccharomyces cerevisiae* cells. *Eur J Biochem* 214:163–172
- Berman SB, Watkins SC, Hastings TG (2000) Quantitative biochemical and ultrastructural comparison of mitochondrial permeability transition in isolated brain and liver mitochondria: evidence for reduced sensitivity of brain mitochondria. *Exp Neurol* 164:415–425
- Berthold DA, Andersson ME, Nordlund P (2000) New insight into the structure and function of the alternative oxidase. *Biochim Biophys Acta* 1460:241–254
- Boles E, Heinisch J, Zimmermann FK (1993) Different signals control the activation of glycolysis in the yeast *Saccharomyces cerevisiae*. *Yeast* 9:761–770
- Brandt U (2006) Energy converting NADH:quinone oxidoreductase (complex I). *Annu Rev Biochem* 75:69–92
- Cabrera-Orefice A, Guerrero-Castillo S, Luevano-Martinez LA, Pena A, Uribe-Carvajal S (2010) Mitochondria from the salt-tolerant yeast *Debaryomyces hansenii* (halophilic organelles?). *J Bioenerg Biomembr* 42:11–19
- Cascante M, Sorribas A, Canela EI (1994) Enzyme-enzyme interactions and metabolite channelling: alternative mechanisms and their evolutionary significance. *Biochem J* 298(Pt 2):313–320
- Cavalheiro RA, Fortes F, Borecky J, Faustinoni VC, Schreiber AZ, Vercesi AE (2004) Respiration, oxidative phosphorylation, and uncoupling protein in *Candida albicans*. *Braz J Med Biol Res* 37:1455–1461
- Cortes P, Castrejon V, Sampedro JG, Uribe S (2000) Interactions of arsenate, sulfate and phosphate with yeast mitochondria. *Biochim Biophys Acta* 1456:67–76
- Chen Q, Vazquez EJ, Moghaddas S, Hoppel CL, Lesnfsky EJ (2003) Production of reactive oxygen species by mitochondria: central role of complex III. *J Biol Chem* 278:36027–36031
- Cheng S, Clancy CJ, Zhang Z, Hao B, Wang W, Iczkowski KA, Pfanner MA, Nguyen MH (2007) Uncoupling of oxidative phosphorylation enables *Candida albicans* to resist killing by phagocytes and persist in tissue. *Cell Microbiol* 9:492–501
- Czarna M, Jarmuszkiewicz W (2005) Activation of alternative oxidase and uncoupling protein lowers hydrogen peroxide formation in amoeba *Acanthamoeba castellanii* mitochondria. *FEBS Lett* 579:3136–3140
- de Souza W, Attias M, Rodrigues JC (2009) Particularities of mitochondrial structure in parasitic protists (Apicomplexa and Kinetoplastida). *Int J Biochem Cell Biol* 41:2069–2080
- den Hollander JA, Ugurbil K, Brown TR, Bednar M, Redfield C, Shulman RG (1986) Studies of anaerobic and aerobic glycolysis in *Saccharomyces cerevisiae*. *Biochemistry* 25:203–211
- Devin A, Rigoulet M (2007) Mechanisms of mitochondrial response to variations in energy demand in eukaryotic cells. *Am J Physiol Cell Physiol* 292:C52–C58
- Diaz-Ruiz R, Averet N, Araiza D, Pinson B, Uribe-Carvajal S, Devin A, Rigoulet M (2008) Mitochondrial oxidative phosphorylation is regulated by fructose 1,6-bisphosphate. A possible role in Crabtree effect induction? *J Biol Chem* 283:26948–26955
- Drakulic T, Temple MD, Guido R, Jarolim S, Breitenbach M, Attfield PV, Dawes IW (2005) Involvement of oxidative stress response genes in redox homeostasis, the level of reactive oxygen species, and ageing in *Saccharomyces cerevisiae*. *FEMS Yeast Res* 5:1215–1228
- Drose S, Brandt U (2008) The mechanism of mitochondrial superoxide production by the cytochrome bc1 complex. *J Biol Chem* 283:21649–21654
- Feniouk BA, Mulkidjanian AY, Junge W (2005) Proton slip in the ATP synthase of *Rhodobacter capsulatus*: induction, proton conduction, and nucleotide dependence. *Biochim Biophys Acta* 1706:184–194
- Fisher N, Bray PG, Ward SA, Biagini GA (2007) The malaria parasite type II NADH:quinone oxidoreductase: an alternative enzyme for an alternative lifestyle. *Trends Parasitol* 23:305–310
- Fisher N, Warman AJ, Ward SA, Biagini GA (2009) Chapter 17 Type II NADH: quinone oxidoreductases of *Plasmodium falciparum* and *Mycobacterium tuberculosis* kinetic and high-throughput assays. *Meth Enzymol* 456:303–320
- Flores-Encarnacion M, Contreras-Zentella M, Soto-Urzua L, Aguilar GR, Baca BE, Escamilla JE (1999) The respiratory system and diazotrophic activity of *Acetobacter diazotrophicus* PAL5. *J Bacteriol* 181:6987–6995
- Forman HJ, Maiorino M, Ursini F (2010) Signaling functions of reactive oxygen species. *Biochemistry* 49:835–842
- Fortes F, Castilho RF, Catisti R, Carnieri EG, Vercesi AE (2001)  $Ca^{2+}$  induces a cyclosporin A-insensitive permeability transition pore in isolated potato tuber mitochondria mediated by reactive oxygen species. *J Bioenerg Biomembr* 33:43–51
- Frank V, Kadenbach B (1996) Regulation of the  $H^+/e^-$  stoichiometry of cytochrome c oxidase from bovine heart by intramitochondrial ATP/ADP ratios. *FEBS Lett* 382:121–124
- Friberg H, Connern C, Halestrap AP, Wieloch T (1999) Differences in the activation of the mitochondrial permeability transition among brain regions in the rat correlate with selective vulnerability. *J Neurochem* 72:2488–2497
- Gincel D, Zaid H, Shoshan-Barmatz V (2001) Calcium binding and translocation by the voltage-dependent anion channel: a possible regulatory mechanism in mitochondrial function. *Biochem J* 358:147–155
- Gonzalez-Hernandez JC, Cardenas-Monroy CA, Pena A (2004) Sodium and potassium transport in the halophilic yeast *Debaryomyces hansenii*. *Yeast* 21:403–412
- Gonzalez-Meler MA, Ribas-Carbo M, Giles L, Siedow JN (1999) The effect of growth and measurement temperature on the activity of the alternative respiratory pathway. *Plant Physiol* 120:765–772
- Gosalvez M, Perez-Garcia J, Weinhouse S (1974) Competition for ADP between pyruvate kinase and mitochondrial oxidative phosphorylation as a control mechanism in glycolysis. *Eur J Biochem* 46:133–140

- Guerin B, Bunoust O, Rouqueys V, Rigoulet M (1994) ATP-induced unspecific channel in yeast mitochondria. *J Biol Chem* 269:25406–25410
- Guerrero-Castillo S, Vazquez-Acevedo M, Gonzalez-Halphen D, Uribe-Carvajal S (2009) In *Yarrowia lipolytica* mitochondria, the alternative NADH dehydrogenase interacts specifically with the cytochrome complexes of the classic respiratory pathway. *Biochim Biophys Acta* 1787:75–85
- Gustafsson L, Norkrans B (1976) On the mechanism of salt tolerance. Production of glycerol and heat during growth of *Debaryomyces hansenii*. *Arch Microbiol* 110:177–183
- Gutierrez-Aguilar M, Perez-Vazquez V, Bunoust O, Manon S, Rigoulet M, Uribe S (2007) In yeast, Ca<sup>2+</sup> and octylguanidine interact with porin (VDAC) preventing the mitochondrial permeability transition. *Biochim Biophys Acta* 1767:1245–1251
- Gutierrez-Aguilar M, Perez-Martinez X, Chavez E, Uribe-Carvajal S (2010) In *Saccharomyces cerevisiae*, the phosphate carrier is a component of the mitochondrial unselective channel. *Arch Biochem Biophys* 494:184–191
- Hashimoto T, Nakamura Y, Nakamura F, Shirakura T, Adachi J, Goto N, Okamoto K, Hasegawa M (1994) Protein phylogeny gives a robust estimation for early divergences of eukaryotes: phylogenetic place of a mitochondria-lacking protozoan, *Giardia lamblia*. *Mol Biol Evol* 11:65–71
- Haworth RA, Hunter DR (1979) The Ca<sup>2+</sup>-induced membrane transition in mitochondria. II. Nature of the Ca<sup>2+</sup> trigger site. *Arch Biochem Biophys* 195:460–467
- Hoefnagel MH, Millar AH, Wiskich JT, Day DA (1995) Cytochrome and alternative respiratory pathways compete for electrons in the presence of pyruvate in soybean mitochondria. *Arch Biochem Biophys* 318:394–400
- Hosler JP, Ferguson-Miller S, Mills DA (2006) Energy transduction: proton transfer through the respiratory complexes. *Annu Rev Biochem* 75:165–187
- Jarmuszkiewicz W, Behrendt M, Navet R, Sluse FE (2002) Uncoupling protein and alternative oxidase of *Dictyostelium discoideum*: occurrence, properties and protein expression during vegetative life and starvation-induced early development. *FEBS Lett* 532:459–464
- Jarmuszkiewicz W, Antos N, Swida A, Czarna M, Sluse FE (2004) The effect of growth at low temperature on the activity and expression of the uncoupling protein in *Acanthamoeba castellanii* mitochondria. *FEBS Lett* 569:178–184
- Jarmuszkiewicz W, Woyda-Ploszczyca A, Antos-Krzeminska N, Sluse FE (2010) Mitochondrial uncoupling proteins in unicellular eukaryotes. *Biochim Biophys Acta* 1797:792–799
- Joseph-Horne T, Hollomon DW, Wood PM (2001) Fungal respiration: a fusion of standard and alternative components. *Biochim Biophys Acta* 1504:179–195
- Jung DW, Bradshaw PC, Pfeiffer DR (1997) Properties of a cyclosporin-insensitive permeability transition pore in yeast mitochondria. *J Biol Chem* 272:21104–21112
- Kadenbach B (2003) Intrinsic and extrinsic uncoupling of oxidative phosphorylation. *Biochim Biophys Acta* 1604:77–94
- Kerscher SJ (2000) Diversity and origin of alternative NADH:ubiquinone oxidoreductases. *Biochim Biophys Acta* 1459:274–283
- Kerscher S, Drose S, Zwicker K, Zickermann V, Brandt U (2002) *Yarrowia lipolytica*, a yeast genetic system to study mitochondrial complex I. *Biochim Biophys Acta* 1555:83–91
- Korshunov SS, Skulachev VP, Starkov AA (1997) High protonic potential actuates a mechanism of production of reactive oxygen species in mitochondria. *FEBS Lett* 416:15–18
- Koshkin V, Wang X, Scherer PE, Chan CB, Wheeler MB (2003) Mitochondrial functional state in clonal pancreatic beta-cells exposed to free fatty acids. *J Biol Chem* 278:19709–19715
- Kovaleva MV, Sukhanova EI, Trendeleva TA, Zyl'kova MV, Ural'skaya LA, Popova KM, Saris NE, Zvyagilskaya RA (2009) Induction of a non-specific permeability transition in mitochondria from *Yarrowia lipolytica* and *Dipodascus (Endomycetes) magnusii* yeasts. *J Bioenerg Biomembr* 41:239–249
- Kowaltowski AJ, Costa AD, Vercesi AE (1998) Activation of the potato plant uncoupling mitochondrial protein inhibits reactive oxygen species generation by the respiratory chain. *FEBS Lett* 425:213–216
- Krauss S, Zhang CY, Lowell BB (2005) The mitochondrial uncoupling-protein homologues. *Nat Rev Mol Cell Biol* 6:248–261
- Kushnareva Y, Murphy AN, Andreyev A (2002) Complex I-mediated reactive oxygen species generation: modulation by cytochrome c and NAD(P)<sup>+</sup> oxidation-reduction state. *Biochem J* 368:545–553
- Leung AW, Varanyuwata P, Halestrap AP (2008) The mitochondrial phosphate carrier interacts with cyclophilin D and may play a key role in the permeability transition. *J Biol Chem* 283:26312–26323
- Luevano-Martinez LA, Moyano E, de Lacoba MG, Rial E, Uribe-Carvajal S (2010) Identification of the mitochondrial carrier that provides *Yarrowia lipolytica* with a fatty acid-induced and nucleotide-sensitive uncoupling protein-like activity. *Biochim Biophys Acta* 1797:81–88
- Luvisetto S, Azzone GF (1989) Local protons and uncoupling of aerobic and artificial delta muH-driven ATP synthesis. *Biochemistry* 28:1109–1116
- Luvisetto S, Conti E, Buso M, Azzone GF (1991) Flux ratios and pump stoichiometries at sites II and III in liver mitochondria. Effect of slips and leaks. *J Biol Chem* 266:1034–1042
- Magnani T, Soriani FM, Martins Vde P, Policarpo AC, Sorgi CA, Faccioli LH, Curti C, Uyemura SA (2008) Silencing of mitochondrial alternative oxidase gene of *Aspergillus fumigatus* enhances reactive oxygen species production and killing of the fungus by macrophages. *J Bioenerg Biomembr* 40:631–636
- Manon S, Guerin M (1997) The ATP-induced K(+) -transport pathway of yeast mitochondria may function as an uncoupling pathway. *Biochim Biophys Acta* 1318:317–321
- Manon S, Guerin M (1998) Investigation of the yeast mitochondrial unselective channel in intact and permeabilized spheroplasts. *Biochem Mol Biol Int* 44:565–575
- Manon S, Roucou X, Guerin M, Rigoulet M, Guerin B (1998) Characterization of the yeast mitochondria unselective channel: a counterpart to the mammalian permeability transition pore? *J Bioenerg Biomembr* 30:419–429
- Mather MW, Vaidya AB (2008) Mitochondria in malaria and related parasites: ancient, diverse and streamlined. *J Bioenerg Biomembr* 40:425–433
- Maxwell DP, Wang Y, McIntosh L (1999) The alternative oxidase lowers mitochondrial reactive oxygen production in plant cells. *Proc Natl Acad Sci USA* 96:8271–8276
- Melo AM, Bandeiras TM, Teixeira M (2004) New insights into type II NAD(P)H:quinone oxidoreductases. *Microbiol Mol Biol Rev* 68:603–616
- Millar AH, Wiskich JT, Whelan J, Day DA (1993) Organic acid activation of the alternative oxidase of plant mitochondria. *FEBS Lett* 329:259–262
- Millenaar FF, Benschop JJ, Wagner AM, Lambers H (1998) The role of the alternative oxidase in stabilizing the in vivo reduction state of the ubiquinone pool and the activation state of the alternative oxidase. *Plant Physiol* 118:599–607
- Monzote L, Gille L (2010) Mitochondria as a promising antiparasitic target. *Curr Clin Pharmacol* 5:55–60
- Moore AL, Siedow JN (1991) The regulation and nature of the cyanide-resistant alternative oxidase of plant mitochondria. *Biochim Biophys Acta* 1059:121–140

- Moreno-Sanchez R, Saavedra E, Rodriguez-Enriquez S, Gallardo-Perez JC, Quezada H, Westerhoff HV (2010) Metabolic control analysis indicates a change of strategy in the treatment of cancer. *Mitochondrion* 10:626–639
- Mourier A, Devin A, Rigoulet M (2010) Active proton leak in mitochondria: a new way to regulate substrate oxidation. *Biochim Biophys Acta* 1797:255–261
- Nakajima-Shimada J, Sakaguchi S, Tsuji FI, Anraku Y, Iida H (2000) Ca<sup>2+</sup> signal is generated only once in the mating pheromone response pathway in *Saccharomyces cerevisiae*. *Cell Struct Funct* 25:125–131
- Nicholls DG, Ferguson SJ (2002) *Bioenergetics* 3. Academic Press, London, ISBN 0125181213
- Nicholls DG, Rial E (1999) A history of the first uncoupling protein, UCP1. *J Bioenerg Biomembr* 31:399–406
- Ohya Y, Umemoto N, Tanida I, Ohta A, Iida H, Anraku Y (1991) Calcium-sensitive *cls* mutants of *Saccharomyces cerevisiae* showing a Pet- phenotype are ascribable to defects of vacuolar membrane H(+)-ATPase activity. *J Biol Chem* 266:13971–13977
- Ovadi J, Saks V (2004) On the origin of intracellular compartmentation and organized metabolic systems. *Mol Cell Biochem* 256–257:5–12
- Perez-Vazquez V, Saavedra-Molina A, Uribe S (2003) In *Saccharomyces cerevisiae*, cations control the fate of the energy derived from oxidative metabolism through the opening and closing of the yeast mitochondrial unselective channel. *J Bioenerg Biomembr* 35:231–241
- Perrone GG, Tan SX, Dawes IW (2008) Reactive oxygen species and yeast apoptosis. *Biochim Biophys Acta* 1783:1354–1368
- Pietrobon D, Azzone GF, Walz D (1981) Effect of funiculosin and antimycin A on the redox-driven H<sup>+</sup>- pumps in mitochondria: on the nature of ‘leaks’. *Eur J Biochem* 117:389–394
- Pietrobon D, Zoratti M, Azzone GF (1983) Molecular slipping in redox and ATPase H<sup>+</sup> pumps. *Biochim Biophys Acta* 723:317–321
- Pozniakovsky AI, Knorre DA, Markova OV, Hyman AA, Skulachev VP, Severin FF (2005) Role of mitochondria in the pheromone- and amiodarone-induced programmed death of yeast. *J Cell Biol* 168:257–269
- Prieto S, Bouillaud F, Ricquier D, Rial E (1992) Activation by ATP of a proton-conducting pathway in yeast mitochondria. *Eur J Biochem* 208:487–491
- Prieto S, Bouillaud F, Rial E (1995) The mechanism for the ATP-induced uncoupling of respiration in mitochondria of the yeast *Saccharomyces cerevisiae*. *Biochem J* 307(Pt 3):657–661
- Rasmusson AG, Soole KL, Elthon TE (2004) Alternative NAD(P)H dehydrogenases of plant mitochondria. *Annu Rev Plant Biol* 55:23–39
- Ricquier D (2005) Respiration uncoupling and metabolism in the control of energy expenditure. *Proc Nutr Soc* 64:47–52
- Rottenberg H, Covian R, Trumper BL (2009) Membrane potential greatly enhances superoxide generation by the cytochrome bc1 complex reconstituted into phospholipid vesicles. *J Biol Chem* 284:19203–19210
- Schmid R, Gerloff DL (2004) Functional properties of the alternative NADH:ubiquinone oxidoreductase from *E. coli* through comparative 3-D modelling. *FEBS Lett* 578:163–168
- Schneider A (2001) Unique aspects of mitochondrial biogenesis in trypanosomatids. *Int J Parasitol* 31:1403–1415
- Segura C, Blair S (2003) Mitochondria in the Plasmodium genera. *Biomedica* 23:351–363
- Siedow JN, Umbach AL (2000) The mitochondrial cyanide-resistant oxidase: structural conservation amid regulatory diversity. *Biochim Biophys Acta* 1459:432–439
- Srere PA (1987) Complexes of sequential metabolic enzymes. *Annu Rev Biochem* 56:89–124
- Starkov AA, Fiskum G, Chinopoulos C, Lorenzo BJ, Browne SE, Patel MS, Beal MF (2004) Mitochondrial alpha-ketoglutarate dehydrogenase complex generates reactive oxygen species. *J Neurosci* 24:7779–7788
- Takeda M (1981) Glucose-induced inactivation of mitochondrial enzymes in the yeast *Saccharomyces cerevisiae*. *Biochem J* 198:281–287
- Thevelein JM (1994) Signal transduction in yeast. *Yeast* 10:1753–1790
- Tovar J, Fischer A, Clark CG (1999) The mitosome, a novel organelle related to mitochondria in the amitochondrial parasite *Entamoeba histolytica*. *Mol Microbiol* 32:1013–1021
- Trumper BL (1990) Cytochrome bc1 complexes of microorganisms. *Microbiol Rev* 54:101–129
- Umbach AL, Siedow JN (2000) The cyanide-resistant alternative oxidases from the fungi *Pichia stipitis* and *Neurospora crassa* are monomeric and lack regulatory features of the plant enzyme. *Arch Biochem Biophys* 378:234–245
- van Dam K, Shinohara Y, Unami A, Yoshida K, Terada H (1990) Slipping pumps or proton leaks in oxidative phosphorylation. The local anesthetic bupivacaine causes slip in cytochrome c oxidase of mitochondria. *FEBS Lett* 277:131–133
- Velazquez I, Pardo JP (2001) Kinetic characterization of the rotenone-insensitive internal NADH: ubiquinone oxidoreductase of mitochondria from *Saccharomyces cerevisiae*. *Arch Biochem Biophys* 389:7–14
- Velours J, Rigoulet M, Guerin B (1977) Protection of yeast mitochondrial structure by phosphate and other H<sup>+</sup>-donating anions. *FEBS Lett* 81:18–22
- Wagner AM, Moore AL (1997) Structure and function of the plant alternative oxidase: its putative role in the oxygen defence mechanism. *Biosci Rep* 17:319–333
- Wallace PG, Pedler SM, Wallace JC, Berry MN (1994) A method for the determination of the cellular phosphorylation potential and glycolytic intermediates in yeast. *Anal Biochem* 222:404–408
- Wilhelm J, Fuksova H, Schwippelova Z, Vytasek R, Pichova A (2006) The effects of reactive oxygen and nitrogen species during yeast replicative ageing. *Biofactors* 27:185–193
- Yamada A, Yamamoto T, Yoshimura Y, Gouda S, Kawashima S, Yamazaki N, Yamashita K, Kataoka M, Nagata T, Terada H et al (2009) Ca<sup>2+</sup>-induced permeability transition can be observed even in yeast mitochondria under optimized experimental conditions. *Biochim Biophys Acta* 1787:1486–1491
- Zitomer RS, Nichols DL (1978) Kinetics of glucose repression of yeast cytochrome c. *J Bacteriol* 135:39–44
- Zundorf G, Kahlert S, Bunik VI, Reiser G (2009) alpha-Ketoglutarate dehydrogenase contributes to production of reactive oxygen species in glutamate-stimulated hippocampal neurons in situ. *Neuroscience* 158:610–616